C.P. No. 4
(10057)
A.R.C. Technical Report

MINISTRY OF SUPPLY

AERONAUTICAL RESEARCH COUNCIL
CURRENT PAPERS

MAXIMUM IMPACT PRESSURES ON SEAPLANE HULL BOTTOMS

By

A. G. Smith, B.Sc., D.I.C., I. W. McCaig, B.Sc.,
W. M. Inverarity, M.A., B.Sc.

LONDON : HIS MAJESTY'S STATIONERY OFFICE

1950

Price 7s. 6d. net.

MAXIMUM IMPACT PRESSURES ON SEAPLANE HULL BOTTOMS

by

A. G. Smith, B.Sc. D.I.C.
I. W. McCaig, B.Sc.
W. M. Inverarity, M.A., B.Sc.

SUMMARY

An investigation has been made to determine the effect of the various impact parameters on the maximum impact pressures on a hull bottom impinging on a water surface.

Pressure measurements were made, using D.V.L. mechanical pressure recorders, on three hulls, each of 3-ft. beam, in the hull launching tank. The dead rise angles of these hulls were 10°, 20°, 30° respectively. They were launched with controlled impact conditions of speed, attitude and acceleration at flight path angles of 8° to 10°, but with freedom in heave and pitch: further tests were made by vertical drops.

Parallel theoretical studies have been made to investigate the effect on the maximum pressure of (1) size of measuring surface, (2) beam loading, (3) freedom to pitch, (4) horizontal velocity, (5) initial vertical acceleration, (6) departure from the simple wedge shape.

Experimental results show that the maximum pressure measured on a diaphragm depends on the diaphragm size and position and that it is not the true maximum pressure at that point. The maximum measured pressures at any given part of the hull can however be expressed in terms of the first impact conditions as

$$p_{max} = \frac{oV_n \quad oV_v \quad \cot^2\theta}{\text{Const. (Area Factor) (Velocity Factor)}} \quad .. \quad .. \quad .. \quad (S.1.)$$

Where oV_n = Resultant velocity normal to the keel at first impact.

oV_v = Vertical velocity at first impact.

θ = Dead rise angle at the point concerned, measured in the section normal to the local keel.

Area factor = correction factor to give measured maximum pressures over the area of surface in terms of the true maximum.

Velocity Factor = correction factor to allow for the reduction in velocity since first impact.

and the Constant has a mean value of 54 when p_{max} is measured in lb./sq.in.

The area and the velocity factors have been evaluated and their applicability determined.

When the velocities V_n, V_v, are those at the time of the pressure occurence, and p_{max} is the true maximum pressure, the above formula becomes -

$$p_{max} = \frac{V_n \, V_v \cot^2\theta}{\text{Const.}}$$

It reduces further to the Wagner theoretical form of $\frac{V_v^2 \cot^2\theta}{\text{Const.}}$ for vertical impacts at zero incidence. A theoretical justification for the form of equation (S.1.) above is given for impacts at flight path angles of the orders of those tested.

Further work both theoretical and experimental, is required to extend these results to include pressures at small flight path angles and in the planing condition.

LIST OF CONTENTS

1. Introduction.

Previous experiments, model and full scale, have shown that the most important parameters affecting the impact pressures on a hull alighting on water are (1) dead rise angle, (2) attitude, (3) velocity normal to the keel. Further there has been deduced the empirical relationship -

$$p_{max.} = \frac{{}_oV_n^2 \cot \phi}{K}$$

where ${}_oV_n$ = the resultant velocity normal to the keel at first impact.

ϕ = the angle between the surface where the pressure is measured and the surface of the water.

K = a constant which increases forward and aft of the C.G. and increases from keel to chine.

This formula has been shown to be a good approximation for regions in the vicinity of first impact both by model tests on a simple wedge[3,4] and by full scale tests on the Southampton[5], and Singapore[6]. The range of impact conditions covered in these tests was considerable, viz.

(1) dead rise angle 5^o to 40^o (including flared forms),

(2) keel attitude 0^o to 23^o,

(3) resultant speeds in the flight path up to 75 knots,

(4) static beam loading coefficients $C_{\Delta o}$ $(= \frac{M}{\rho b^3})$ = 0.5 (approx.),

(5) initial downward accelerations 0 to 1 g.,

(6) angular velocities at or subsequent to first impact of up to 15^o per sec. (full scale only).

The above formula is however deficient in several respects.

Firstly, it is based only on measurements, in all positions[4], model and full scale, of the mean maximum pressure on the surfaces of 2 inch diameter diaphragms. Therefore it is not obvious that the true peak pressure which is of a transient nature and extends only over a very small width near the edge of the wetted area is given by the above formula as it stands.

Secondly, for the important practical purpose of stressing it is desirable to know the mean maximum pressure over any required area. Hence an investigation is made in this report of the 'area factor' which is defined as the ratio of the true peak pressure to the mean maximum pressure.

Lastly the variation of the constant with position on the hull requires examination. To do this we define "velocity factor" as the ratio of the constant evaluated on the velocities at first impact to that evaluated on the velocities at the time of maximum pressure on the diaphragm in question. This velocity factor will therefore be seen to depend only on the variation of velocity during the impact and not on the pressure measured on the diaphragm.

The objects of the report are therefore to examine -

(1) the relationship between the true peak pressures and the impact parameters.

(2) the area factor.

(3) the velocity factor.

The experimental results with their analysis form the body of the report, theoretical results and calculations are in the appendices.

The authors wish to acknowledge the considerable contributions to the experimental work and to the report of F. O'Hara M.A., P.E. Naylor, B.A. B.Sc., J. M. Bird B.Sc., and E. K. Greatrix B.Sc.

2. Pressure Measurements with the Hull Launching Tank.

2.1 Description of Tests.

The experiments were made in the M.A.E.E., Hull Launching Tank; a description of this tank and the method of operating it is given in ref. 1. Three hulls, each of 3 ft. beam and of the same basic form, were tested. The dead rise angles at the step were 10°, 20°, 30°. This dead rise was constant from keel to chine and also forward for about half the forebody length.

The hull and link bars correspond to a flying boat of 1370 lb. while the moment of inertia about a transverse axis through the C.G. was 6550 lb. ft.^{2}. Hull lines and leading dimensions are given in Figs. 1 to 3.

The hulls were launched free to heave and to pitch about the C.G. position, at keel attitudes of +9° to -8°, at horizontal speeds of 0 to 35 ft. per sec. and vertical speeds of 5 to 8 ft. per sec. Flight path angles available were 8° to 14°, corresponding to stalled landings; some vertical drops were also made. Details are given in Tables 4, 5, 6.

For each drop time records of pressures, attitudes, and speeds were made for each of the 15 diaphragms. Details of the positions of these diaphragms are given in Tables 1, 2, 3. Different sizes of diaphragms were used to investigate the area factor.

The effect of vertical acceleration was studied by varying the balance of the parallel link bar motion; a range from 0 to 6.3 ft./sec^2 was obtained.

Damping in pitch was investigated on the 10° hull using the damper illustrated in Fig. 4. This was of a simple friction clutch type. A wire attached to the bow and stern of the hull was wound round a drum (A). This drum was constrained in rotation by the pressure from the spring (B); this could be adjusted by the lock nut (C) thus varying the damping.

2.2 Results.

In this section only the maximum recorded pressures and the corresponding initial and local impact conditions are given and no attempt is made at this stage to express these quantities in a generalised form.

Results on the 20° hull are given first as these included the greatest variation of speed and attitude. Also the dead rise of 20° is more representative of present day practice. A list of runs is given in Table 4 and the dimensions and position of the diaphragms are given in Table 1 and Fig. 1. The results are detailed in Figs. 5 - 23.

The table at the top of these figures gives the maximum pressures recorded on each of the 15 diaphragms and two sets of speeds and attitudes. The first set gives the conditions just before impact i.e. at time t_o. The vertical and horizontal velocities are those of the pressure points at that time and the attitude that of the local keel. This set is of use for stressing purposes where these conditions are assumed known. The second set refer to conditions at time t_1 of maximum pressure on the diaphragm and are primarily of use for checking against theory and establishing the law connecting pressures and impact velocities and geometry. The vertical acceleration due to gravity is shown at the top of the table. The diagram below the tables gives a time history of each drop, showing the variation of attitude and vertical velocity of the C.G. with time. A record of the times of maximum pressures on the diaphragms is also shown.

Figs. 24 - 36 give the results on the 30° hull. A list of runs is given in Table 5 and particulars of the diaphragms in Table 2 and Fig. 2. All runs on this hull were made with horizontal velocity.

A list of runs on the 10° dead rise hull is given in Table 6 and the results in Figs. 37 - 53. Particulars of the diaphragms are given in Table 3 and Fig. 3. On this hull some damping in pitch was applied as indicated on the figure. The maximum pressures measured on this hull were considerably greater than expected and a high rate of diaphragm failure occurred. It was not possible to repeat the tests with new diaphragms.

The time at which the maximum pressures are recorded is measured directly from the record. This pressure is generally built up under one hundredth of a second, the smaller the dead rise angle the shorter the time. The time at which the first keel impact occurs was not measured directly but estimated from the geometry of impact, knowing the variation with time of attitude, velocity and vertical distance of the step above the water.

3. Method of Reduction

To use the above results to estimate the maximum pressures in any landing case it is necessary to express them as a function of impact velocities and attitudes. A survey of the theoretical aspects of the problem is given in Appendix I and further details in Appendices II to IV.

The results of Jones and others, using 2 in. diameter diaphragms, gave good agreement with the formula -

$$p_{max.} = \frac{{}_oV_n^{\,2} \cot \emptyset}{K}$$

where ${}_oV_n$ is the velocity normal to the keel at first impact and $\emptyset$ is the angle between the plane of the side of the wedge and the water surface. The Hull Launching Tank results were first reduced in terms of this formula, values of the constant K being estimated in terms of the velocity at the first impact (K_1) and further in terms of the velocity at the time of the maximum pressure measurements (K_3). On analysing the Hull Launching Tank results it was found that both K_1 and K_3 varied widely with attitude, increased with speed at positive attitudes and decreased rapidly with decrease of deadrise angle. The applicability of the above formula is therefore questionable and further reduction was made in terms of the relation arrived at in Appendix I

viz:-

$$p_{max} = \frac{V_n \, V_v \cot^2 \theta}{D \text{ (Area Factor)}}$$

As in the first analysis two values of D were calculated, D_1 in terms of initial impact velocities and D_3 in terms of impact velocities at time of maximum pressure. Thus the ratio $\frac{D_1}{D_3}$ was the experimental value of the velocity factor that is examined theoretically in Appendix I.

4. The Relations between the Measured Maximum Pressures and the Impact Parameters at the Time of Pressure Measurement

4.1 The Velocity Parameter

The variation in K (in $p_{max} = \frac{{}_oV_n^{\,2} \cot \emptyset}{K}$) was first investigated for systematic error by plotting log K_1 against log ${}_oV_n$ and log K_3 against log V_n for several diaphragms near the main step on the 20° hull. These plots are shown in Figs. 54 - 57 for diaphragms 9 and 10. The points plotted on these graphs represent all the runs made on the hull with 2.1 ft./sec^2 vertical acceleration due to gravity. The initial vertical velocity during these runs varied between 4 and 6 ft./sec. and were taken as sensibly constant, the horizontal velocity varied between 0 and 36.6 ft./sec. and the attitude between -6° and $+9^{\circ}$. A line with slope unity has been drawn through these points and it can be seen to be a fair mean. The slope of this mean line indicated that the maximum pressure varies according to the law.

$$p_{max} = \frac{{}_oV_n}{\text{constant}} \cdot \cot \emptyset$$

Where the constant has dimensions $\left[L^{2}\right]\left[T\right]\left[M^{-1}\right]$ and is therefore of the form $f\left(\frac{1}{\rho V}\theta\right)$ where V is a velocity. As the vertical velocity in these tests was sensibly constant the velocity term would appear to be V_v. A theoretical argument for a $V_n V_v$ form for impact is given in ref. 15 where it is also shown that there is no justification for the use of cot ϕ rather than cot θ. The reduction equation was therefore taken as

$$p_{max} = \frac{V_n V_v \cot \theta}{C}$$

Pressure was then reduced on this basis, which is the velocity basis indicated theoretically in Appendix I. C_1 is the value of the constant in terms of time of first impact and C_3 in terms of time of p_{max} measurement.

4.2 Area of Diaphragm.

As the peak of the pressure wave on landing is very sharp the use of a diaphragm of practicable size to measure the peak gives an incorrect result, since only the average pressure over the diaphragm is measured. The Area Factor is established for vertical drops in Appendix II where a correction is given for rectangular and circular diaphragms. The correction depends on the ratio $\frac{\text{width of diaphragm}}{\text{distance from keel}} = \frac{d}{c}$, and angle of deadrise, and is given in Fig. 58 - 59 for dead rise angles of 10°, 20° and 30°.

This area factor, based on the theoretical pressure distribution in vertical drops [11], has been checked for

(a) vertical drops,
(b) drops with horizontal velocity.

The check for vertical drops could only be made on the 20° hull on which such drops were made. Here values of C_3 were compared for diaphragms in the region of the step over a range of the ratio $\frac{d}{c}$. Observed values of C_3 are given in Table 7 together with their corresponding values of $\frac{d}{c}$. These values of C_3, then reduced to C_3 at zero $\frac{d}{c}$ by the correction of Fig. 58 are given in the last column. It can be seen that the average value of this last column is approximately 19 and although there is considerable scatter round this value it is purely of a random nature, and is not in itself a function of $\frac{d}{c}$. Table 8 gives the average values for the same diaphragms on this hull for runs with horizontal velocity and here again the average value of C_3 reduced to zero is approximately 19.

Comparison between diaphragms of different $\frac{d}{c}$ values on the 30° hull is given in Table 9 for runs with horizontal velocity. More scatter is obtained on this hull but no consistent different of the reduced value of C_3 with the ratio $\frac{d}{c}$ is apparent.

Mean values of C_3 observed during nose up impacts on the 10° hull are given in Table 10. Here C_3 increases in value towards the bow so in Table 10 the hull is divided transversely and C_3 compared at constant values of the ratio -

$$\frac{L}{b} = \frac{\text{Distance forward of C.G.}}{\text{Beam at step.}}$$

Values compared on this basis shows the theoretical correction to be slightly too great for higher values of $\frac{d}{c}$.

4.3 Deadrise Angle, θ

Average values of the local impact constant C_3 were obtained for the 3 hulls, where

$$p_{max} = \frac{V_n V_v \cot \theta}{C_3 \text{ (Area Factor)}}$$

(a) Over the constant deadrise section of the forebody.

(b) Over diaphragms of equal deadrise on the warped section of the forebody.

(c) Over the region behind the step.

Average values of C_3 in section (a) reduced to zero are given in Table 11 for the 3 deadrise angles tested. It can be seen from this table that C_3 varies considerably with deadrise angle. Wagner[11] indicated that p_{max} is nearly proportional to $\cot^2\theta$ rather than $\cot\theta$ so these values were multiplied by $\cot\theta$ and a constant D_3 defined by $p_{max} = \dfrac{V_n V_v \cot^2\theta}{D_3(\text{Area Factor})}$.

Values of D_3 are given in Table 12 along with the theoretical value of Wagner for vertical drops. It can be seen that both theoretical and experimental values are in close agreement and that D_3 is nearly constant with deadrise.

On the warped section of the forebody values of D_3 reduced to zero $\frac{d}{c}$ are given as averages over sections of equal deadrise in Table 13. These values of D_3 are higher than the values on the unwarped part of the forebody on the 10° hull and lower on the 30° hull. On the 20° hull they are approximately the same.

Results for the region aft of the step are most complete on the 20° hull. On this hull it was found that results measured in vertical drops and rear step landings gave a higher value of D_3 than these in which the main step touched first. The average value of D_3 reduced to zero for the first group was 92 and for the second 45. On the 30° and 10° hulls the values of D_3 for the afterbody were 47 and 42 respectively showing a slight fall off with decrease in forebody deadrise. No variation of D_3 fore and aft along the afterbody was found.

5. Relation between Maximum Local Pressures and Impact Parameters at Time of First Impact

It can be seen from the above that the maximum pressure measured on a given area can best be expressed in terms of

$$p_{max} = \frac{V_n V_v}{D_3} \qquad \frac{\cot^2\theta}{(\text{Area Factor})}$$

where the value of D_3 is closely the same as the theoretical Wagner value of 58 for vertical drops with small deadrise angles. In terms of the velocities at first keel impact, $_oV_n$, $_oV_v$, the constant D_3 is replaced by D_1 and the ratio of these observed values as defined by $\frac{D_1}{D_3}$ is the observed value of the velocity factor for the hulls tested. The value of the velocity factor is independent of the form of the maximum pressure relationship assumed for the same impact conditions and diaphragm position on a given hull. Its evaluation also obviated any inaccuracies in measuring the pressure itself.

The value of this velocity factor will depend theoretically on the value of the ratio of the associated mass of water to the mass of the hull, (Appendix I).

5.1 Attitude and Position of Pressure Measurement

The attitude of the hull changes between the time of first keel impact and the maximum pressure measurement. It is convenient to determine what effect this has on the velocity factor. If we write

$$\frac{D_1}{D_3} = \frac{D_1}{D_2} \cdot \frac{D_2}{D_3}$$

where D_2 is a factor calculated from the formula

$$P_{max} = \frac{{}_2V_n \; {}_oV_v \cot^2\theta}{D_2 \text{ (Area Factor)}}$$

and ${}_oV_v$ = vertical speed at first impact

${}_2V_n = {}_oV_v \cos\alpha_1 + V_H \sin\alpha_1$

V_H = horizontal velocity

α_1 = hull attitude at time of maximum pressure at the diaphragm.

then $\frac{D_1}{D_2}$ explores the effect of change of attitude between the first and diaphragm impacts, and its variation with initial attitude and initial angular velocity. This variation of $\frac{D_1}{D_2}$ was investigated for 3 diaphragms on the 20° hull, these were

No. 5 near the bow
No. 10 near the main step
No. 15 near the rear step

and $\frac{D_1}{D_2}$ was plotted against initial attitude (αo) in Figs. 60 - 62 for varying angular velocities, $\dot{\alpha} o$. Whilst it is evident from the figures that $\frac{D_1}{D_2}$ varies with αo there appears to be little variation of $\frac{D_1}{D_2}$ with change of attitude after first impact or with initial angular velocity. Thus, within the limits of experimental error, the effects of angular velocity on the velocity factor for any diaphragm may be neglected and the velocity factor may be taken as a function of first impact attitude only.

There therefore remains only the investigation of the dependence of the ratio $\frac{D_1}{D_3}$ on attitude and diaphragm position. A plot of $\frac{D_1}{D_3}$ against initial attitude was therefore made (for runs with 2.1 ft./sec.^{2} initial acceleration) for all the diaphragms on each hull. Specimens of these are given in Figs. 63 - 65 for diaphragms 5, 10, and 15 on the 20° hull. These figures show considerable scatter due to experimental error but the general form and position of a mean line can be seen. Cross plotting these mean values of $\frac{D_1}{D_3}$ against $\frac{2c}{b} = \frac{\text{local wetted beam}}{\text{beam at step}}$ for constant values of $\frac{L}{b} = \frac{\text{distance forward of C.G.}}{\text{beam at step}}$ at attitudes of -5°, 0°, 5°, and 10° give graphs shown in Figs. 66 - 69 for the 20° hull. On the afterbody where there was only one diaphragm on each cross section a constant value of $\frac{D_1}{D_3}$ was taken across its width. Results on the 30° hull were analysed in a similar manner and identical mean values obtained. Sufficient results were not obtained at any one damping on the 10° hull to draw a similar figure.

From Fig. 66 - 69 the velocity factor is known for this hull and hence the maximum pressure distribution for any landing.

5.2 Hull Weight

The velocity factors obtained in paragraph 5.1 will be modified for other hulls of different weights as shown theoretically in Appendix III. No experimental evidence has yet been obtained from the hull launching tank experiments to confirm these estimated values, which are based on the vertical impact case of Wagner. Approximately the velocity factor is decreased and the maximum pressure increased at a given point by the multiplying factor

$$\left(1 + \frac{2\mu}{1 + \mu}\right) \frac{\delta M}{M}$$

where μ is the ratio of the associated mass of water to the mass of the hull and δM is the change in the mass of the hull M. Its value is therefore dependent on the unknown factor μ. It will be negligible for small immersions, near the keel, but increase to the order of 10 per cent near the chines near the C.G. or 20 per cent forward for a 20 per cent increase of mass.

The effect is further increased with distance of impact from the C.G. because of the inertia effect increasing the value of μ by the factor $(1 + \frac{a^2}{k^2})$. The loading per wetted beam determines the value of μ for any given immersion, so that the effect of mass can be considered in terms of the static beam loading coefficient

$$C_{\Delta o} = \frac{M}{\rho b^3}$$

Where ρ is mass density of water

b is beam at the step.

This is not accurate unless the maximum beam is wetted but is a convenient criterion. More accurately the beam at the position considered must be used, but this also requires a knowledge of the effective mass of water displaced.

The beam loading of the hulls tested is of the same order as that of present day hulls.

5.3 Pitching Moment of Inertia

The pitching moment of inertia will also have some effect on the maximum pressure when impact takes place away from the C.G. so that momentum can be absorbed in both rotation and translation. No experimental evidence was obtained but theoretical values for a range of values of μ and $\frac{a^2}{k^2}$ are given in Appendix IV. It is shown that pressures are increased or velocity factors decreased by the factor.

$$\left[1 + \left(\frac{\mu}{1 + \mu}\right) \frac{a^2}{k^2}\right]^2$$

where a is the distance of the resultant impact force from the C.G. and k is the radius of gyration. The corrections to the velocity factors obtained on the experimental hulls are thus known only very approximately.

5.4 Vertical Acceleration at First Impact

The vertical acceleration due to gravity was varied between 0 and 6.5 ft./sec.^{2} during the tests by changing the weight of the counterbalance on the swinging arm. The variation had no effect on the value of D_3 as this was dependent only on local velocities. The effect of D_1 can therefore be seen from the variation of $\frac{D_1}{D_3}$ with initial vertical acceleration.

Figs. 70 - 72 show this effect for diaphragms 5, 10, and 15 the points with different initial acceleration being given different symbols. From these figures there appears to be little consistent variation with acceleration due to gravity; so over the range of accelerations tested the effect can be ignored. A theoretical treatment of the problem is given in Appendix III, which also shows the effect to be small.

5.5 Damping in Pitch

The effect of damping was only explored on the 10° hull where runs were made with zero, 1/3, 2/3, and full damping. The effect of these on ratio $\frac{D_1}{D_3}$ is shown in Figs. 73 and 74 for diaphragms 5 and 10. From these it can be seen that at high attitudes on diaphragm 5 which is near the bow; damping appears to increase the pressure in that region. It is however emphasised that this conclusion is based on 3 points and the mean curve for observations made on the 20° hull which were undamped gives lower values of $\frac{D_1}{D_3}$ than any of the points with damping.

5.6 Water Resistance

The effect of water resistance is included in the velocity parameter; it is small

6. Comparison of Hull Launching Tank and Earlier Maximum Pressure Measurements

In this section previous work both model and full scale is analysed and compared with the results obtained from the Hull Launching Tank; first (6.1) gives the comparison with the Model Scale Work on Wedges, then (6.2) with the full scale dropping tests on a Singapore, and lastly (6.3) examines the full scale landing tests made on a Southampton.

6.1 Model Scale Measurements

An extensive series of Model Scale measurement was made by Jones on a wedge dropped into water[4]. These drops were made to investigate a variety of impact conditions, and included a range of attitudes from 0° to 23° and angles of descent from 90° to 16°. Dead rise angles from 0° to 22° were examined but results are compared in this section for angles of 16° and 22° only as dead rise angles of less than this are not used in present day seaplanes.

These results were re-analysed on the basis of the reduction formula

$$p_{max} = \frac{{}_oV_n \, {}_oV_v}{D_1} \cot^2 \theta \qquad \cdot\cdot \quad \cdot\cdot \quad \cdot\cdot \quad 6.1.$$

and the average value of D_1 corrected for area factor was 110 for 16° and 93 for 22° dead rise angle. This value is higher than that found for a similar position in the Hull Launching Tank, possibly due to an increased value of Pabst's correction on the comparatively short wedges used.

Jones in his analysis obtained the empirical law

$$p_{max} - \frac{{}_oV_n^2}{K} \cot \phi \qquad \cdot\cdot \quad \cdot\cdot \quad \cdot\cdot \quad 6.2.$$

where the average value of K was 55. A comparison of the curves of (6.1) and (6.2) and the experimental points is given in Figs. 82 and 83 for the two dead rise angles tested. Both curves show reasonable agreement with the experimental points which are very scattered.

6.2 Dropping Tests

These were done on a Singapore and pressure measurements were made on seven diaphragms positioned at the step. A comparison between these measurements and pressure estimates based on the formulae evolved in this report are given in Table 14. The values agree well for diaphragms near the keel but discrepancies appear near the chine when the Singapore has a marked flare not represented on the Hull Launching Tank models.

6.3 Full Scale Landing Tests

A comparison is given here between estimated and measured pressures on the Southampton for two landings. Pressures obtained during the landing shown in Fig. 28 of reference 5 are given in Table 15 for four diaphragms near the keel. A comparison between these and the estimated pressures show them to be approximately twice the calculated values. This is due to the aircraft striking a swell (made evident by the rapidly recurring pressure peaks) on landing, thus increasing its effective rate of descent relative to the local water surface. Table 16 is a comparison between estimated pressures and pressures given in Fig. 35 of reference 5. The diaphragms for which pressures are given cover most of the forebody. Agreement between measured and calculated pressure is, in this case, fairly good and shows that the impact formulae given are reasonably accurate over the forebody.

7. Conclusions

Experiments in the Hull Launching Tank show that for the range of flight path angles tested the maximum pressures obtained at any one point of a hull for impact on a horizontal water surface can be expressed as

$$p_{max} = \frac{V_n \, V_v}{D_3} \cot^2 \theta$$

where V_n and V_v are respectively the velocities normal to the keel and vertical measured at the time of the maximum pressure, θ is the dead rise angle at the point considered measured on a section normal to the local keel and D_3 is a constant. The experimental value of D_3 is equal to 54, and is of the same order as the theoretical value given by Wagner for the vertical drop of a simple wedge at zero incidence.

When the maximum pressure is measured or required over a finite area than a correction factor, the area factor, will give the maximum value of distributed pressure over that area, as:-

$$p_{max} = \frac{V_n V_v \cot^2 \theta}{D_3 \text{ (Area Factor)}}$$

The value of this area factor can be taken as equal to the theoretical value given in Appendix II and is calculable from the theoretical pressure distribution given by Wagner for vertical drops.

The application of this result to stressing purposes requires that it be expressed in terms of the impact conditions at first impact. A velocity factor has therefore been estimated from the experimental results which represents the effect of the change of velocity and attitude between the first and local impacts, then

$$p_{max} = \frac{{}_oV_n \, {}_oV_v \cot^2 \theta}{D_3 \text{ (Area factor)(Velocity factor)}}$$

where ${}_oV_n$ and ${}_oV_v$ are the velocities at first impact measured respectively normal to the keel and vertically.

The velocity factor varies with the position of the diaphragm on the hull and with the attitude at first impact. Its value for the hulls tested can be obtained from position and impact condition from Figs. 66 to 69. It is unity for all keel positions at first impact, but increases with depth of immersion.

This factor is shown theoretically to be also dependent on the beam loading and pitching moment of inertia. The application of the velocity factor values to other hulls therefore needs correction for these terms. The order of the corrections is only known theoretically for vertical impacts and is difficult to apply, so that experiments to ascertain its value experimentally are required. The correction can be very important in regions near the chines.

Experiment shows that the effect of vertical acceleration at first impact and damping in pitch (change of attitude during immersion) are of negligible importance. The first result is supported by theory but the second needs further experimental verification.

Analysis of the results obtained in earlier Vee shape dropping tests and full scale shows that these are better satisfied by this new result than by the earlier emperical form, viz:-

$$p_{max} = \frac{V_n^2}{K} \cot \phi$$

However some lack of agreement full scale is found when the flight path angle is small.

Further Developments

Due to limitations in the apparatus, and to the techniques both of measurement and reduction of the results, having to be developed in the course of this, the first major undertaking with the Hull Launching Tank, the scope of the present survey is somewhat limited.

In particular the flight path angle has been restricted to the order of 8^o and over - the stalled on case - so that the known range of validity of the $V_n V_v$ law is very restricted. Hence it is desirable that both experimental and theoretical investigations should be extended to low flight path angles - the fly on case - in which the effect of horizontal planing forces will become evident. This case is also of importance for the ditching of landplanes. Further systematic information is also required on the effects of beam loading, moment of inertia in pitch and damping in pitch.

As the tank length is not great enough for more than first impact measurement the study of the effect of the horizontal planing forces at low flight angles would be facilitated by catapult launching on to the sea of models large enough to carry the requisite pressure recording apparatus.

Full scale tests covering the complete time history of impact are also desirable.

Both model and full scale tests require extension to the case of waves.

Lastly the application of this work to stressing requirements requires an investigation of the relative severity of the strains imposed by the peak pressure and the maximum pressure over a given area.

REFERENCES

Ref. No.	Author.	Title.	Report No.
1.	A. G. Smith G. C. Abel W. Morris	The Hull Launching Tank (Descriptive).	F/Res/161. A.R.C. 6804
2.	H. M. Garner	Recent Full Scale and Model Research on Seaplanes.	Lecture to Lilienthal Gesellschaft 1938.
3.	E. T. Jones.	Some Measurements of Pressure over a V-shape when dropped into water	F/Res/78. A.R.C. 1714
4.	E. T. Jones P. W. Blundell	Force and Pressure Measurements on V-shapes on impact with water compared with Theory and with Seaplane Alighting Results.	R. & M. 1932.
5.	E. T. Jones W. H. Davies	Measurements of Water Pressure on Hull of a Boat Seaplane.	R. & M. 1638.
6.	E. T. Jones G. Douglas C. E. Stafford R. K. Cushing	Measurement of Acceleration and Water Pressure on a Seaplane when dropped into water.	R. & M. 1807.
7.	Th. V. Karman	The Impact on Seaplane Floats during Landing.	N.A.C.A. T.N.321.
8.	H. Wagner.	Phenomena associated with Impact and Gliding on a Liquid Surface.	Z.A.M.M. Vol. 12 1932. A.R.C. 2575.
9.	W. Pabst.	Landing Impact of Seaplanes.	Z.F.M. 1930, 1931.
10.	L. Sedov	On the Impact of a Solid Body on the Surface of an Incompressible Liquid.	Cahi Report No. 187, 1934. A.R.C. 2246
11.	R. L. Kreps.	Experimental Investigation of Impact in Landing on Water.	N.A.C.A. T.M. 1046.
12.	I. W. McCaig.	Preliminary Note on the Impact of an Inclined Wedge on Water.	H/Res/190. A.R.C. 8747.

LIST OF SYMBOLS

p = pressure.

M = mass of hull.

m = mass of associated quantity of water.

μ = $\frac{m}{M}$

ρ = density of water.

b = beam at step.

$2c$ = local wetted beam.

ℓ = wetted length.

λ = $\frac{2c}{\ell}$.

L = distance forward of C.G.

a = distance of resultant impact force on hull from C.G.

k = radius of gyration.

d = diaphragm breadth.

$\bar{\Phi}$ = a potential function.

θ = dead rise angle in section normal to local keel.

φ = angle between water surface and surface on which pressure is measured.

ψ = sweep in angle.

γ = angle of flight path to horizontal at first impact.

α = keel attitude.

α_o = keel attitude at first impact.

α_1 = attitude at time of maximum pressure on diaphragm.

V_n = velocity normal to the keel.

${}_oV_n$ = velocity normal to the keel at first impact.

${}_1V_n$ = velocity along line of greatest slope.

${}_2V_n$ = ${}_oV_v \cos \bar{\alpha}_1 + V_H \sin \alpha_1$.

V_v = vertical velocity.

${}_oV_v$ = vertical velocity at first impact.

V_T = velocity parallel to the keel.

V_H = horizontal velocity.

S = area factor.

f_1 = aspect ratio factor.

f_2 = factor for finite dead rise angle.

δ = $\frac{2}{\pi^2} C_D . \tan \theta$

$C_{\Delta o}$ = static beam loading = $\frac{M}{\rho b^3}$

K, K_1, K_3
C_1, C_2, C_3
D_1, D_2, D_3 } = constants defined where they occur.

Other non-recurring symbols are defined where they are used.

LIST OF TABLES

LIST OF FIGURES

FIGURE NUMBER	TITLE

APPENDIX I

A Summary of Theoretical Work on Impact Pressures

1. Introduction

In this appendix an outline is given of how the original theory on the dropping of straight wedges at zero attitude into water has been extended to give the formulae used in this report in which account is taken of attitude, freedom in pitch, horizontal and vertical velocity, varying deadrise angle etc. Details of some proofs are referred to later appendices.

2.1 Maximum pressure at the keel

In the original theory of Von Karman[7] a wedge of great length, small deadrise angle, and dropped at zero attitude into water was considered. Assuming that the associated mass of water was that of a half cylinder, of radius equal to that of the wetted width, the mean pressure over the wetted surface defined by the intersection of the wedge and the undisturbed water surface was shown to be

$$p_{mean} = \frac{1}{2}\pi\rho\, {}_oV_v^{\,2} \cot\theta \, \frac{1}{(1+\mu)^3} \tag{1.1}$$

where ${}_oV_v$ = vertical velocity at first impact.

θ = dead rise angle

ρ = density of water

$$\mu = \frac{\text{mass of the associated water}}{\text{mass of wedge}} = \frac{1}{2}\pi\rho\frac{c^2 \ell}{M}$$

where $2c$ = wetted beam, ℓ = wetted length

M = mass of wedge

From this the maximum pressure at the keel becomes

$$p_{max} = \frac{1}{2}\pi\rho\, {}_oV_v^2 \cot\theta \tag{1.2}$$

or $$p_{max} = \frac{{}_oV_v^2 \cot\theta}{46}$$

in lb./sq.in.

2.2 Effect of Splash and Finite Immersion

Wagner[8] showed that, where x is the beam at the point considered, a velocity potential $\Phi = V_c\sqrt{c^2 - x^2}$ satisfied the conditions of impact, also that the wetted beam, $2c$, for a straight wedge at zero incidence was $\frac{\pi}{2}$ that given by the intersection of the wedge sides and the still water surface. His consequent formula for the pressure at any immersion defined by $\frac{3}{4}$ was –

$$p = \frac{1}{2}\pi\rho\, {}_oV_v^2 \cot\theta \frac{1}{(1+\mu)^2}\left[\frac{1}{\sqrt{1-\frac{x^2}{c^2}}} - \frac{2\mu}{1+\mu}\sqrt{1-\frac{x^2}{c^2}} - \frac{\frac{2}{\pi}\tan\theta}{2\left(\frac{c^2}{x^2}-1\right)}\right] \tag{1.3}$$

For p_{max}, which occurs very close to the wetted leading edge this gives

$$p_{max} = \frac{1}{8}\pi^2\rho\, {}_oV_v^2 \cot^2\theta \frac{1}{(1+\mu)^2}\left[1 + \frac{1-3\mu}{1+\mu}\,\frac{4}{\pi^2\cot^2\theta}\right] \tag{1.4}$$

From Fig. 75 a graph of the second term in the bracket – it is seen that equation (1.4) can be written approximately as

$$p_{max} = \frac{1}{8} \pi^2 \rho \, {}_oV_v^2 \cot^2 \theta \frac{1}{(1 + \mu)^2} \qquad (1.5)$$

The minimum pressure at first immersion is given by x = o, i.e. at the keel and is

$$p_{min} = \frac{1}{2} \pi \rho \, {}_oV_v^2 \cot \theta \, . \, \frac{1 - \mu}{(1 + \mu)^3} \qquad (1.6)$$

which reduces to von Karman's result at the keel when $\mu = o$

The mean pressure for finite immersion is given by –

$$p_{mean} = \frac{1}{4} \pi^2 \rho \, {}_oV_v^2 \cot \theta \frac{1}{(1 + \mu)^3} \qquad (1.7)$$

and the maximum pressure at the keel is

$$p_{max} = \frac{1}{4} \pi^2 \rho \, {}_oV_v^2 \cot \theta \qquad (1.8)$$

Wagner's results therefore compared with von Karman, increase the mean and the keel maximum pressures by $\frac{\pi}{2}$ and, more important, make the peak pressures proportional to $\cot^2\theta$.

2.3 Corrections for Finite Length

Pabst[9] from experimental evidence, provides a correction for a finite aspect ratio equivalent to a correction of the wetted length to

$$n = \frac{\ell}{\sqrt{1 + \lambda^2}} \left[1 - \frac{0.425\lambda}{1 + \lambda^2} \right] \qquad (1.9)$$

where $\lambda = \frac{2c}{\ell}$

This leads to the following correction factor to the Wagner expressions above viz:-

$$\frac{1}{\sqrt{1 + \lambda^2}} \left[1 + \frac{\lambda (1.27 + \lambda)}{2(1 + \lambda^2)} + \frac{0.635\lambda^3}{(1 + \lambda^2)^3} \right]$$

The correction factor of (1.9) is graphed in Fig. 76; this factor approximates to 1 for $\lambda > \frac{2}{3}$.

2.4 Correction for Finite Dead Rise Angle.

The correction for this to the associated mass was given by Sedov[10], on theoretical grounds, as the factor –

$$\frac{2 \tan \theta}{\pi} \quad \frac{\rho(\frac{3}{2} - \frac{\theta}{\pi}) \, . \, \rho(\frac{\theta}{\pi})}{\rho(\frac{1}{2} + \frac{\theta}{\pi}) \, . \, \rho(1 - \frac{\theta}{\pi})}$$

where $\rho_o(\theta)$ is the Euler function; for small dead rise angles this reduces to $1 - \frac{\theta}{\pi}$.

2.5 Correction for the frictional resisting force of the water

Kreps[11] in an analysis of this for vertical drops at zero incidence, relates the velocity at any instant to the initial velocity by

$$V_v = \frac{{}_oV_v}{(1 + \mu)^{1 + \delta}} \qquad (1.10)$$

where the correction for resistance

$$\delta = \frac{2}{\pi^2} C_D \tan\theta$$

and C_D is the resistance of a flat plate.

From this it follows that equations (1.5), (1.6), (1.7), (1.8) become

$$p_{max} = \frac{1}{8} \pi^2 \rho \, {}_oV_v^2 \cot^2\theta \frac{1}{(1+\mu)^2 + 2\delta} \quad .. \quad .. \qquad (1.11)$$

$$p_{min} = \frac{1}{2} \pi\rho \, {}_oV_v^2 \cot\theta \frac{1-\mu}{(1+\mu)^3 + 2\delta} \left[1 - \frac{4\mu \, C_D}{\pi^2 \cot\theta \, (1-\mu)}\right] \quad .. \qquad (1.12)$$

$$p_{mean} = \frac{1}{4} \pi^2\rho \, {}_oV_v^2 \cot\theta \frac{1}{(1+\mu)^3 + 2\delta} \left[1 - \frac{2C_D}{\pi^2} \cdot \frac{\mu}{\cot\theta}\right] \quad .. \quad .. \qquad (1.13)$$

$$p_{max_{keel}} = \frac{1}{4} \pi^2\rho \, {}_oV_v^2 \cot\theta \quad .. \quad .. \quad .. \quad .. \qquad (1.14)$$

2.6 Impacts with Finite Incidence

In a perfect fluid the pressures act normal to the wetted surface of the hull. Neglecting gravity the resultant forces must (for symmetrical impacts) be perpendicular to the directions on the hull bottom which make the greatest slope. In Appendix VII the direction of these lines (for hulls whose dead rise is constant or only varies in a fore and aft direction) is shown to be normal to the local keel at the position considered. The associated mass must be considered in this direction. The effective dead rise, for this purpose is shown in Appendix VII to be defined by –

$$\sin\xi = \frac{1}{1 + \tan^2\psi + \cot^2\theta} \quad .. \quad .. \qquad (1.15)$$

where θ = dead rise angle in a plane normal to the keel at the step

ψ = sweep in angle i.e. equivalent dead rise angle measured in a horizontal plane parallel to the keel at the step.

2.7 Freedom to Pitch

Freedom to pitch permits the absorption of some of the momentum of impact in angular motion; a relief of impact acceleration normal to the keel is obtained. In Appendix IV it is shown that this relief is equivalent to multiplying the associated mass term by

$$1 + \frac{a^2}{k^2} \cos^2\alpha \doteq 1 + \frac{a^2}{k^2}$$

where a = distance of resultant impact force from the C.G.

k = the radius of gyration

α = the angle of incidence.

2.8 Impacts with Horizontal and Vertical Velocities

From the results of ref. 12, in which horizontal and vertical velocities are taken into account, the mean pressure at finite immersion is given by

$$p_{mean} = \frac{1}{4} \pi^2\rho \, V^2 \cot\theta \frac{1}{(1+\mu)^3} \cdot \sin(\alpha+\gamma) \, (\sin\gamma - \mu\sin\alpha) \qquad (1.16)$$

or $$p_{mean} = \frac{1}{4} \pi^2\rho \, {}_oV_n \, {}_oV_v \cot\theta \frac{1}{(1+\mu)^3} \left(1 - \frac{\mu \sin\alpha}{\sin\gamma}\right) \quad .. \qquad (1.17)$$

where V = resultant velocity in flight path at first impact,

γ = angle of flight path to horizontal at first impact,

α = attitude of keel at first impact,

${}_oV_n$ = resultant velocity normal to keel,

${}_oV_v$ = resultant vertical velocity,

The maximum pressure at the keel at first impact becomes

$$p_{max} = \frac{1}{4}\pi^2\rho\, {}_oV_n\, {}_oV_v \cot\theta \quad .. \quad .. \quad (1.18)$$

When $\mu \sin\alpha \ll \sin\gamma$ i.e. when μ, α, γ, are all small quantities of the same order eq (1.17) becomes

$$p_{mean} = \frac{1}{4}\pi^2\rho\, {}_oV_n\, {}_oV_v \cot\theta \frac{1}{(1+\mu)^3} \quad .. \quad (1.19)$$

When $\gamma = 90^\circ$ (1.18), (1.19) become of the same form as (1.8) and (1.7) derived by Wagner.

The importance of these results is the replacement of ${}_oV_n^2$ used in all previous work, by ${}_oV_n\, {}_oV_v$. The simple ${}_oV_n\, {}_oV_v$ form (1.19) is only applicable for

(1) impacts where the change in horizontal velocity can be neglected; this is usually so,

(2) impacts of finite immersion when either the flight path angle is of the order of stalled on landings or first impacts when μ is small. For these same conditions, the value for p_{max} by the analogy of equation (1.18) (1.19) with (1.8) (1.7) (1.6) gives

$$p_{max} = \frac{1}{8}\pi^2\rho\, {}_oV_n\, {}_oV_v \cot^2\theta \frac{1}{(1+\mu)^2} \quad .. \quad (1.20)$$

This relationship for peak pressures has been used in the analysis of the Hull Launching Tank results.

2.9 Maximum Pressures measured on Finite Areas

The mean maximum pressure over an area will be less than the peak pressures and more than the mean pressure discussed above. The value of this area factor is discussed in Appendix II and is denoted by S in the result.

$$p_{max} = \frac{1}{8}\pi^2\rho\, {}_oV_n\, {}_oV_v \cot^2\theta \frac{1}{S(1+\mu)^2} \quad .. \quad (1.21)$$

It is assumed to be generally applicable.

3. Conclusions

Incorporating all results arrived at above we get

$$p_{max} = \frac{1}{8}\pi^2\rho\, {}_oV_n\, {}_oV_v \cot^2\theta \frac{1}{\left[1+\mu\left(1+\frac{a^2}{k^2}\right)\right]^{2+2\delta}} \frac{f_1\, f_2}{S} \quad (1.22)$$

where θ = dead rise angle taken in the direction of greatest slope relative to the plane of symmetry,

$_oV_n$ = resultant velocity normal to the keel at first impact,

$_oV_v$ = resultant vertical velocity normal to the keel at first impact,

δ = the correction factor for resistance (Kreps),

f_1 = the correction factor for aspect ratio (Pabst),

f_2 = the correction factor for finite dead rise angle (Sedov),

S = area factor,

a = distance of the resultant impact force from the C.G.,

k = the radius of gyration,

It follows that the theoretical value of the velocity factor is -

$$\frac{\left[1 + \mu(1 + \frac{a^2}{k^2})\right]^{2 + 2\delta}}{f_1 \; f_2}$$

and it independent of constant dead rise angle and velocity of impact.

APPENDIX II

The Area Factor

When a pressure wave has a sharply-defined peak, a diaphragm of finite width will not in general measure the peak pressure but some lower value dependent on the average pressure over the diaphragm. Thus, if AB denotes the diaphragm in Fig. 77 the pressure indicated will not be the peak pressure DN but an average pressure given by the area ABCDE divided by AB. This average pressure depends on

(i) the sharpness of the peak.

(ii) the width of the diaphragm AB.

(iii) the position of the diaphragm.

To relate the maximum value of the average pressure to the true pressure peak DN, it is first necessary to calculate the position of the diaphragm AB to make the average pressure a maximum.

In Fig. 77 let AB = d and let B be specified by the co-ordinate z, then it is required to choose z so that F(d) is a maximum where

$$F(d) = \int_{z-d}^{z} p(y) \; dy \qquad \text{and } y = \frac{x}{c}$$

On differentiating F(d) with respect to z, the value of z for a maximum average pressure is given by the equation -

$$p(z) - p(z - d) = 0 \qquad \text{(II.1)}$$

For the vertical impact of a V-shape at zero incidence on water, Wagner's theory gives the pressure p, as

$$p(y) = \frac{1}{2}\pi\rho\, {}_o V_v^2 \frac{1}{(1+\mu)^2}\cot\theta\left[\frac{1}{\sqrt{1-y^2}} - \frac{2\mu}{1+\mu}\sqrt{1-y^2} - \frac{\frac{1}{2}\mu y^2}{1-y^2}\right]$$

where $\mu = \frac{2}{\pi}\tan\theta$.

Thus neglecting variation of μ over the time taken for one diaphragm to to be wetted we may choose a unit of pressure in such a way that

$$p = \cot\theta\left[\frac{1}{\sqrt{1-y^2}} - \frac{2\mu}{1+\mu}\sqrt{1-y^2} - \frac{\frac{1}{2}\mu y^2}{1-y^2}\right]$$

As a first approximation the term $\frac{2\mu}{1+\mu}\sqrt{1-y^2}$ may be neglected as it is small near $y = 1$. Hence we obtain -

$$p(y) = \cot\theta\left[\frac{1}{\sqrt{1-y^2}} - \frac{1}{2}\frac{\mu y^2}{1-y^2}\right] \qquad \text{(II.2)}$$

Substituting (II.2) in (II.1) gives

$$\frac{1}{\sqrt{1-z^2}} - \frac{1}{\sqrt{1-(z-d)^2}} - \frac{1}{2}\frac{\mu z^2}{1-z^2} + \frac{1}{2}\frac{\mu(z-d)^2}{1-(z-d)^2} = 0 \qquad \text{(II.3)}$$

as the condition of maximum average pressure on the diaphragm.

From equations II.2 the maximum average pressure measured by a diaphragm of width "d", is

$$\frac{F(d)}{d} = \frac{1}{d}\int_{z-a}^{z}\cot\theta\left[\frac{1}{\sqrt{1-y^2}} - \frac{1}{2}\frac{\mu y^2}{1-y^2}\right]dy$$

$$= \frac{\cot\theta}{d}\left[\sin^{-1}_{y} + \frac{\mu y}{2} - \frac{\mu}{4}\log\frac{1+y}{1-y}\right]_{z-a}^{z}$$

where z is chosen to satisfy equation II.3.

If we define the area factor of the diaphragm to be the ratio of the true peak to the maximum average pressure measured by the diaphragm then

$$\text{area factor } S = \frac{dp_{max}}{F(d)}$$

$$\text{but } p_{max} \doteq \cot\theta\left[\frac{1}{2\mu} + \frac{\mu}{2}\right]$$

$$\text{and thus } S = \frac{d\left[\frac{1}{2\mu} + \frac{\mu}{2}\right]}{\sin^{-1}z - \sin^{-1}(z-d) + \frac{\mu d}{2} - \frac{\mu}{4}\log\frac{1+z}{1-z}\,D + \frac{\mu}{4}\log\frac{1+z-d}{1-z+d}} \qquad \text{(II.4)}$$

In any particular case the values of d and θ are known and the value of z to give a maximum average pressure can be determined from equation II.3. Hence the area factor may be determined by means of equation II.4 for square or rectangular diaphragms. For circular diaphragms as commonly used the values are slightly less. The area factors in this case are obtained by integrating the values obtained for rectangular diaphragms over a circle. Results for the two forms of measuring surfaces are given in Figs. 58 and 59.

APPENDIX III

The Effect of Beam Loading

The variation of maximum pressures with beam loading for a given Vee-bottom may be derived from the theoretical work of Wagner who gives the peak pressures as

$$p_{max} = {}^1/_8 \, \pi^2 \frac{\rho \, {}_oV_v{}^2}{(1 + \mu)^2} \cot^2 \theta = \frac{{}_oV_v{}^2}{K} \cot^2 \theta$$

where $K = \frac{8}{\rho\pi^2}(1 + \mu)^2$

By differentiation $\frac{\delta K}{K} = \frac{2 \, \delta\mu}{(1 + \mu)}$

but $\mu = \frac{m}{M}$

therefore $\frac{\delta K}{K} = \frac{-2 \, \mu}{1 + \mu} \quad \frac{\delta m}{M}$ .. .. (III.1)

Figures 78 is a plot of $\frac{\delta K}{K}$ against $\frac{\delta m}{M}$, the increase in beam loading. Thus for a hull of known geometry, for which μ is calculated the increase of maximum pressure with increase in the beam loading may be estimated.

APPENDIX IV

The Effect of Freedom in Pitch

In this appendix the general case of a wedge, free to pitch, dropping at a finite attitude into water is considered. The effect of initial angular velocity is also examined.

Consider a wedge of Mass M, (Fig. 79) dropping vertically into the water so that at first impact it has attitude α_o, and angular velocity $\dot{\alpha}_o$. Let its point of first impact be P and let point P be distance "a" from the centre of gravity, then the momentum equations will be

$$M({}_oV_v - V_v) = m(V_v - a \, \dot{\alpha} \cos \dot{\alpha})$$

$$M \, k^2(\dot{\alpha} - \dot{\alpha}_o) = m(V_v - a \, \dot{\alpha} \cos \dot{\alpha}) \, a \cos \dot{\alpha},$$

where m = associated mass of water,

k = radius of Gyration of wedge,

V_v = vertical velocity.

Putting $\mu = \frac{m}{M}$ and $z = V_v - a \, \dot{\alpha} \cos \dot{\alpha}$,

this becomes

$${}_oV_v - V_v = \mu \, z \quad .. \quad .. \quad (IV.1)$$

$$k^2(\dot{\alpha} - \dot{\alpha}_o) = a \, \mu \, z \cos \dot{\alpha} \quad .. \quad .. \quad (IV.2)$$

Multiplying equation (IV.1) by k^2 and (IV.2) by $\dot{\alpha}$ cos $\dot{\alpha}$ and adding we get

$$k^2({}_oV_v - a\dot{\alpha}_o \cos \dot{\alpha}) = k^2 z \left[1 + \mu \left(1 + \frac{a^2}{k^2}\cos^2\dot{\alpha}\right)\right]$$

$$\text{i.e. } V_v - a\dot{\alpha} \cos \dot{\alpha} = \frac{{}_oV_v - a\dot{\alpha}_o \cos \dot{\alpha}}{1 + \mu \left(1 + \frac{a^2}{k^2}\cos^2 \dot{\alpha}\right)} .$$

That is, the effect of freedom to pitch is to increase the associated mass term by the factor $(1 + \frac{a^2}{k^2}\cos^2\dot{\alpha})$. On applying this result to the formula for maximum pressures in the region near point of first impact.

$$p_{max} = \frac{1}{8} \pi^2 \rho \frac{{}_oV_v^2 \cot^2 \theta}{(1 + \mu)^2}$$

becomes

$$p_{max} = \frac{1}{8} \pi^2 \rho \frac{({}_oV_v - a\dot{\alpha}_o \cos \dot{\alpha})^2 \cot^2 \theta}{\left[1 + \left(1 + \frac{a^2}{k^2}\cos^2 \dot{\alpha}\right) \mu\right]^2}$$

but as ${}_oV_v - a\dot{\alpha}_o \cos \dot{\alpha}$ is the initial local vertical velocity, this means that for similar local impact velocities the peak pressure is reduced by the factor -

$$\frac{1}{\left(1 + \frac{\mu}{1 + \mu}\frac{a^2}{k^2}\cos^2 \dot{\alpha}\right)^2}$$

APPENDIX V

The Effect of Acceleration due to Gravity

The formula given by Wagner for maximum pressures was

$$p_{max} = \frac{1}{8} \pi^2 \rho V_v^2 \cot^2 \theta \quad .. \quad .. \quad (V.1)$$

If gravity is neglected this can be written in terms of first impact conditions as

$$p_{max} = \frac{1}{8} \pi^2 \rho \frac{{}_oV_v^{\,2}}{(1 + \mu)^2} \cot^2 \theta \quad .. \quad .. \quad (V.2)$$

In this Appendix the effect of the acceleration due to gravity on V_v is examined and a correction to equation (V.2) obtained.

The equation of motion during the impact of a wedge on the water is

$$\frac{d}{dt} (M + m) V_v = Mg$$

On dividing through by M

$$\frac{d}{dt}\left[(1+\mu)\,V_v\right] = g \qquad .. \qquad .. \qquad (V.3)$$

for a wedge dropped with its keel at angle α to the water.

But
$$\mu = \frac{1}{3M}\,\rho\,c^3\,\frac{\tan\theta}{\tan\alpha}$$

therefore we can write $\mu = nc^3$ and equation (V.3) becomes

$$\frac{d}{dt}\left[(1+nc^3)\,V_v\right] = g$$

$$\therefore\ (1+nc^3)\frac{dV_v}{dt} + 3nc^2\,\dot{c}\,V_v = g$$

but $\frac{dV_v}{dt} = \frac{dV_v}{dc}\cdot\dot{c}$ and $\dot{c} = \frac{1}{2}\pi\cot\theta\,V_v$

$$\therefore\ (1+nc^3)\cdot\frac{1}{2}\pi\cot\theta\,V_v\,\frac{dV_v}{dc} + 3nc^2\,V_v^2\cot\theta = g$$

or, dividing throughout by $\frac{1}{2}\pi\cot\theta$,

$$(1+nc^3)\,V_v\,\frac{dV_v}{dc} + 3nc^2\,V_v^2 = \frac{2g}{\pi}\tan\theta \qquad .. \qquad (V.4)$$

$$\text{Let } V_v^2 = u\ ,\ \text{i.e. } 2V_v\,dV_v = du$$

Substituting this in the above equation (V.4) gives

$$(1+nc^3)\frac{du}{dc} + 6nc^2u = \frac{4g}{\pi}\tan\theta\ .$$

$$\text{or } \frac{d}{dc}\left[(1+nc^3)^2\,u\right] = \frac{4g}{\pi}\tan\theta\,(1+nc^3)$$

On integrating this becomes -

$$(1+nc^3)^2\,V_v^2 = \frac{4g\,c\tan\theta}{\pi}\left(1+\frac{1}{4}nc^3\right) + \text{constant of integration.}$$

$$\text{At } c = 0,\ V_v = {}_oV_v,$$

$$\therefore\ \text{constant of integration} = {}_oV_v^2.$$

Substituting this value and putting $\mu = nc^3$ gives

$$V_v^2 = \frac{{}_oV_v^2}{(1+\mu)^2} + \frac{4g\,c\tan\theta}{\pi}\left[\frac{1+\frac{1}{4}\mu}{(1+\mu)^2}\right] \qquad .. \qquad .. \qquad (V.5)$$

Substituting (V.5) in (V.1) gives the maximum pressure as

$$p_{max} = \frac{1}{8}\pi^2\rho\,\frac{{}_oV_v^2}{(1+\mu)^2}\cot^2\theta + \frac{1}{2}\pi\rho g\,c\cot\theta\left[\frac{1+\frac{1}{4}\mu}{(1+\mu)^2}\right]$$

that is a further term

$$\Delta p = \frac{1}{2}\pi\rho\,g\,c\cot\theta\left[\frac{1+\frac{1}{4}\mu}{(1+\mu)^2}\right]$$

is to be added to the pressure obtained from equation (V.2) to allow for the effect of gravity.

If the wedge on impact is however partially balanced such that the force due to gravity is represented by F(g), then the term g in equation (V.3) is replaced by $\frac{F(g)}{M}$ and Δ p becomes –

$$\Delta p = \frac{1}{2} \pi \rho c \frac{F(g)}{M} \cot \theta \left[\frac{1 + \frac{1}{4}\mu}{(1 + \mu)^2} \right]$$

A graph of Δ p is given in Fig. 80 for a range of values of μ and $\frac{F(g)}{M}$. It can be seen from these graphs that the correction for gravity is small.

APPENDIX VI

Velocity and Dead Rise Angle in Direction of Greatest Slope.

In Appendix I it is shown that peak pressures vary approximately for a straight wedge as

$$P_{max} = \frac{Vn^{V_v}}{C} \cot^2 \theta$$

where V_n = velocity normal to keel.

V_v = vertical velocity.

C = a constant.

θ = dead rise angle.

As θ, the dead rise angle, is taken in the direction of greatest slope on the wedge, and V_n is also taken in this direction it follows that if the wedge is warped so as to have a sweep in angle ψ, θ, the dead rise angle, will be replaced by ξ, the angle of the greatest slope. Similarly, the value of V_n will be that for a direction given by the line of intersection of the plane of symmetry and the plane containing this angle.

Consider (Fig. 81) a circular diaphragm OAB on the side of a Vee-bottom. Let its centre O be the origin of rectangular co-ordinates with Ox and Oz normal, and Oy parallel to datum. Let the Line OD, be the intersection of the plane of the diaphragm with a plane inclined at an angle β to the plane xOz. Then OD is itself inclined at an angle ξ to Oz and it is required to find the value of β for which ξ is a maximum and slope is a maximum.

Let the Planes ZOx, ZOy intersect the diaphragm perimeter at the points A, B. Then A is the point (r sin θ, o, r cos θ) and B (o, r cos ψ, – r sin ψ) and thus the plane containing the diaphragm has the equation

$$- x \cot \theta + y \tan \psi + z = 0$$

The plane making an angle with plane XOA has equation –

$$x \tan \beta + y = 0$$

and so the line OD, intersection of these two planes, has direction ratios

$$1 \; ; \; - \tan \beta \; ; \; (\tan \beta \tan \psi + \cot \theta),$$

and therefore the angle ξ, between OD and OZ is given by -

$$\cos \xi = \frac{\tan \beta \tan \psi + \cot \theta}{\sqrt{\left[1 + \tan^2 \beta + (\tan \beta \tan \psi + \cot \theta)^2\right]}}$$

Differentiating this with respect to β we find ξ a maximum when

$$\tan \beta = \frac{\tan \psi}{\cot \theta}$$

giving $$\cos \xi_{max} = \sqrt{\left[\frac{\tan^2 \psi + \cot^2 \theta}{1 + \tan^2 \psi + \cot^2 \theta}\right]}$$

i.e. $$\sin \xi_{max} = \frac{1}{\sqrt{\left[1 + \tan^2 \psi + \cot^2 \theta\right]}}$$

The velocity along the line of greatest slope, ${}_1V_n$ is given by -

$${}_1V_n = V_n \cos \beta + V_T \sin \beta, \text{ where } \tan \beta = \frac{\tan \psi}{\cot \theta}$$

and V_n = velocity normal to keel

V_T = velocity parallel to keel

hence $${}_1V_n = \frac{V_n \cot \theta + V_T \tan \psi}{\sqrt{\left[\cot^2 \theta + \tan^2 \psi\right]}}$$

TABLE I

Position and Size of Pressure Recorders on 20° Hull

No. of Diaphragm	Diameter (ins)	$\frac{d}{c} = \frac{\text{Diameter}}{\text{Distance from Keel}}$	θ (Degrees)	ψ (Degrees)	Angle Between Local Keel and Keel at Step $= \alpha^1 - \alpha$
1	1.00	0.200	32.7	9.3	10.3
2	1.00	0.100	24.2	7.8	4.2
3	1.00	0.143	24.2	6.75	4.2
4	1.00	0.077	24.2	8.3	4.2
5	1.36	0.195	20.0	0	0
6	1.36	0.100	20.0	0	0
7	1.00	0.182	20.0	0	0
8	1.00	0.096	20.0	0	0
9	1.36	0.088	20.0	0	0
10	1.00	0.159	20.0	0	0
11	1.00	0.070	20.0	0	0
12	5.00	0.834	20.0	0	0
13	1.00	0.134	29.3	0	-6.6
14	1.00	0.154	28.8	0	-6.6
15	1.00	0.200	27.9	0	-6.6

TABLE II

Position and Size of Pressure Recorders on 30° Hull

No. of Diaphragm	Diameter (ins.)	$\frac{d}{c} = \frac{\text{Diameter}}{\text{Distance from Keel}}$	θ (Degrees)	ψ (Degrees)	Angle between Local Keel and Keel at Step $= \alpha^1 - \alpha$
1	1.00	0.200	39° 00'	4° 45'	8° 30'
1a	1.00	0.200	46° 15'	5° 00'	14° 30'
1b	1.00	0.071	39° 00'	9° 15'	8° 30'
2	1.00	0.178	33° 30'	0° 50'	4° 30'
3	1.00	0.095	33° 30'	1° 00'	4° 30'
4	1.00	0.066	33° 30'	0° 45'	4° 30'
5	1.00	0.143	30° 15'	0° 30'	1° 45'
6	1.00	0.091	30° 15'	0	1° 45'
7	1.00	0.179	30° 00'	0	0
8	1.00	0.095	30° 00'	0	0
9	1.00	0.065	30° 00'	0	0
10	1.00	0.167	30° 00'	0	0
11	1.00	0.069	30° 00'	0	0
12	5.00	0.835	30° 00'	0	0
13	1.00	0.132	29° 15'	0	-6° 36'
14 (Not corrected)	1.00	-	29° 00'	0	-6° 36'
15	1.00	0.200	28° 00'	0	-6° 36'

TABLE III

Position and Size of Pressure Recorders on 10° Hull

No. of Diaphragm	Diameter (ins.)	$\frac{d}{c}$ = Diameter / Distance from Keel	θ (Degrees)	ψ (Degrees)	Angle between Local Keel and Keel at Step = $\alpha^1 - \alpha$
1	1.00	0.250	21° 50'	1° 25'	10° 12'
1a	1.00	0.222	30° 00'	6° 00'	10° 45'
1b	1.00	0.131	23° 00'	8° 40'	16° 35'
2	1.00	0.250	13° 40'	2° 20'	5° 25'
3	1.00	0.114	14° 00'	12° 36'	5° 25'
4	1.00	0.074	14° 20'	17° 10'	5° 25'
5	1.00	0.182	10°	1° 00'	0°
6	1.00	0.083	10°	8° 30'	0°
7	1.00	0.200	10°	0°	0°
8	1.00	0.105	10°	0°	0°
9	1.00	0.071	10°	0°	0°
10	1.00	0.200	10°	0°	0°
11	1.00	0.077	10°	0°	0°
12	5.00	0.862	10°	0°	0°
13	1.00	0.132	29°	0°	-6° 36'
14 (Not corrected)	1.00	-	29°	0°	-6° 36'
15	1.00	0.200	28°	0°	-6° 36'

TABLE IV

Impacts of Hull with 20° Dead Rise

Figure Number	Vertical Acceleration Due to Gravity (ft./sec^2)	Horizontal Velocity of Carriage at First Impact (ft./sec.)	Vertical Velocity at First Impact (ft./sec.)	Attitude At First Impact (degrees)
5	2.1	36.6	5.2	5.62
6	2.1	36.5	4.2	2.65
7	2.1	36.14	6.4	0.25
8	2.1	36.1	5.3	8.26
9	2.1	35.8	5.0	11.95
10	2.1	31.3	5.8	-2.05
11	2.1	25.3	6.0	9.25
12	2.1	25.2	5.7	-0.70
13	2.1	25.2	4.9	-6.00
14	2.1	25.2	5.0	+4.85
15	2.1	0	6.4	1.85
16	2.1	0	5.22	6.64
17	2.1	0	6.0	9.15
18	2.1	0	6.1	-3.42
19	0	0	6.8	6.50
20	4.2	0	7.7	6.47
21	4.2	26.5	6.4	1.07
22	5.2	0	7.75	6.57
23	6.3	25.8	6.25	1.2

TABLE V

Impacts of Hull with 30° Dead Rise

Figure Number	Vertical Acceleration Due to Gravity (ft./sec.^{2})	Horizontal Velocity of Carriage at First Impact (ft./sec.)	Vertical Velocity at First Impact (ft./sec.)	Attitude at First Impact (degrees)
24	2.1	33.1	6.2	0.35
25	2.1	39.8	5.1	5.50
26	2.1	40.0	6.5	9.10
27	2.1	37.7	6.5	2.35
28	2.1	37.6	5.0	4.82
29	2.1	35.8	3.4	-5.92
30	2.1	36.0	7.6	2.34
31	0	37.4	6.7	5.18
32	0	37.9	8.2	10.45
33	4.2	40.0	6.9	1.55
34	4.2	40.6	6.0	0.80
35	6.3	40.1	6.2	4.40
36	6.3	37.6	6.6	2.22

TABLE VI

Impact of Hull with 10° Dead Rise

Figure Number	Vertical Acceleration Due to Gravity (ft./sec.^{2})	Horizontal Velocity of Carriage at First Impact (ft./sec.)	Vertical Velocity at First Impact (ft./sec.)	Attitude at First Impact (degrees)
37	2.1	32.5	6.1	1.95
38	2.1	32.0	6.0	6.75
39	2.1	33.5	5.9	0.8
40	2.1	33.8	6.1	6.7
41	2.1	34.0	5.6	7.6
42	2.1	33.1	5.5	-3.2
43	2.1	34.0	6.9	-2.9
44	2.1	32.1	5.4	-7.4
45	2.1	32.4	4.9	-6.0
46	2.1	32.2	6.7	-8.0
47	2.1	30.8	6.2	-2.1
48	2.1	35.4	6.1	-2.7
49	0	33.0	5.9	-3.0
50	4.2	32.4	6.2	2.1
51	4.2	36.4	5.8	-2.4
52	6.3	34.4	6.6	-2.7
53	6.3	36.4	5.6	2.3

TABLE VII

Variation of Observed Values of C_3 with Ratio $\frac{d}{c}$
during Vertical Drops on 20° Dead Rise Hull

Number of Diaphragm	$\frac{\text{Diameter}}{\text{Distance from Keel}} = \frac{d}{c}$	Average Value of C_3 (observed)	Average Value of C_3 (corrected to zero $\frac{d}{c}$)
11	0.070	20.1	18.6
9	0.088	26.1	23.3
8	0.096	22.4	19.7
10	0.159	22.1	18.9
7	0.182	21.6	18.0
12	0.834	39.8	22.1

TABLE VIII

Variation of Observed Values of C_3 with Ratio $\frac{d}{c}$
during Runs with Horizontal Velocity on 20° Dead Rise Hull

Number of Diaphragm	$\frac{\text{Diameter}}{\text{Distance from Keel}} = \frac{d}{c}$	Average Value of C_3 (observed)	Average Value of C_3 (corrected to zero $\frac{d}{c}$)
11	0.070	24.7	22.6
9	0.088	17.2	15.7
8	0.096	21.9	19.6
10	0.159	21.1	17.9
7	0.182	24.2	20.2
12	0.834	37.0	20.6

TABLE IX

Variation of Observed Values of C_3 with Ratio $\frac{d}{c}$ for 30° Dead Rise Hull

Number of Diaphragm	Diameter / Distance from Keel $= \frac{d}{c}$	Average Value of C_3 (observed)	Average Value of C_3 (corrected to zero $\frac{d}{c}$)
9	0.065	20.8	20.0
11	0.069	21.1	20.3
8	0.095	27.7	26.0
10	0.167	20.4	18.8
7	0.179	30.0	27.3
12	0.835	34.6	26.0

TABLE X

Variation of Observed Value of C_3 with Ratio $\frac{d}{c}$ and Distance Forward of the Step for 10° Hull

Number of Diaphragm	Diameter / Distance from Keel $= \frac{d}{c}$	Average Value of C_3 (observed)	Average Value of C_3 (corrected to zero $\frac{d}{c}$)	Distance Forward of C.G. Beam
5	0.182	21.8	11.5	1.11
6	0.083	22.6	15.6	
8	0.105	16.1	10.2	0.46
9	0.071	26.5	18.9	
10	0.200	10.2	5.3	0.28
11	0.077	8.8	6.1	

TABLE XI

Variation of C_3 with Dead Rise angle, θ

Dead Rise Angle θ	C_3
10°	10
20°	19
30°	24

TABLE XII

Variation of D_3 with Dead Rise Angle, θ

Dead Rise Angle θ	Experimental Value of D_3	Theoretical Value of D_3
10°	56	57
20°	54	56
30°	48	51

TABLE XIII

Values of D_3 at $\frac{d}{c} = 0$ near the Bows

10° Hull		20° Hull		30° Hull	
θ	D_3 (corrected)	θ	D_3 (corrected)	θ	D_3 (corrected)
30°	59.3	-	-	46°	38.7
22°	79.2	33°	39.9	39°	36.1
14°	82.1	24°	63.3	33°	36.0

TABLE XIV

Comparison of Pressures measured during dropping Tests on Singapore with Results Computed from H.L.T. Formula. V_v = 11.0 ft./sec.

Station	$p_{max} = \frac{V_n V_v \cot^2\theta}{54}$	$\frac{2c}{b}$	Velocity Factor	$\frac{d}{c}$	Area Factor	μ (full scale)	μ (model scale)	Beam Loading Correction	p_{max} corrected	p_{max} observed
1	31.1	0.71	1.30	0.04	1.15	0.155	0.062	1.18	17.6	7.5
2	18.2	0.55	1.20	0.06	1.08	0.087	0.035	1.10	10.7	8.6
3	10.3	0.30	1.10	0.11	1.10	0.019	0.008	1.02	8.4	8.6
4	8.2	0.15	1.05	0.18	1.12	0.002	0.001	1.00	6.9	6.0
5	8.6	0.10	1.02	0.30	1.20	0.001	0.000	1.00	6.5	7.0
6	11.3	0.33	1.10	0.09	1.10	0.019	0.008	1.02	9.3	7.7
7	42.0	0.84	1.37	0.04	1.20	0.301	0.121	1.35	18.9	12.3

TABLE XV

Comparison between Results of H.L.T. Formula with Keel Pressures measured during a Landing in a Southampton

at $_oV_v$ = 3.0 ft./sec. V = 135 ft./sec. $\alpha = -0.5$

Diaphragm	$p_{max} = \frac{V_n V_v \cot^2\theta}{54}$	$\frac{d}{c}$	Area Factor	Velocity Factor	μ	p_{max} corrected	p_{max} observed
5	2.6	0.16	1.08	1.02	negligible	2.4	7.5
7	2.7	0.45	1.35	1.01	"	1.9	4.0
10	2.5	0.13	1.15	1.01	"	2.1	4.8
12	negligible	-	-	-	-	-	0.5

TABLE XVI

Comparison of Results of H.L.T. Formula and Pressure Measurements made during a landing in a Southampton

at ${}_oV_v = 9.5$ ft./sec. $V = 84$ ft./sec. and $\alpha = 4.5^o$

Diaphragm	(Corrected for Bank)	${}_oV_n$	${}_oV_v$	$\frac{{}_oV_n \, {}_oV_v \cot^2\theta}{54}$	$\frac{d}{c}$	Area Factor	$\frac{L}{b}$	$\frac{c}{b}$	Velocity Factor	μ Full Scale	Beam Loading Correction	p_{max} Corrected	p_{max} Observed
5	24.0	24.7	9.5	22.0	0.16	1.13	1.25	0.26	2.00	0.45	1.24	7.9	13.0
6	24.0	24.7	9.5	22.0	0.07	1.06	1.25	0.63	2.75	0 68	1.32	5.7	4.5
7	20.4	22.2	9.5	28.2	0.45	1.45	0.81	0.12	1.50	0.15	1.10	11.8	19.0
8	20.4	22.2	9.5	28.2	0.08	1.10	0.81	0.48	1.80	0.32	1.17	12.2	21.0
10	16.5	19.7	9.5	39.5	0.13	1.35	0.38	0.32	1.30	0.03	1.02	22.1	29.0
11	16.5	19.7	9.5	39.5	0.06	1.20	0.38	0.66	1.50	0.22	1.12	19.6	26.5
12	13.2	16.0	9.5	51.0	0.29	1.70	0.13	0.14	1.03	0.00	1.00	29.1	27.5
13	13.2	16.0	9.5	51.0	0.13	1.50	0.13	0.32	1.10	0.03	1.02	30.2	27.5
14	13.2	16.0	9.5	51.0	0.04	1.20	0.13	0.89	1.40	0.22	1.12	27.1	20.0

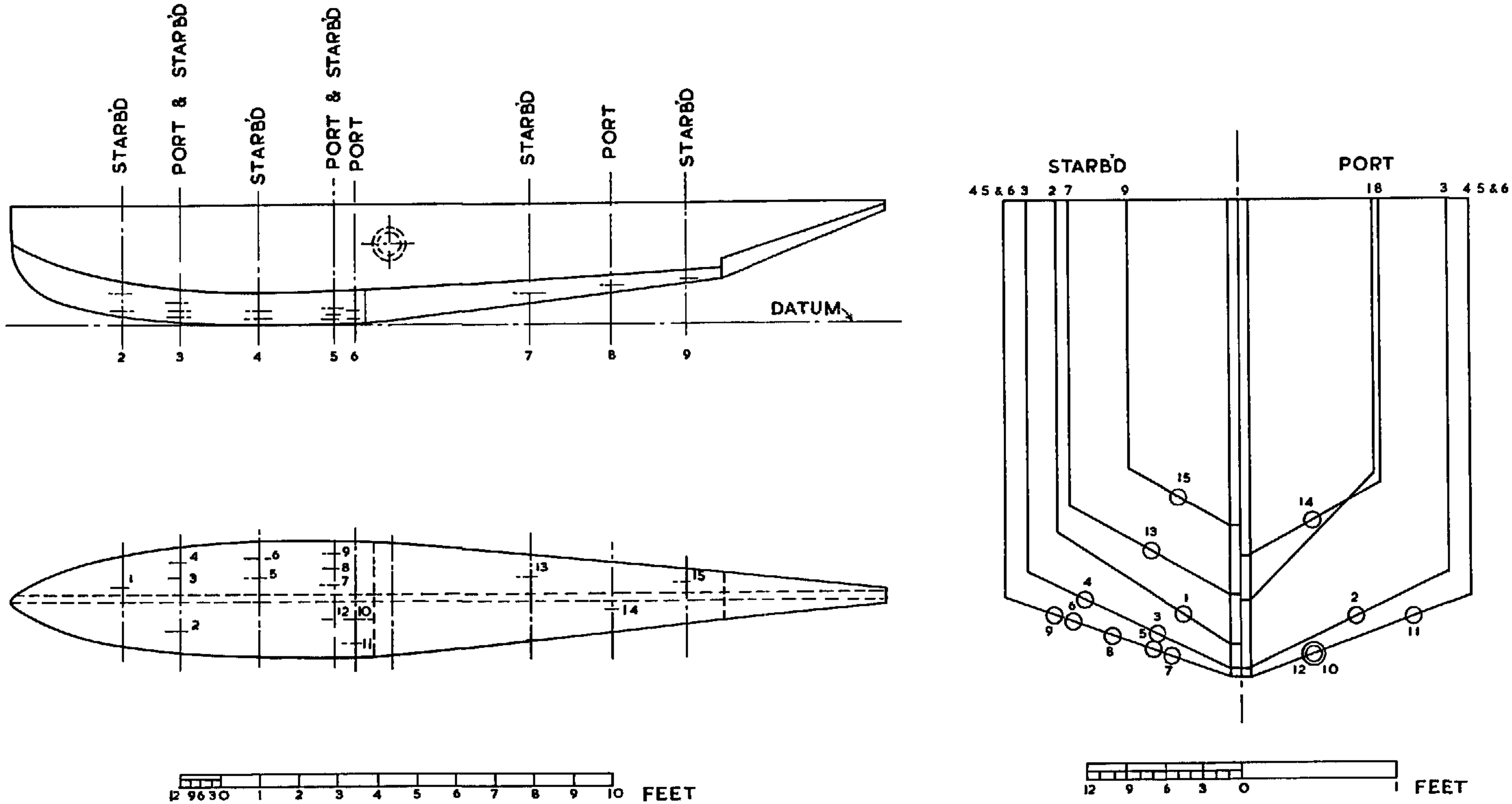

DEADRISE ANGLE AT STEP 20°

Hull Lines and Positions of Fitted Pressure Recorders

FIG 2

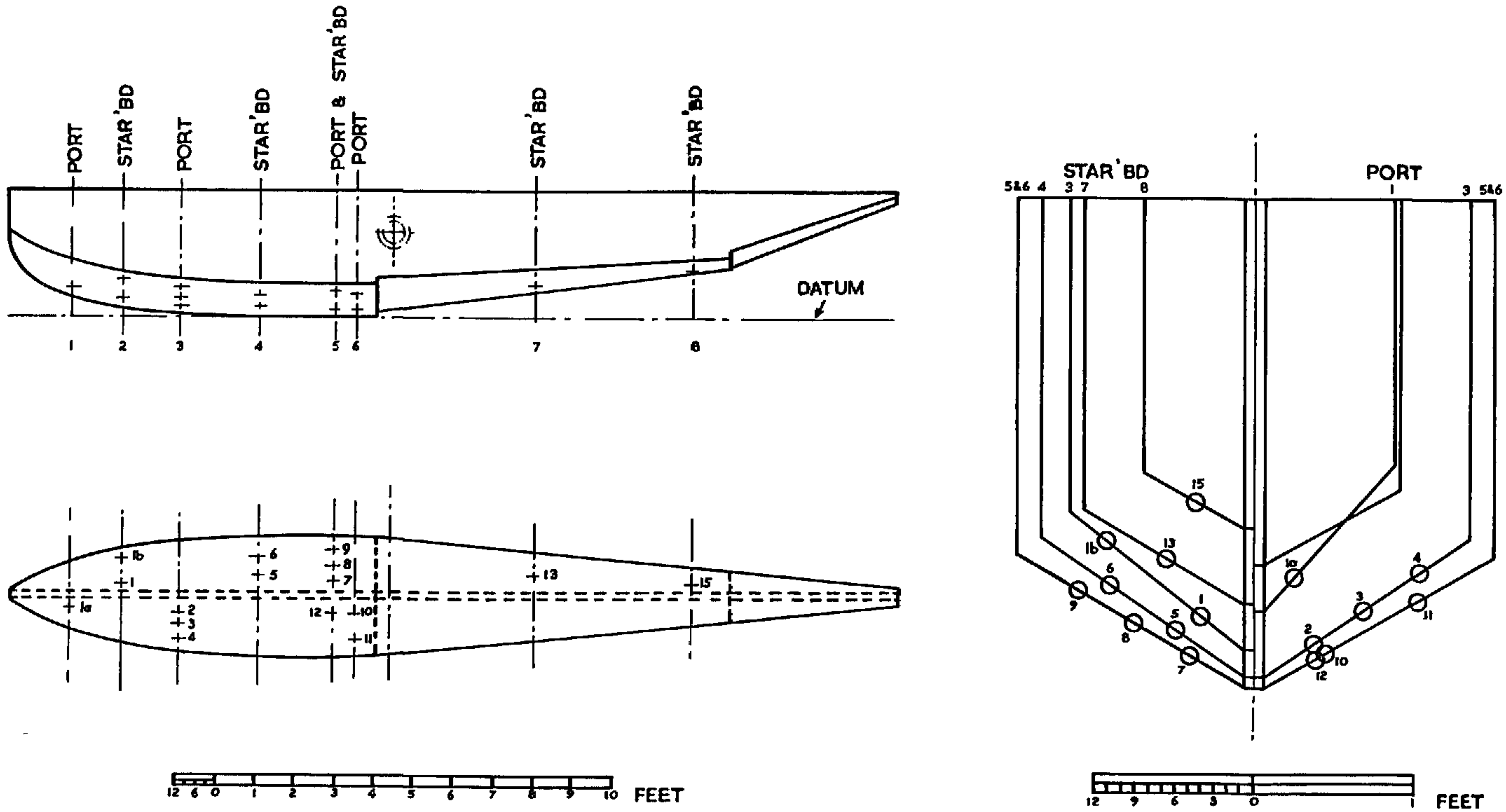

DEADRISE ANGLE AT STEP 30°

Hull Lines and Positions of Fitted Pressure Recorders

FIG 3

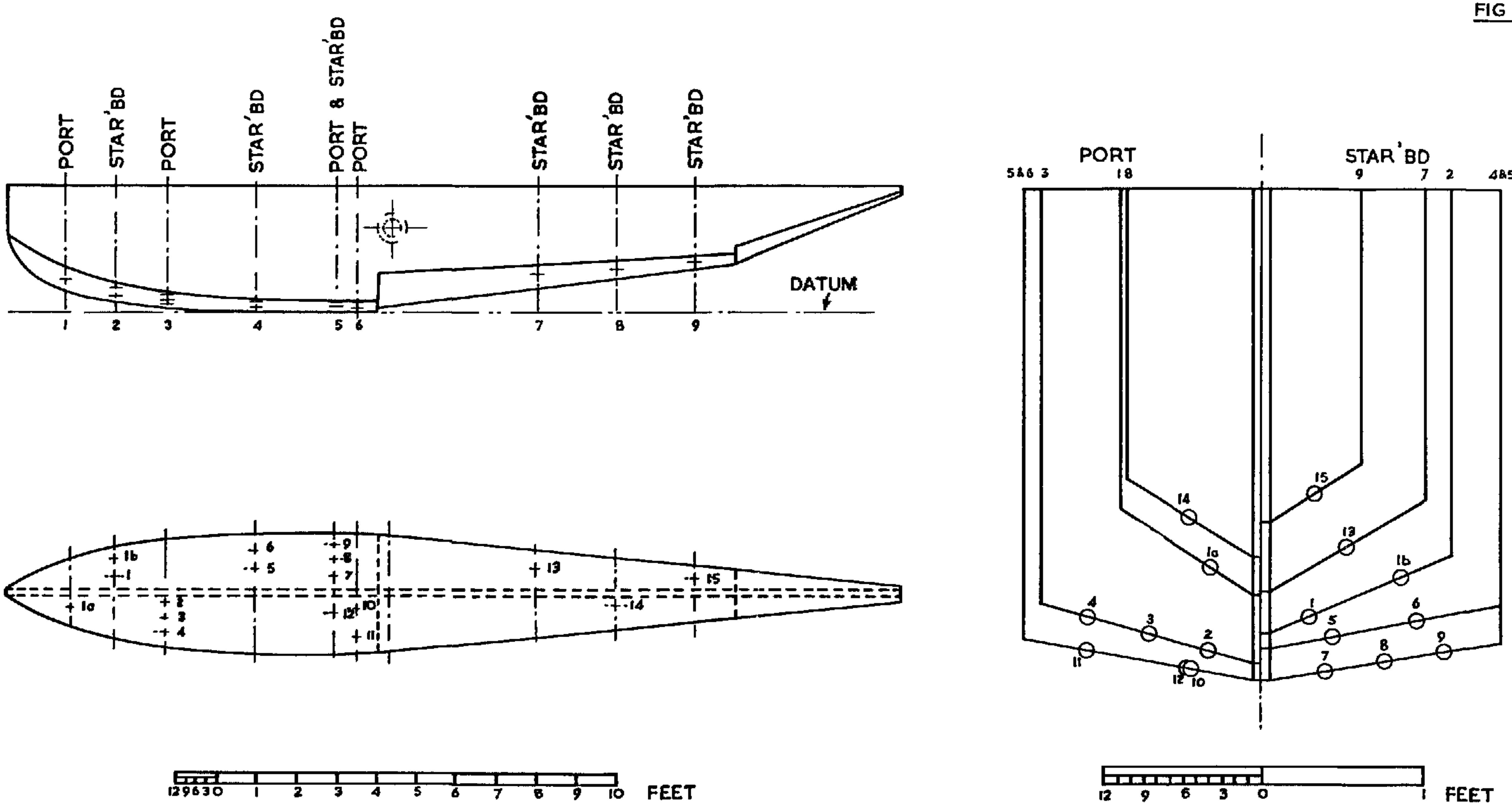

DEADRISE ANGLE AT STEP 10°

Hull Lines and Positions of Fitted Pressure Recorders

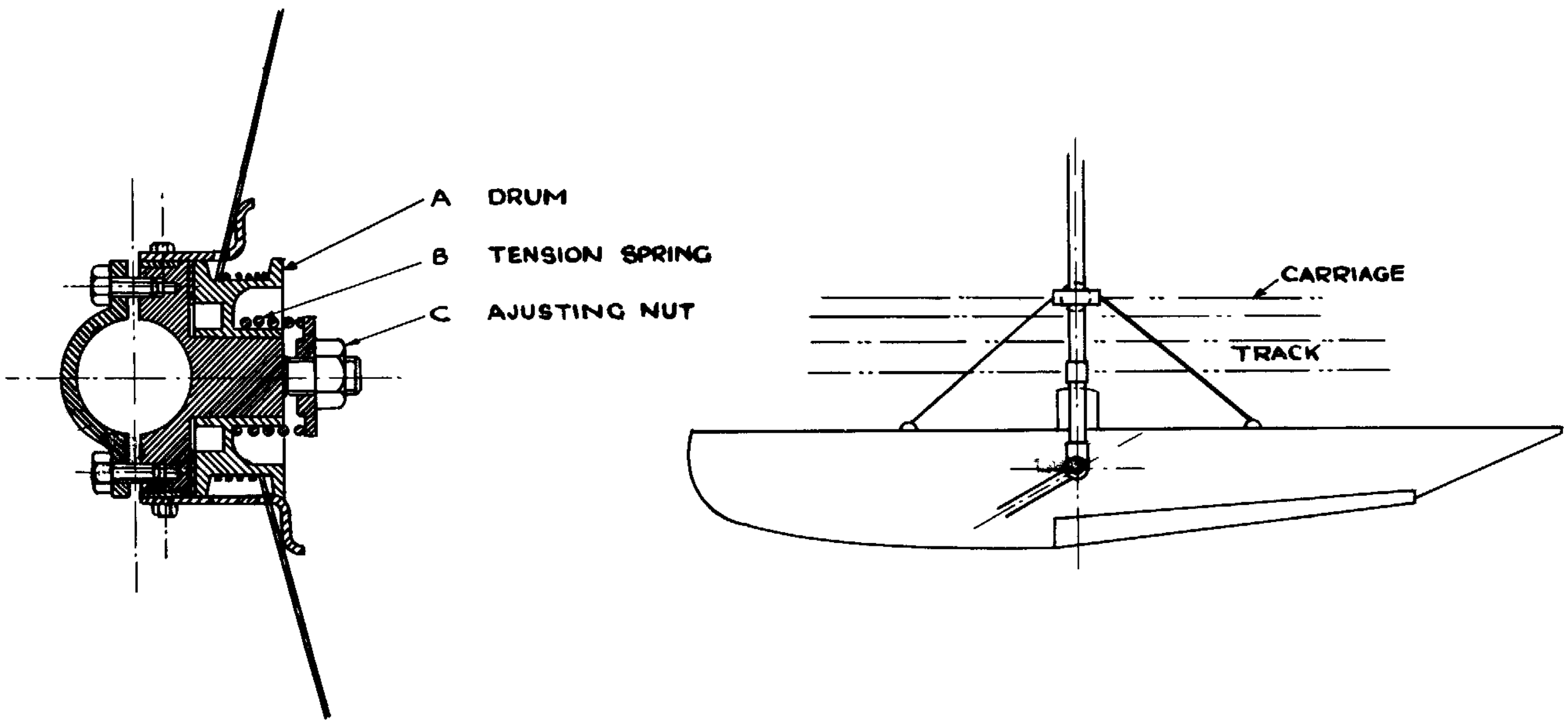

GENERAL ARRANGEMENT OF DAMPER

FIG.4

FIG.5

ACCELERATION DUE TO GRAVITY = 2·1 FT/SEC²							
DIAPHRAGM	$P_{MAX.}$	INITIAL CONDITIONS			LOCAL IMPACT CONDITIONS		
		V_H	V_V	α	V_H	V_V	α
1							
2							
3							
4							
5	3·43	37·0	4·40	5·62	36·3	3·08	6·06
6	1·72	36·9	4·38	5·62	36·0	0·37	6·86
7	5·07	37·0	4·83	5·62	36·9	4·50	5·56
8	4·27	37·0	4·82	5·62	37·0	3·73	5·90
9	4 06	37·0	4·82	5·62	36·2	3·32	6·09
10	4·33	37·0	4·87	5·62	36·8	3·89	6·02
11	4·60	37·0	4·90	5·62	36·5	5·00	5·44
12	2·86	37·0	4·83	5·62	36·9	4·50	5·53
13	1·13	37·0	5·96	−0·38	36·2	2·46	0·20
14	0·98	37·0	6·46	−0·38	36·1	3·65	−0·46
15	1·58	37·0	6·93	−0·38	36·2	4·30	0·02

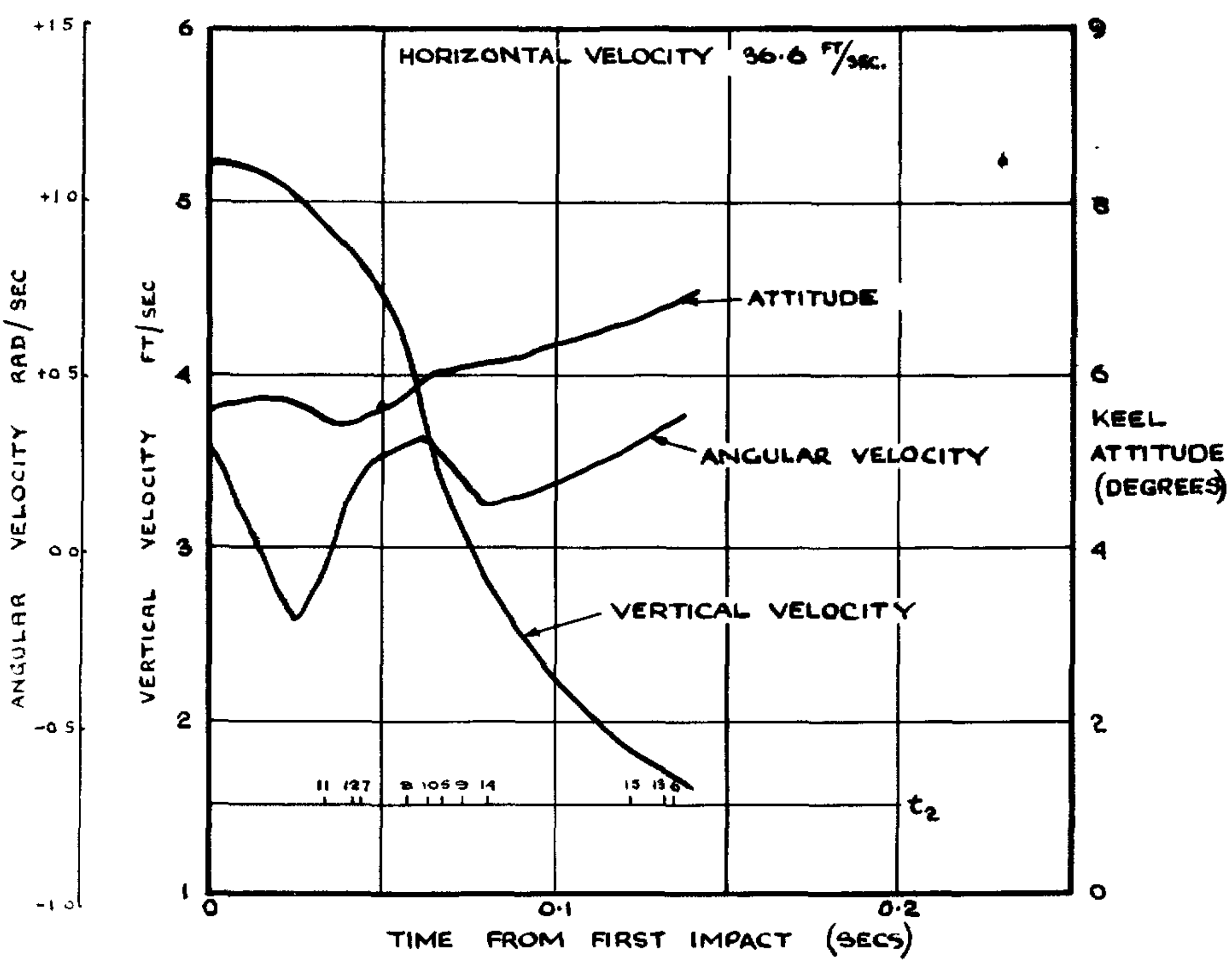

FIG. 6

ACCELERATION DUE TO GRAVITY = 2·1 FT/SEC²							
DIAPHRAGM	P_{MAX}	INITIAL CONDITIONS			LOCAL IMPACT CONDITIONS		
		V_H	V_V	α	V_H	V_V	α
1							
2							
3							
4							
5							
6							
7	2·81	38·8	2·35	2·65	35·8	4·78	3·65
8	2·56	38·6	2·29	2·65	37·3	3·09	4·32
9	2·80	38·5	2·28	2·65	36·3	2·69	4·54
10	3·62	38·1	2·23	2·65	36·5	3·33	4·41
11	3·47	38·7	2·72	2·65	35·7	4·78	3·44
12	1·90	38·8	2·35	2·65	35·7	4·92	3·45
13	1·10	38·4	8·35	− 3·95	37·1	4·7	− 1·74
14	0·99	38·3	10·96	− 3·95	37·2	6·31	− 1·47
15	2·06	38·2	13·47	− 3·95	37·8	5·98	− 1·85

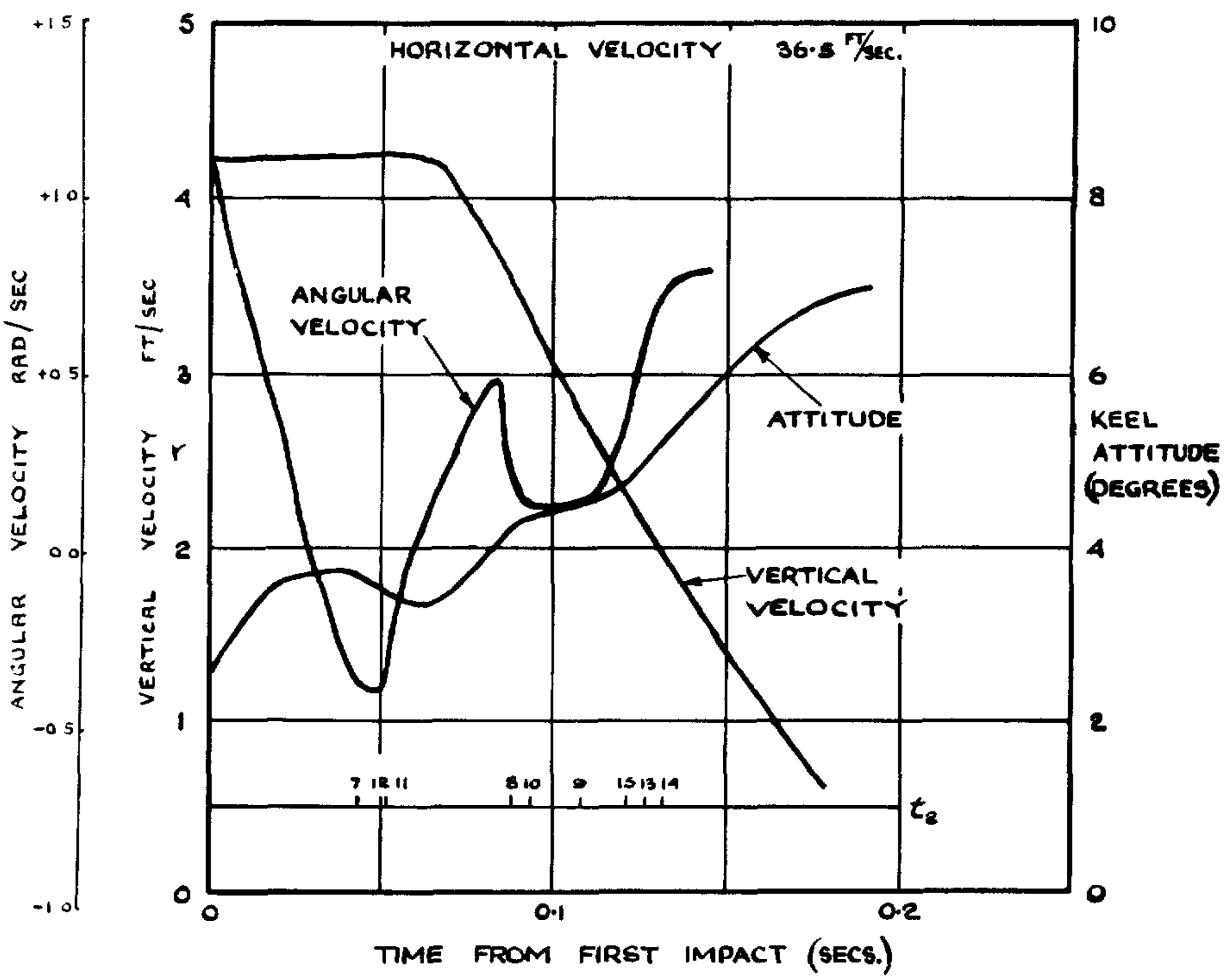

FIG. 7

ACCELERATION DUE TO GRAVITY = 2·1 FT/SEC²							
DIAPHRAGM	$P_{MAX.}$	INITIAL CONDITIONS			LOCAL IMPACT CONDITIONS		
		V_H	V_V	α	V_H	V_V	α
1							
2							
3							
4							
5	3·8	35·2	8·1	2·25	35·5	7·01	1·53
6	3·86	35·3	8·14	2·25	36·0	5·63	1·46
7							
8	4·44	35·2	7·18	2·25	35·3	5·85	1·50
9	3·36	35·3	7·18	2·25	35·7	5·10	1·46
10	4·34	35·2	6·93	2·25	35·6	6·25	1·46
11	3·53	35·2	7·00	2·25	35·7	6·93	1·95
12	2·70	35·2	7·16	2·25	35·6	7·05	2·04
13	1·82	35·4	5·69	− 4·35	36·0	3·73	0·05
14	1·60	35·4	3·62	− 4·35	35·8	4·54	0·25
15	2·0	35·5	2·59	− 4·35	35·8	5·96	0·36

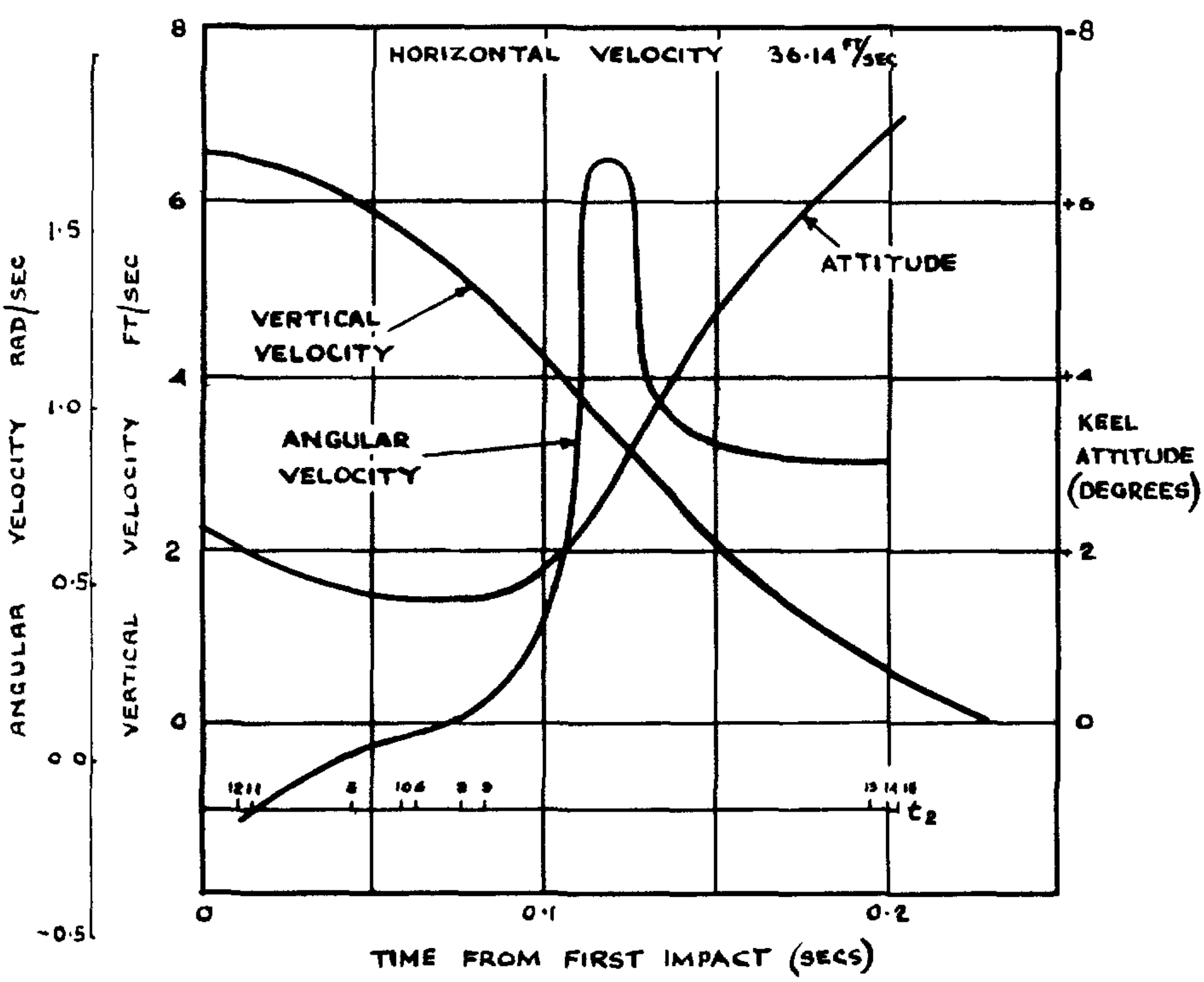

FIG. 8

ACCELERATION DUE TO GRAVITY = 2·1 FT/SEC²

DIAPHRAGM	P_{MAX}	INITIAL CONDITIONS			LOCAL IMPACT CONDITION		
		V_H	V_V	α	V_H	V_V	α
1							
2							
3							
4							
5	4·06	35·793	5·988	8·26	35·57	2·65	7·30
6	0·44	35·859	5·995	8·26	35·59	0·08	7·48
7	5·56	35·759	5·627	8·26	35·26	4·56	7·86
8	6·14	35·790	5·634	8·26	35·11	4·47	7·48
9	5·80	35·912	5·632	8·26	35·12	4·11	7·20
10	5·14	35·78	5 538	8·26	35·38	4·13	7·52
11	6·14	35·770	5·567	8·26	35·55	4·62	8·03
12	3·72	35·759	5·627	8 26	35·20	4·47	7·77
13	0·48	35·735	4·680	1·66	35·06	2·83	7·47
14	1·03	35·707	4·268	1·66	35·49	3·53	8·20
15	1·96	35·684	3·870	1·66	26·20	5·69	8·63

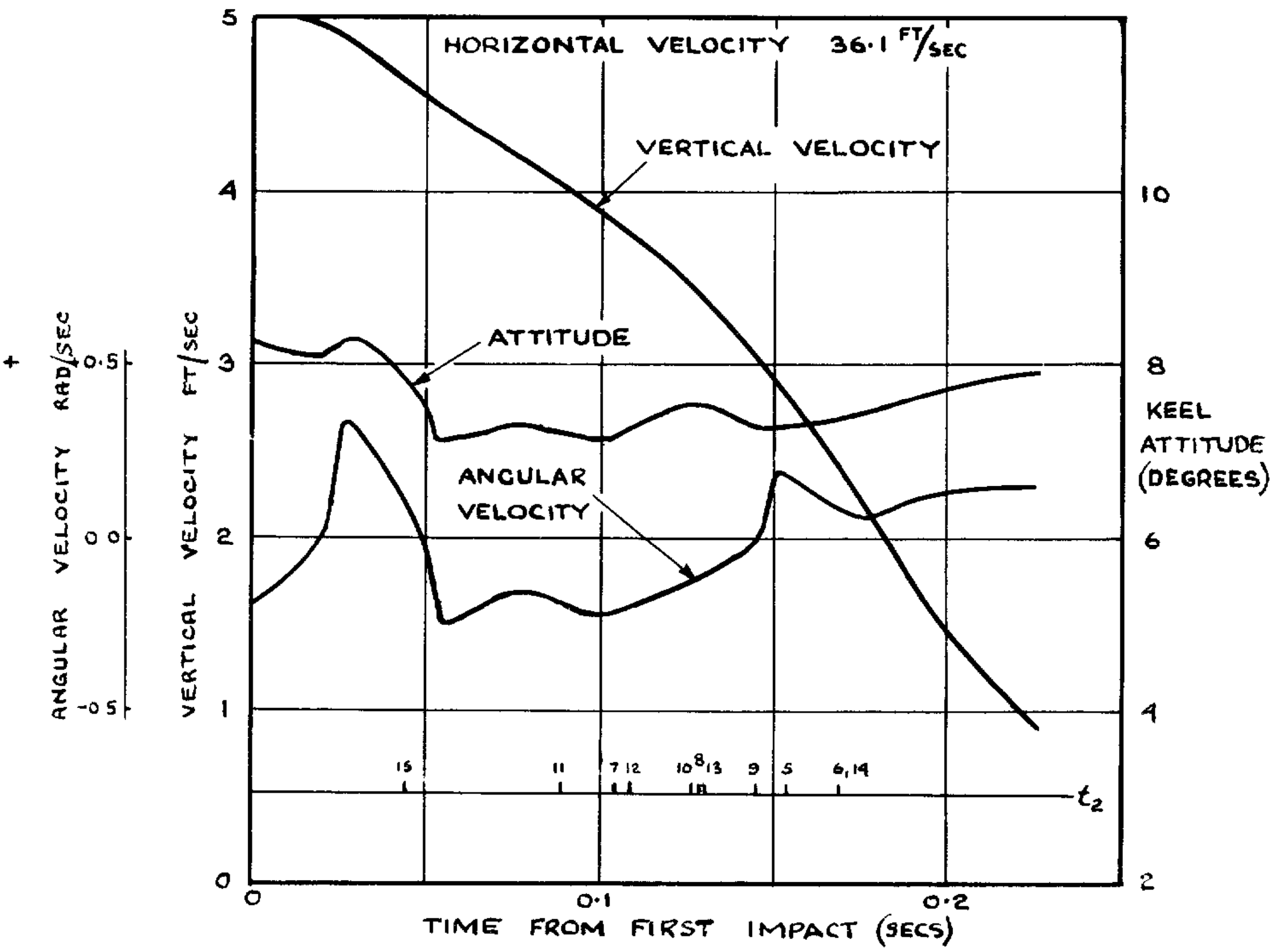

FIG.9

ACCELERATION DUE TO GRAVITY = 2·1 FT/SEC²							
DIAPHRAGM	$P_{MAX.}$	INITIAL CONDITIONS			LOCAL IMPACT CONDITIONS		
		V_H	V_V	α	V_H	V_V	α
1							
2							
3							
4							
5							
6	2·2	35·8	5·37	11·95	35·3	1·23	7·23
7	6·0	35·7	5·18	11·95	35·1	6·55	10·85
8	4·83	35·7	5·18	11·95	34·8	4·27	7·58
9	4·61	35·8	5·18	11·95	34·9	4·27	7·43
10	4·65	35·7	5·14	11·95	34·8	4·08	7·53
11	6·5	35·7	5·15	11·95	34·4	4·38	7·71
12	3·95	35·7	5·18	11·95	35·0	4·39	7·86
13	0·40	35·7	4·69	5·35	34·7	2·24	0·75
14	0·50	35·7	4·48	5·35	35·1	3·07	3·43
15	1·10	35·6	4·27	5·35	35·5	3·86	5·15

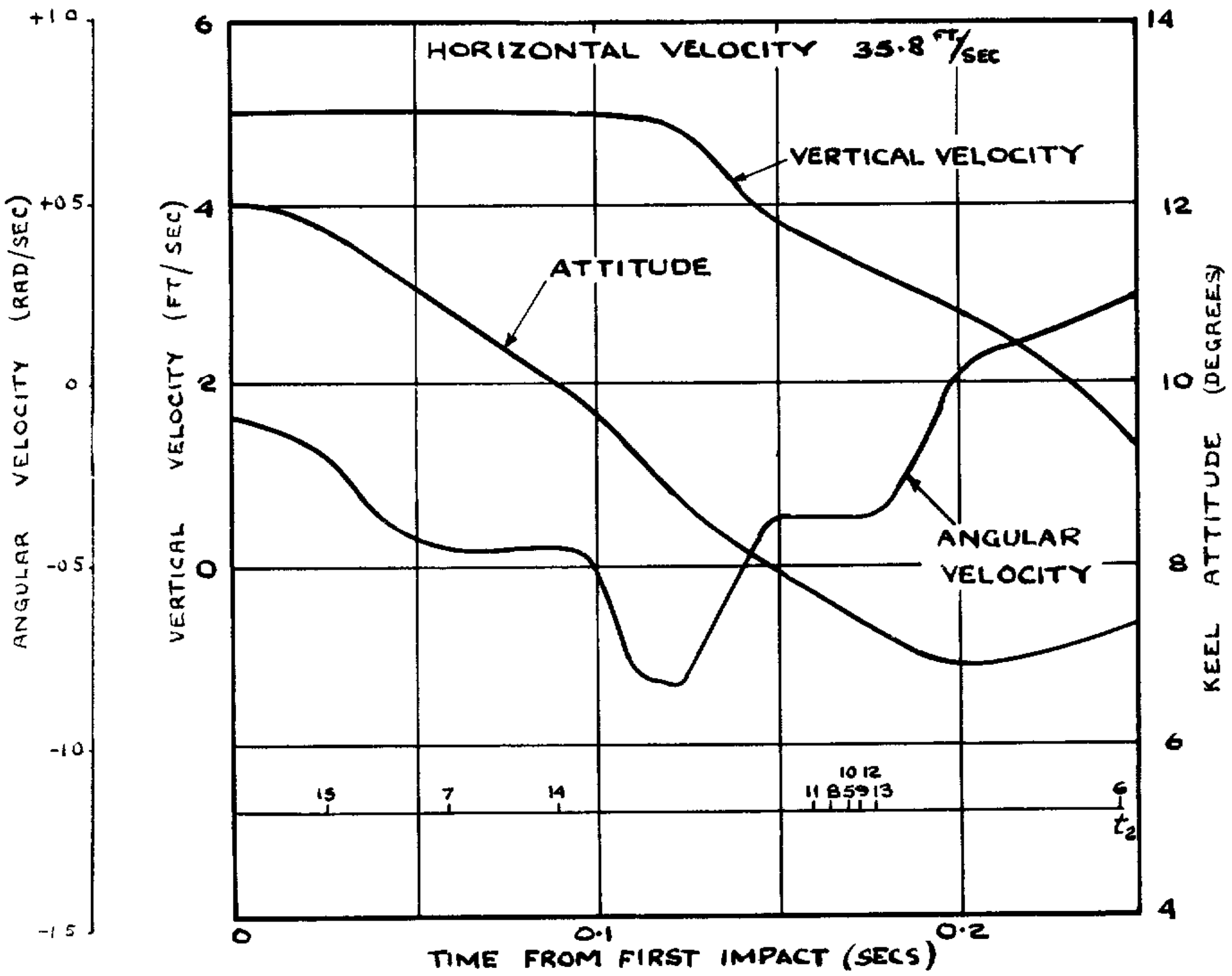

FIG.10

ACCELERATION DUE TO GRAVITY = 2·1 FT/SEC.²							
DIAPHRAGM	$P_{MAX.}$	INITIAL CONDITIONS			LOCAL IMPACT CONDITIONS		
		V_H	V_V	α	V_H	V_V	α
1	2·05	31·692	4·08	8·25	30·829	1·94	8·00
2	1·40	31·754	4·44	2·15	28·775	6·796	2·14
3							
4	1·36	31·744	4·44	2·15	31·106	3·284	2·35
5	1·70	31·830	5·01	− 2·05	30·69	4·643	− 2·23
6	1·30	31·746	4·786	− 2·05	30·88	3·200	− 2·60
7	1·50	31·789	5·496	− 2·05	30·754	4·673	− 2·55
8	1·26	31·751	5·470	− 2·05	30·917	4·230	− 2·45
9	1·30	31·722	5·467	− 2·05	32·026	2·335	0·20
10							
11							
12							
13	1·85	31·598	6·720	− 6·65	31·296	5·504	− 3·00
14	1·65	31·536	7·260	− 6·65	31·745	10·06	− 4·50
15	1·66	31·542	7·780	− 6·65	31·227	8·93	− 2·70

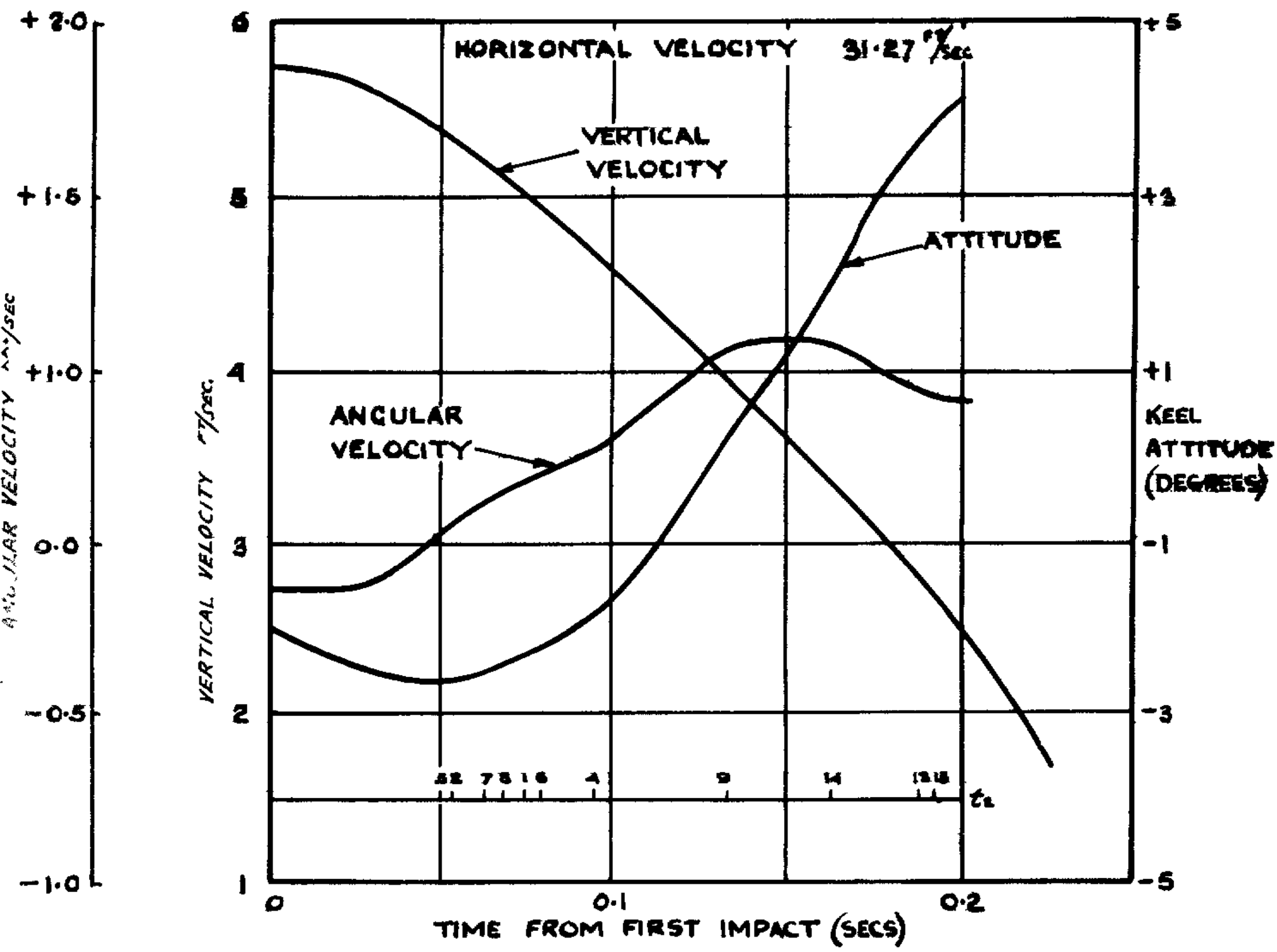

FIG. 11

ACCELERATION DUE TO GRAVITY = 2·1 FT/SEC²							
DIAPHRAGM	$P_{MAX.}$	INITIAL CONDITONS			LOCAL IMPACT CONDITION		
		V_H	V_V	α	V_H	V_V	α
1							
2							
3							
4	0·74	25·40	5·10	13·45	24·2	0·12	11·65
5	3·41	25·50	5·43	9·25	24·0	2·74	7·35
6	2·10	25·50	5·41	9·25	23·7	1·40	7·25
7	4·66	25·60	5·73	9·25	24·3	4·94	8·40
8	4·51	25·50	5·72	9·25	24·10	4·47	8·17
9	3·60	25·50	5·73	9·25	23·90	3·37	7·53
10	3·85	25·60	5·80	9·25	24·10	4·26	8·10
11	4·74	25·60	5·77	9·25	24·30	4·98	8·48
12	3·14	25·60	5·72	9·25	24·60	4·55	8·22
13							
14	0·75	25·60	6·84	2·65	24·80	3·20	2·74
15	1·34	25·70	7·16	2·65	25·30	6·03	2·82

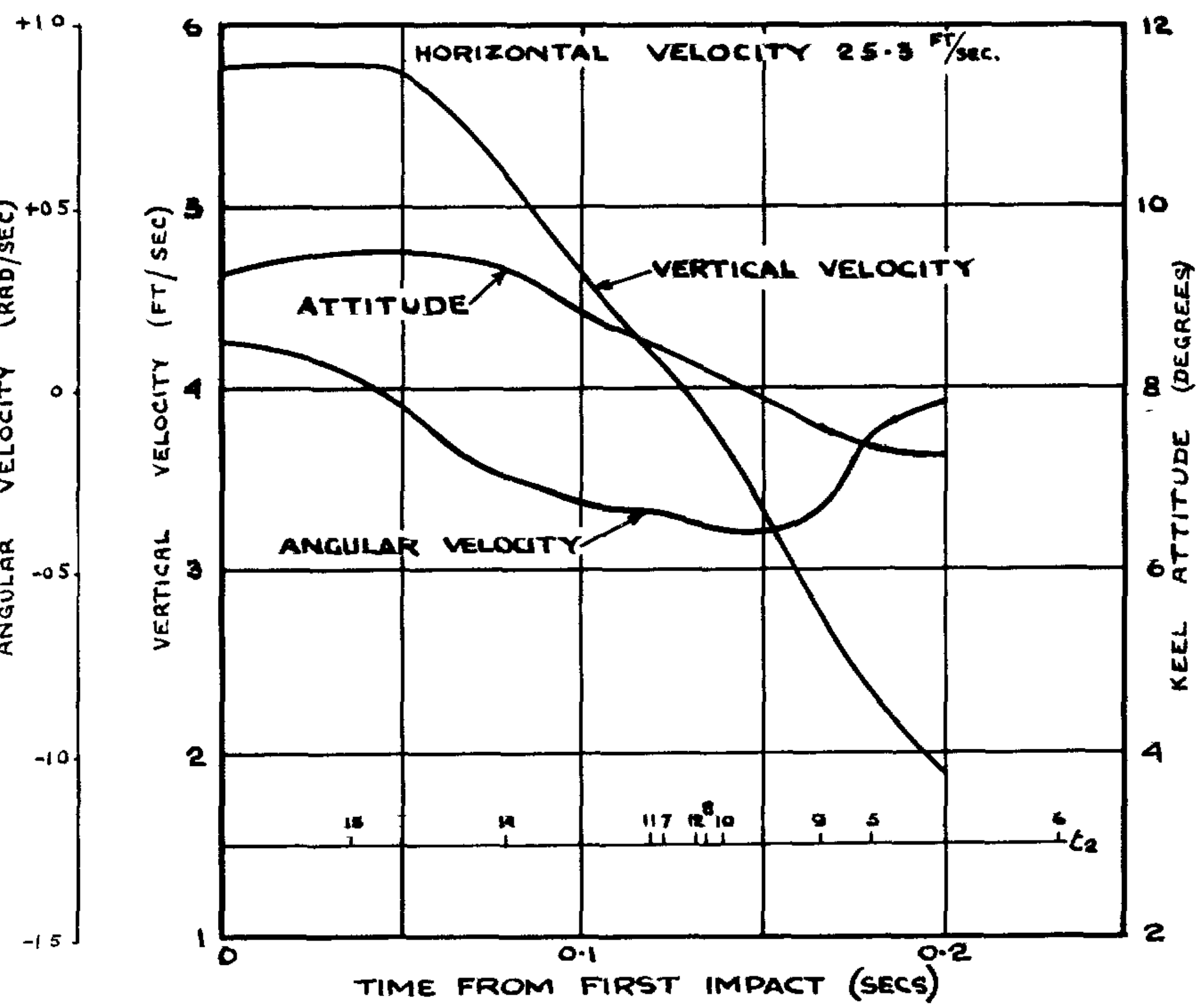

FIG. 12

ACCELERATION DUE TO GRAVITY = 2·1 FT/SEC²							
DIAPHRAGM	P_{MAX}	INITIAL CONDITIONS			LOCAL IMPACT CONDITIONS		
		V_H	V_V	α	V_H	V_V	α
1							
2							
3	1·82	25·21	5 667	3·50	25·51	3·51	7·94
4	0·84	25·21	5·667	3·50	26·08	0·00	5·12
5	1·70	25·21	5·667	– 0·70	25·60	3·604	0·36
6	1·26	25·21	5·667	– 0·70	26·22	0·43	2·46
7	2·10	25·21	5·667	– 0·70	25·41	5·051	– 0·34
8	1·93	25·21	5·667	– 0·70	25·64	4·25	– 0·14
9	1·92	25·21	5·667	–0·70	25 90	3·840	0·42
10	2·06	25·21	5·667	–0·70	25·75	4·363	0·19
11	2·00	25·21	5·667	–0·70	25·30	5·170	– 0·37
12	1·23	25·21	5·667	–0·70	25·54	4·615	–0·25
13	1·84	25·21	5·667	– 7·30	25·75	5·554	– 1·90
14	1·42	25·21	5·667	– 7·30	26·20	8·900	– 3·10
15	1·68	25·21	5·667	– 7·30	25·92	9·940	– 2·22

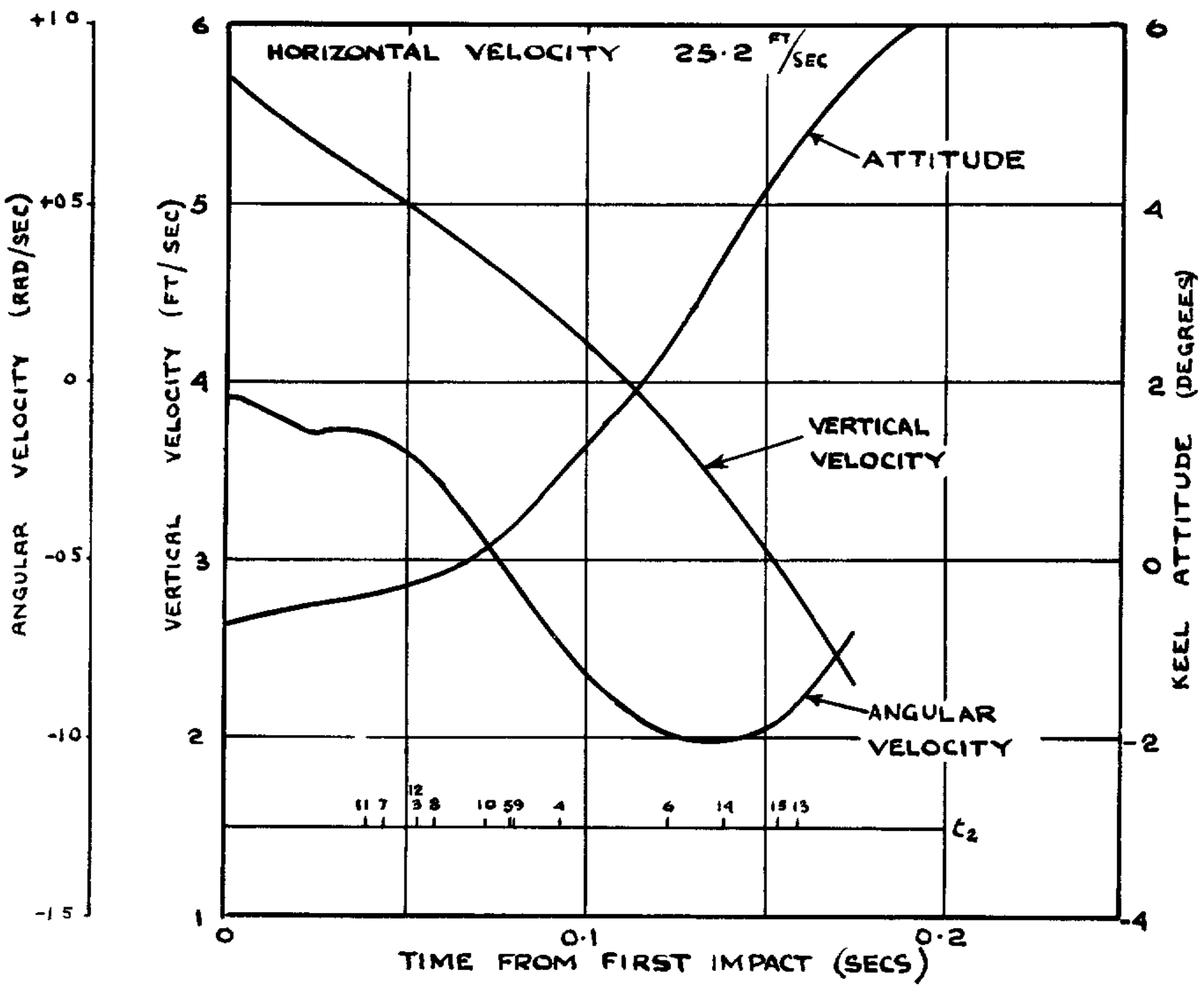

FIG. 13

ACCELERATION DUE TO GRAVITY = 2·1 FT/SEC²							
DIAPHRAGM	$P_{MAX.}$	INITIAL CONDITIONS			LOCAL IMPACT CONDITION		
		V_H	V_V	α	V_H	V_V	α
1	1·40	25·20	4·92	4·30	25·60	3·74	4·60
2	0·80	25·20	4·92	−1·80	25·70	3·88	−1·50
3	0·85	25·20	4·92	−1·80	25·70	4·02	−1·75
4	1·10	25·20	4·92	−1·80	25·60	3·87	−1·40
5	0·50	25·20	4·92	−6·00	26·00	3·94	−5·50
6							
7	1·20	25·20	4·92	−6·00	27·00	3·90	−4·40
8	0·80	25·20	4·92	−6·00	26·80	3·87	−4·10
9	0·60	25·20	4·92	−6·00	26·30	4·14	−1·60
10	1·30	25·20	4·92	−6·00	26·80	4·30	−4·50
11	1·35	25·20	4·92	−6·00	26·90	4·18	−4·30
12	0·55	26·20	4·92	−6·00	27·00	3·94	−4·70
13	1·70	25·20	4·92	−12·60	26·80	6·47	−5·30
14	1·53	25·20	4·92	−12·60	25·20	5·98	−3·00
15	1·95	25·20	4·92	−12·60	26·20	8·92	−0·45

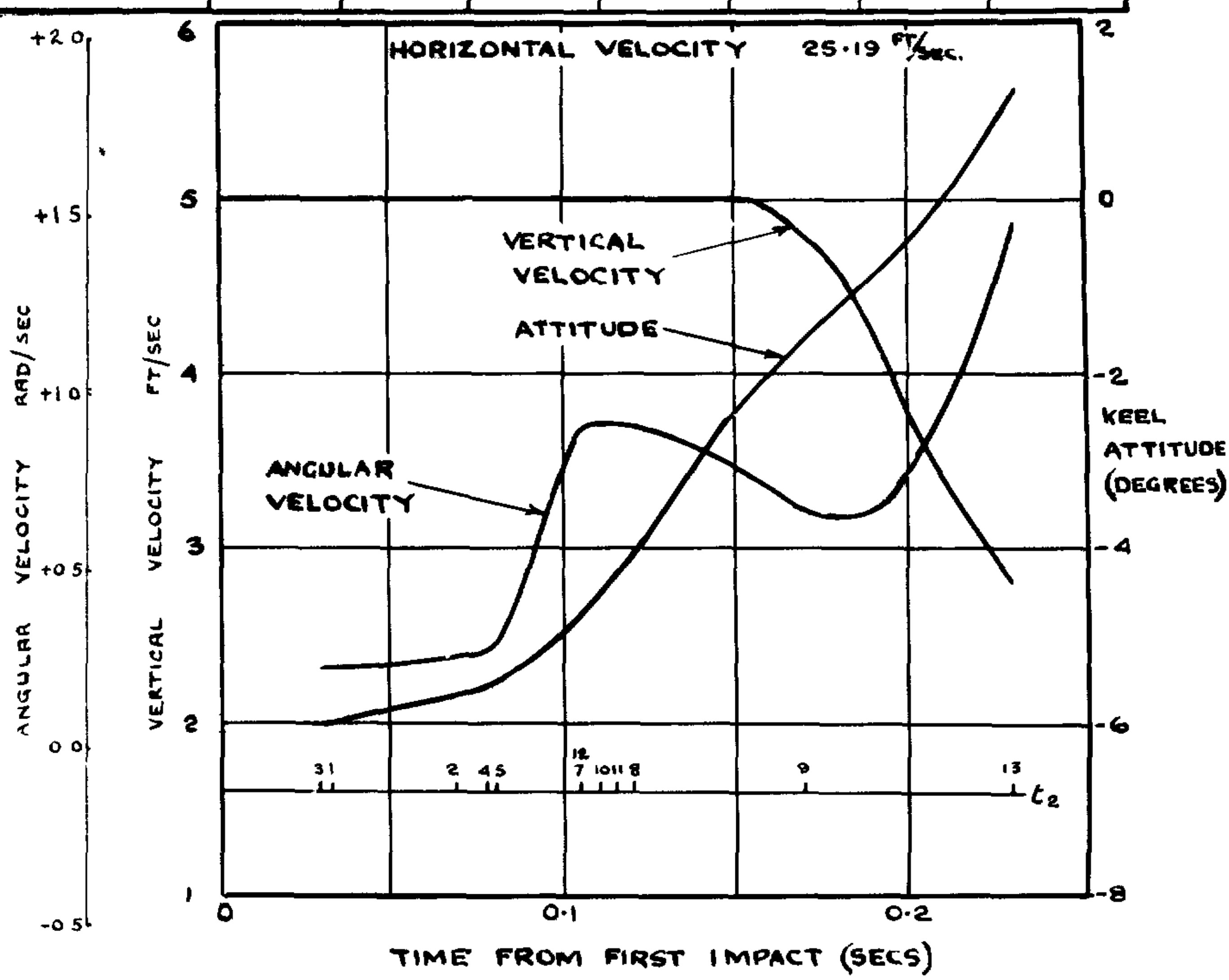

FIG.14

ACCELERATION DUE TO GRAVITY = 2·1 FT/SEC²							
DIAPHRAGM	$P_{MAX.}$	INITIAL CONDITIONS			LOCAL IMPACT CONDITIONS		
		V_H	V_V	α	V_H	V_V	α
1							
2							
3							
4	0·90	25·270	4·717	9·046	24·37	−0·35	10·73
5	2·50	25·30	4·826	4·845	25·24	2·52	5·80
6	2·06	25·283	4·823	4·845	25·06	2·20	6·26
7	3·30	25·304	4·92	4·845	25·21	4·04	5·23
8	3·80	25·296	4·919	4·845	25·12	3·60	5·29
9	3·12	25·290	4·918	4·845	25·18	2·80	5·88
10	3·95	25·297	4·943	4·845	25·20	4·10	5·26
11	3·85	25·300	4·925	4·845	25·41	4·76	5·11
12	2·18	25·304	4·920	4·845	25·21	4·04	5·21
13							
14	0·88	25·296	5·274	−1·755	25·26	5·03	−0·80
15	1·20	25·296	5·377	−1·785	25·27	5·61	−0·76

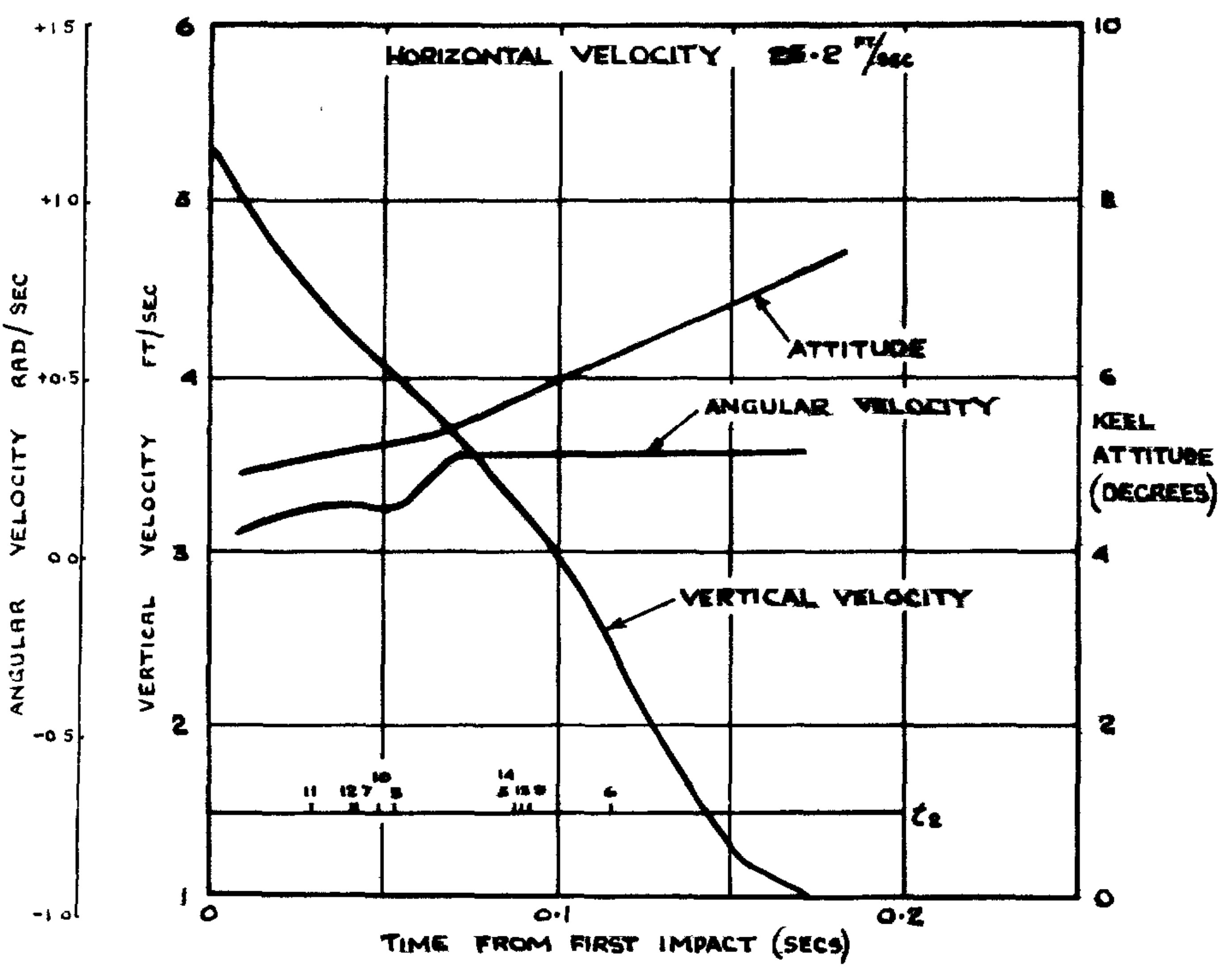

FIG. 15

ACCELERATION DUE TO GRAVITY = 2·1 FT/SEC²							
DIAPHRAGM	$P_{MAX.}$	INITIAL CONDITIONS			LOCAL IMPACT CONDITIONS		
		V_H	V_V	α	V_H	V_V	α
1							
2	0·70	0·60	7·71	6·05	1·42	2·69	8·70
3	1·29	0·57	7·72	6·05	2·23	3·43	6·29
4	0·52	0·61	7·75	6·05	1·37	2·81	8·65
5	2·10	0·50	7·20	1·85	2·07	5·82	1·70
6	1·70	0·58	7·22	1·85	2·22	4·26	2·10
7	3·80	0·51	7·75	1·85	1·76	6·25	1·71
8	2·73	0·55	6·76	1·85	2·29	5·18	1·86
9	2·20	0·57	6·77	1·85	2·64	4·87	2·07
10	2·80	0·55	6·65	1·85	2·35	5·30	1·90
11	2·68	0·53	6·85	1·85	1·76	6·23	1·70
12	1·68	0·51	6·75	1·85	1·76	6·25	1·73
13	1·93	0·57	5·61	−4·75	2·70	7·45	−3·00
14	1·675	0·57	5·11	−4·75	2·37	7·89	−2·60
16	1·57	0·57	4·62	−4·75	2·08	8·06	−2·20

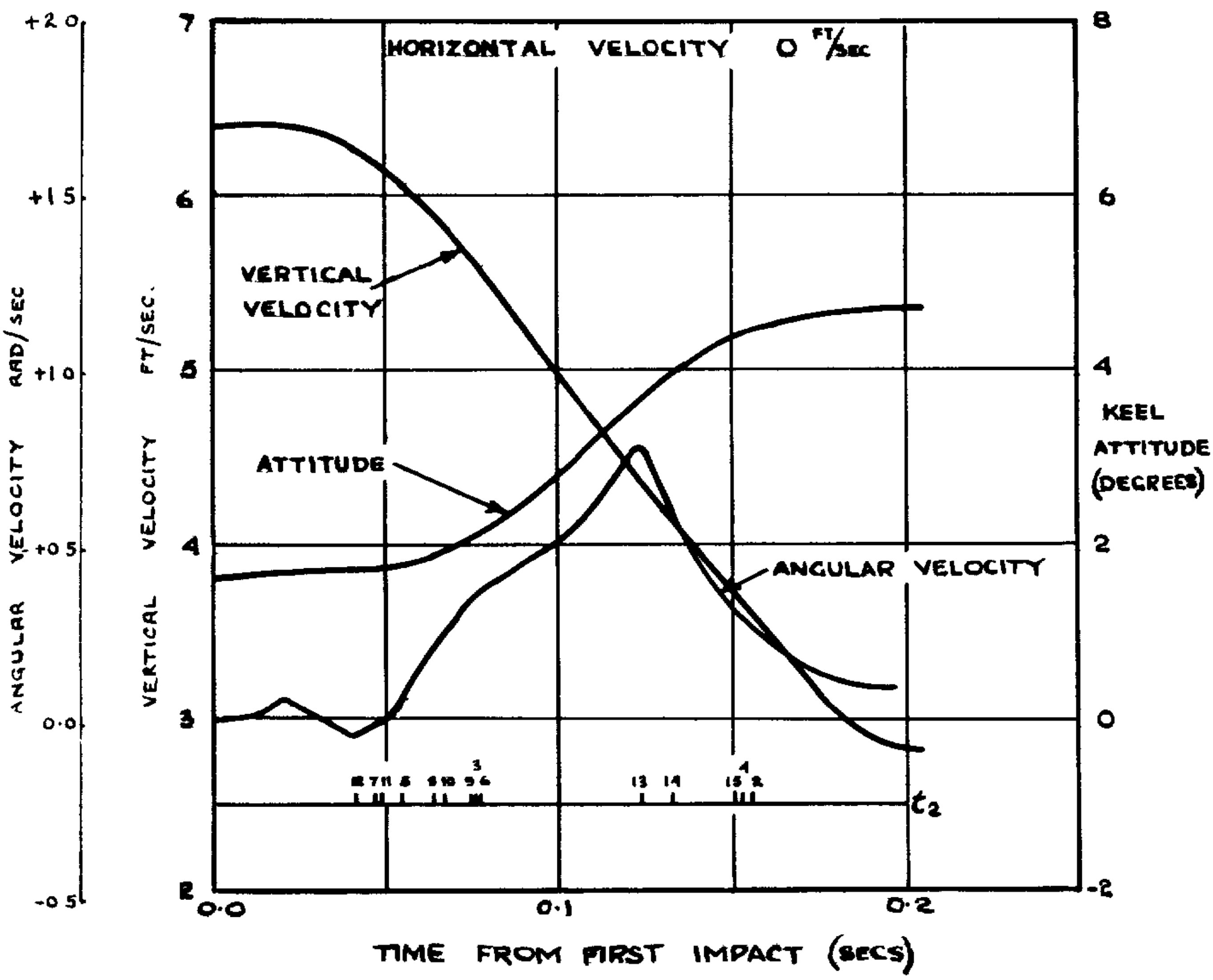

FIG. 16

ACCELERATION DUE TO GRAVITY = 2·1 FT/SEC²							
DIAPHRAGM	P_{MAX}	INITIAL CONDITIONS			LOCAL IMPACT CONDITIONS		
		V_H	V_V	α	V_H	V_V	α
1							
2							
3	1·5	1·55	5·365	10·84	1·018	3·382	9·97
4	0·92	1·554	5·365	10·84	0·713	2·457	9·87
5	2·55	1·537	5·310	6·64	1·179	5·350	6·30
6	1·80	1·546	5·309	6·64	1·038	4·896	6·08
7	3·20	1·534	5·261	6·64	1·227	5·210	6·45
8	3·50	1·538	5·262	6·64	1·292	5·202	6·43
9	2·75	1·541	5·262	6·64	1·205	5·063	6·25
10	3·50	1·538	5·251	6·64	1·190	4·879	6·37
11	3·45	1·536	5·253	6·64	1·415	5·413	6·50
12	3·66	1·534	5·261	6·64	1·467	5·397	6·55
13	0·96	1·535	5·138	0·04	1·179	4·279	− 0·22
14	0·90	1·533	5·085	0·04	1·158	3·945	− 0·32
15	0·87	1·531	5·032	0·04	1·695	4·341	− 0·35

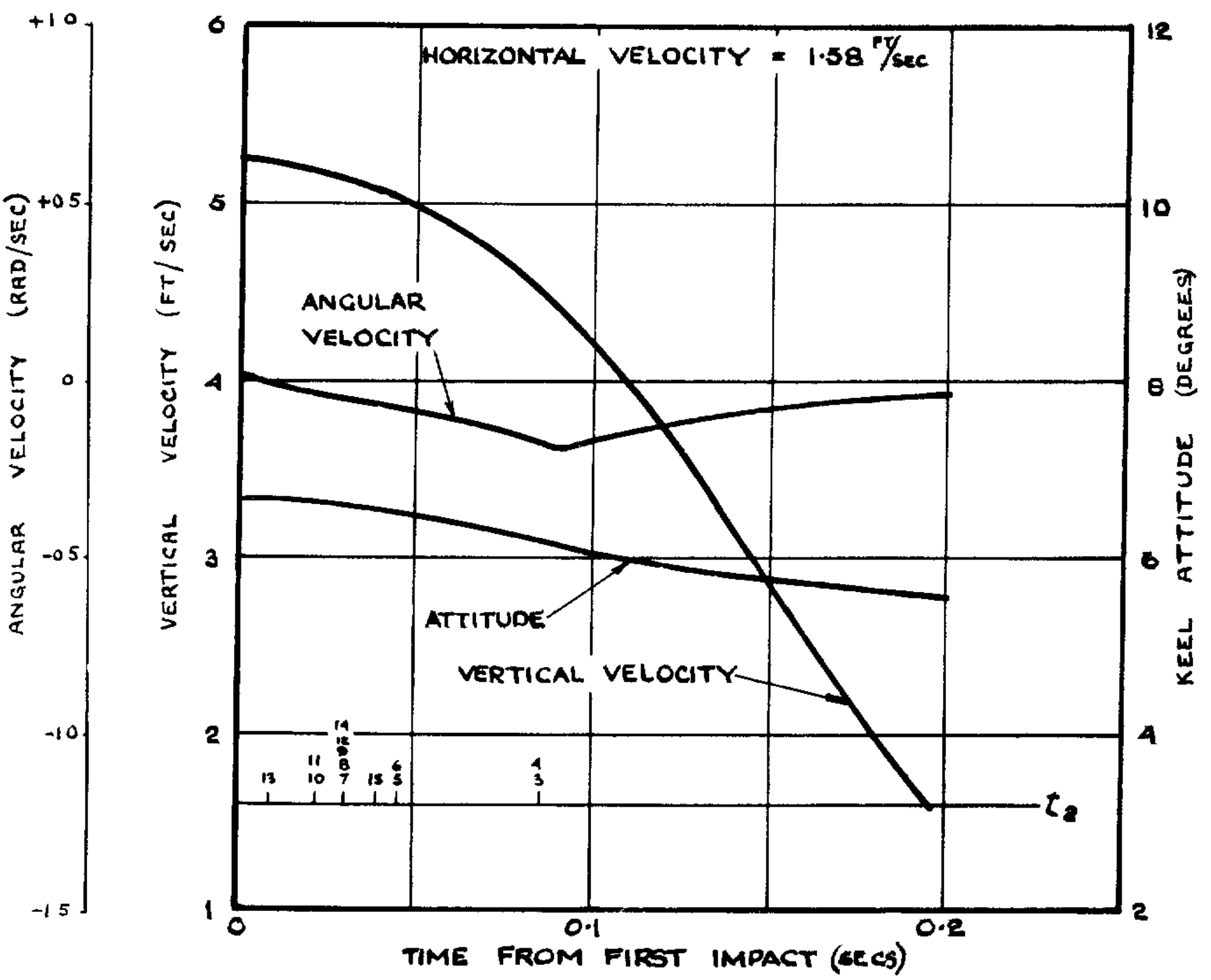

FIG.17

ACCELERATION DUE TO GRAVITY = 2·1 FT/SEC²							
DIAPHRAGM	$P_{MAX.}$	INITIAL CONDITIONS			LOCAL IMPACT CONDITIONS		
		V_H	V_V	α	V_H	V_V	α
1	0·30	1·81	6·00	19·45	0·50	2·99	16·30
2	1·05	1·81	6·00	13·35	0·52	3·64	10·65
3	1·59	1·81	6·00	13·35	0·53	4·18	10·90
4	1·02	1·81	6·00	13·35	0·61	4·19	10·85
5	2·55	1·81	6·00	9·15	0·64	4·19	7·37
6	1·90	1·81	6·00	9·15	0·64	4·04	7·25
7	3·20	1·81	6·00	9·15	0·35	4·96	8·45
8	3·10	1·81	6·00	9·15	0 44	4·97	8·10
9	2·50	1·81	6·00	9·15	0·29	4·69	7·60
10	2·90	1·81	6·00	9·15	0·51	4·54	8·60
11	3·25	1·81	6·00	9·15	0·64	4·55	8·60
12	1·70	1·81	6·00	9·15	0·65	4·69	8·80
13	0·96	1·81	6·00	2·55	0·39	5·71	1·90
14	1·10	1·81	6·00	2·55	0·47	6·76	2·80
15	2·06	1·81	6·00	2·55	0·17	7·87	1·60

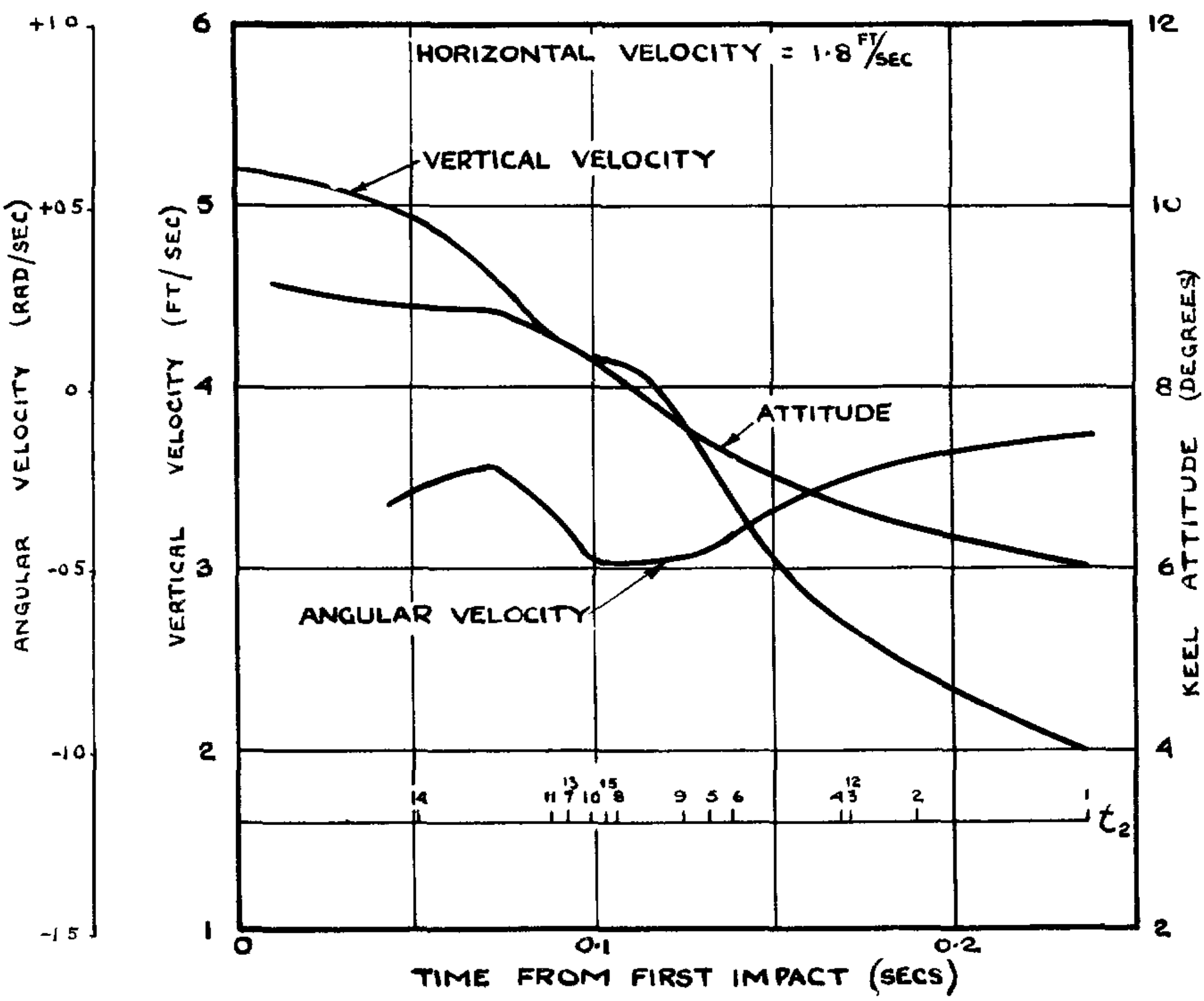

FIG.18

ACCELERATION DUE TO GRAVITY = 2·1 FT/SEC²							
DIAPHRAGM	$P_{MAX.}$	INITIAL CONDITIONS			LOCAL IMPACT CONDITIONS		
		V_H	V_V	α	V_H	V_V	α
1	1·14	1·85	6·13	6 88	2·233	2·168	7·30
2							
3							
4							
5							
6							
7	2·90	1·85	6·13	− 3·42	2·317	4·174	− 3·10
8	2·25	1·85	6·13	− 3·42	2·411	4·386	− 2·77
9							
10	2·20	1·85	6·13	− 3·42	2·910	4·281	− 1·90
11	2·40	1·85	6·13	− 3·42	2·424	4·509	− 2·75
12	1·30	1·85	6·13	− 3·42	2·186	4·552	− 3·24
13							
14	1·42	1·85	6·13	− 10·02	2·085	6·097	− 3·60
15							

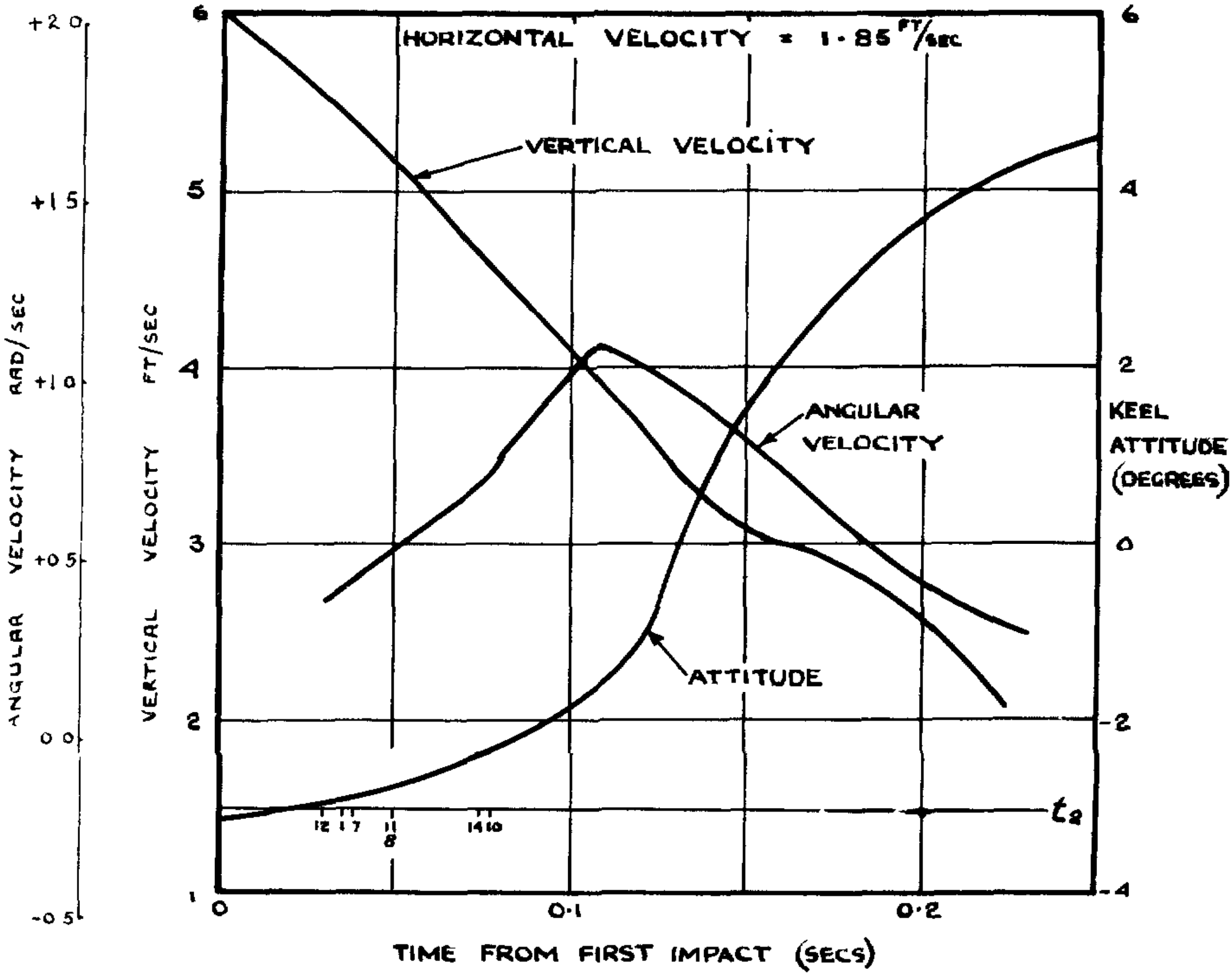

FIG. 19

ACCELERATION DUE TO GRAVITY = ZERO							
DIAPHRAGM	$P_{MAX.}$	INITIAL CONDITIONS			LOCAL IMPACT CONDITIONS		
		V_H	V_V	α	V_H	V_V	α
1	0·30	2·072	6·544	16·8	0·64	3·17	15·89
2	0·80	2·091	6 595	10·70	0·743	4·019	9·99
3	1·06	2·094	6·595	10·70	1·124	3·989	10·11
4	0·77	2·089	6·588	10·70	0·787	3·252	9·86
5	2·43	2·112	6·673	6·50	1·488	6·536	6·29
6	1·60	2·099	6·671	6·50	1·221	4·425	5·93
7	2·91	2·116	6·740	6·50	1·711	5·991	6 38
8							
9	2·67	2 106	6·739	6·50	0 917	5 648	6·31
10	2·48	2·112	6·757	6·50	1·717	5·971	6 38
11	3·72	2·114	6·752	6·50	1·691	6·090	6·42
12	1·63	2·116	6·740	6·50	1·705	6·095	6·41
13	1·07	2·115	6·718	− 0·10	1·710	5·780	− 0·25
14							
15							

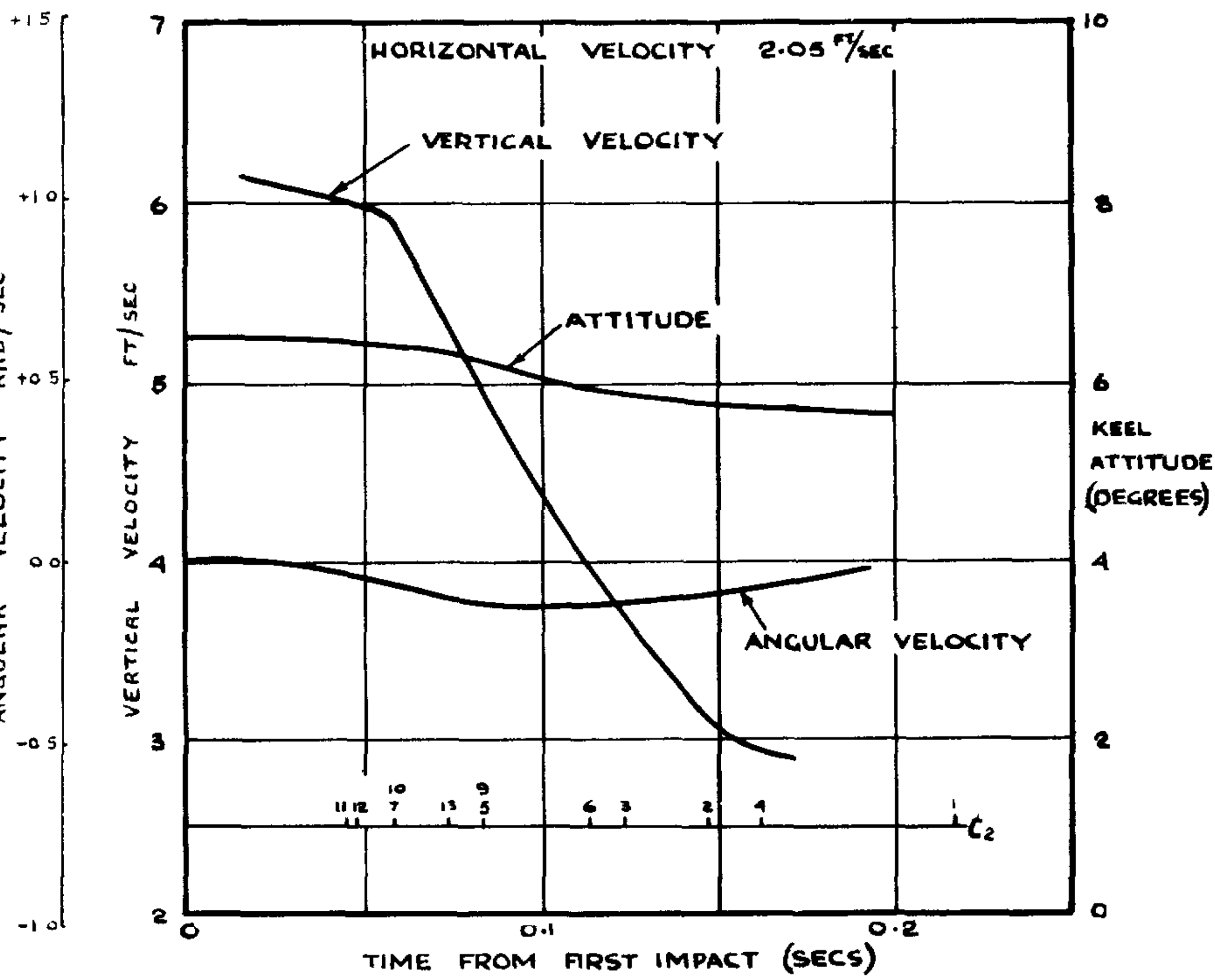

FIG. 20

DIAPHRAGM	$P_{MAX.}$	INITIAL CONDITIONS			LOCAL IMPACT CONDITIONS		
		V_H	V_V	α	V_H	V_V	α
ACCELERATION DUE TO GRAVITY = 4·2 FT/SEC²							
1	0·54	2·314	7·885	16·77	0·47	2·75	15·83
2	1·15	2·301	7·848	10·67	1·06	4·47	9·93
3	1·67	2·298	7·848	10·67	1·16	4·81	9·96
4	1·02	2·303	7·848	10·67	1·00	4·15	9·90
5	3·26	2 286	7·792	6·47	1·11	5·28	6·07
6	4·45	2·294	7 793	6·47	1·09	4·81	5·95
7							
8	4·13	2·287	7·744	6·47	1·78	7·11	6·32
9	3·85	2·290	7·743	6·47	1·45	6·39	6·30
10	3·82	2·285	7·731	6·47	1·16	5·54	6·25
11	4·08	2·284	7·735	6·47	2·27	7·91	6·45
12	2·15	2·282	7·748	6·47	2·24	7·95	6·42
13	1·32	2·283	7·614	– 0·13	1·19	4·50	– 0·36
14	1·08	2·281	7·558	– 0·13	1·40	4·74	– 0·35
15	0·85	2·279	7·505	– 0·13	1·18	3·66	– 0·35

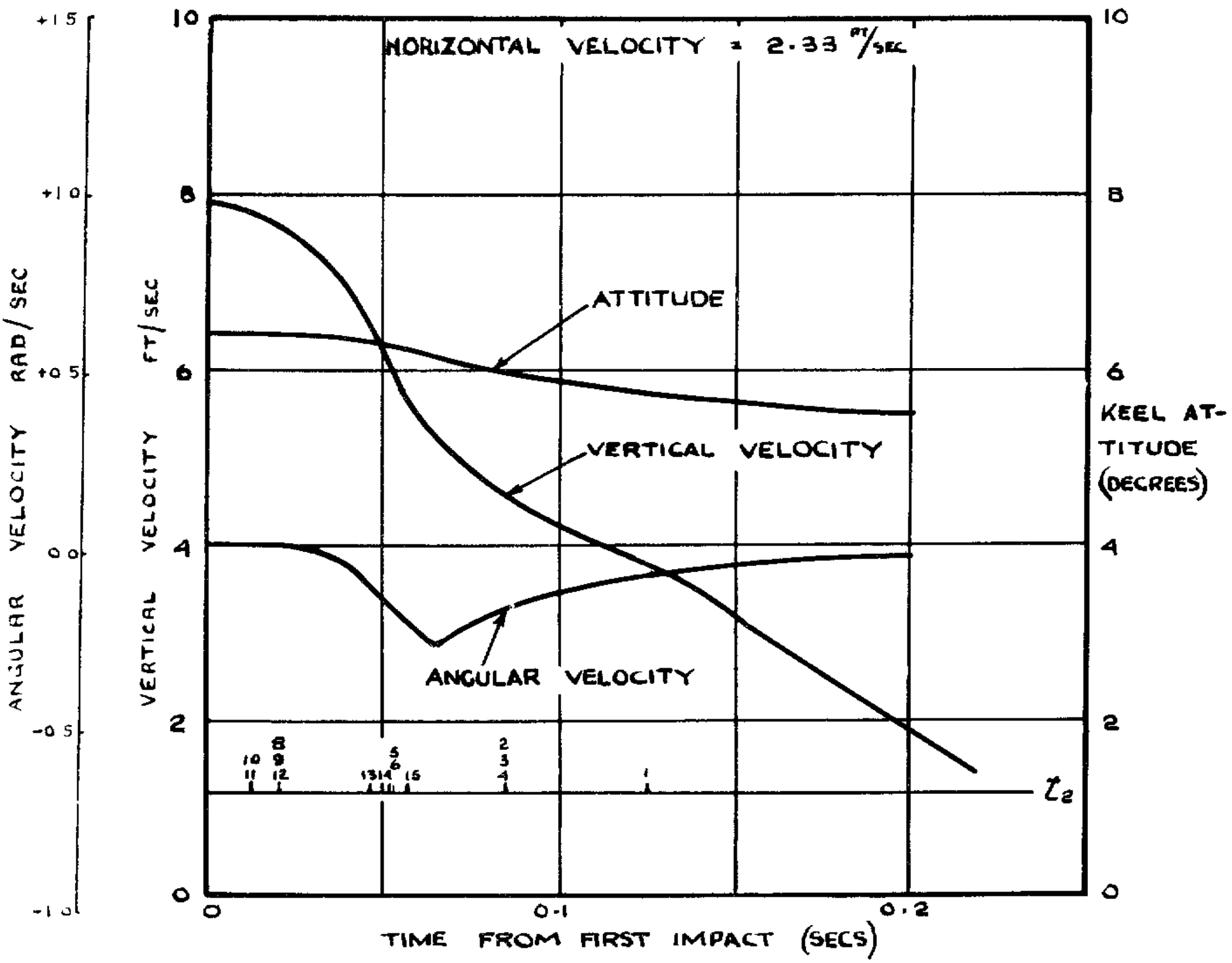

FIG.22

ACCELERATION DUE TO GRAVITY = 5·2 FT/SEC²							
DIAPHRAGM	P_{MAX}	INITIAL CONDITIONS			LOCAL IMPACT CONDITIONS		
		V_H	V_V	α	V_H	V_V	α
1	0·43	2·33	7·75	16·87	0·84	2·61	16·03
2	1·00	2·33	7·75	10·77	1·08	4·26	10 11
3	1·49	2·33	7·75	10·77	1·01	4·07	10·06
4							
5	3·20	2·33	7·75	6·57	1·12	4·67	6·33
6							
7	3·25	2·33	7·75	6·57	1·46	5·18	6·42
8	3·74	2·33	7·75	6·57	1·38	4·97	6·38
9	3·14	2·33	7·75	6·57	1·42	4·99	6·39
10	3·41	2·33	7·75	6·57	1·20	4·51	6·37
11	3·72	2·33	7·75	6·57	1·55	5·48	6·42
12	1·96	2·33	7·75	6·57	1·57	5·58	6·43
13	1·62	2·33	7·75	−0·03	1·11	3·94	−0·27
14	0 90	2·33	7·75	−0 03	1·42	4 71	−0·22
15	0·93	2·33	7·75	−0 03	1·43	4·68	−0·21

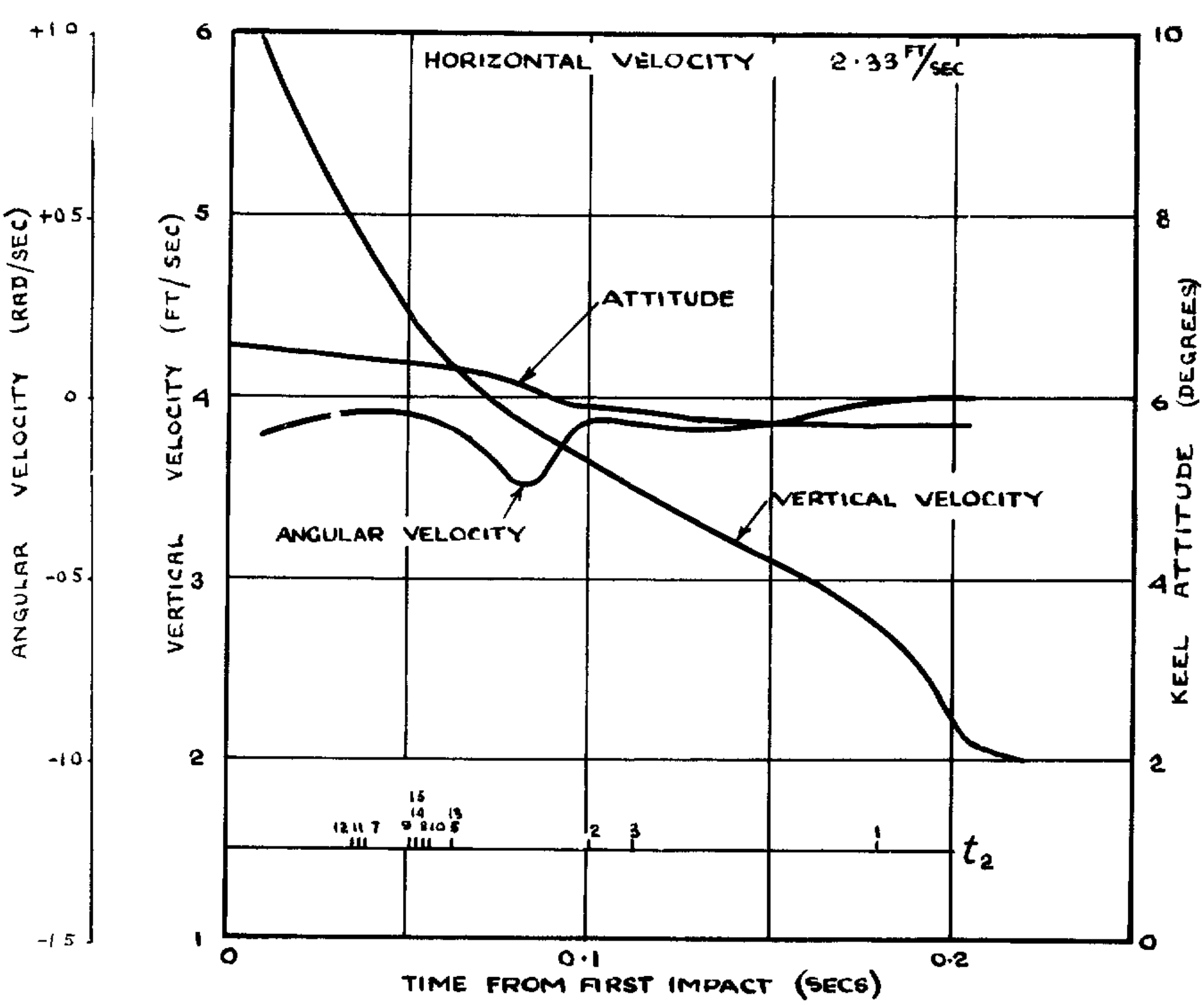

FIG.23

ACCELERATION DUE TO GRAVITY = 6·3 FT/SEC²							
DIAPHRAGM	P_{MAX}	INITIAL CONDITIONS			LOCAL IMPACT CONDITIONS		
		V_H	V_V	α	V_H	V_V	α
1	2·35	25·631	6·96	9·10	26·90	0·566	9·10
2	2·20	25·598	6·81	3·00	26·015	5·04	2·35
3							
4	1·95	25·607	6·81	3·00	27·075	1·686	2·90
5	2·70	25·570	6·58	− 1·20	25·800	6·25	− 1·95
6	2·50	25·603	6·69	− 1·20	28·320	0·560	− 0·65
7	2·30	25·583	6·39	− 1·20	26·686	5 245	− 1·62
8	2·20	25·598	6·40	− 1·20	26·785	5·024	− 1·50
9	2·17	25·610	6·40	− 1·20	26·740	5·054	− 1·50
10							
11	3·0	25 594	6·36	− 1·20	26·350	5·585	− 1·75
12	1·50	25·583	6·39	− 1·20	25·820	6·33	− 1·95
13	2·05	25·652	5·89	− 7·80	27·610	9·818	− 1·30
14	1·60	25·674	5·68	− 7·80	27·008	9·433	0·10
15	1·90	25 696	5·47	− 7·80	28 52	17·02	− 3·10

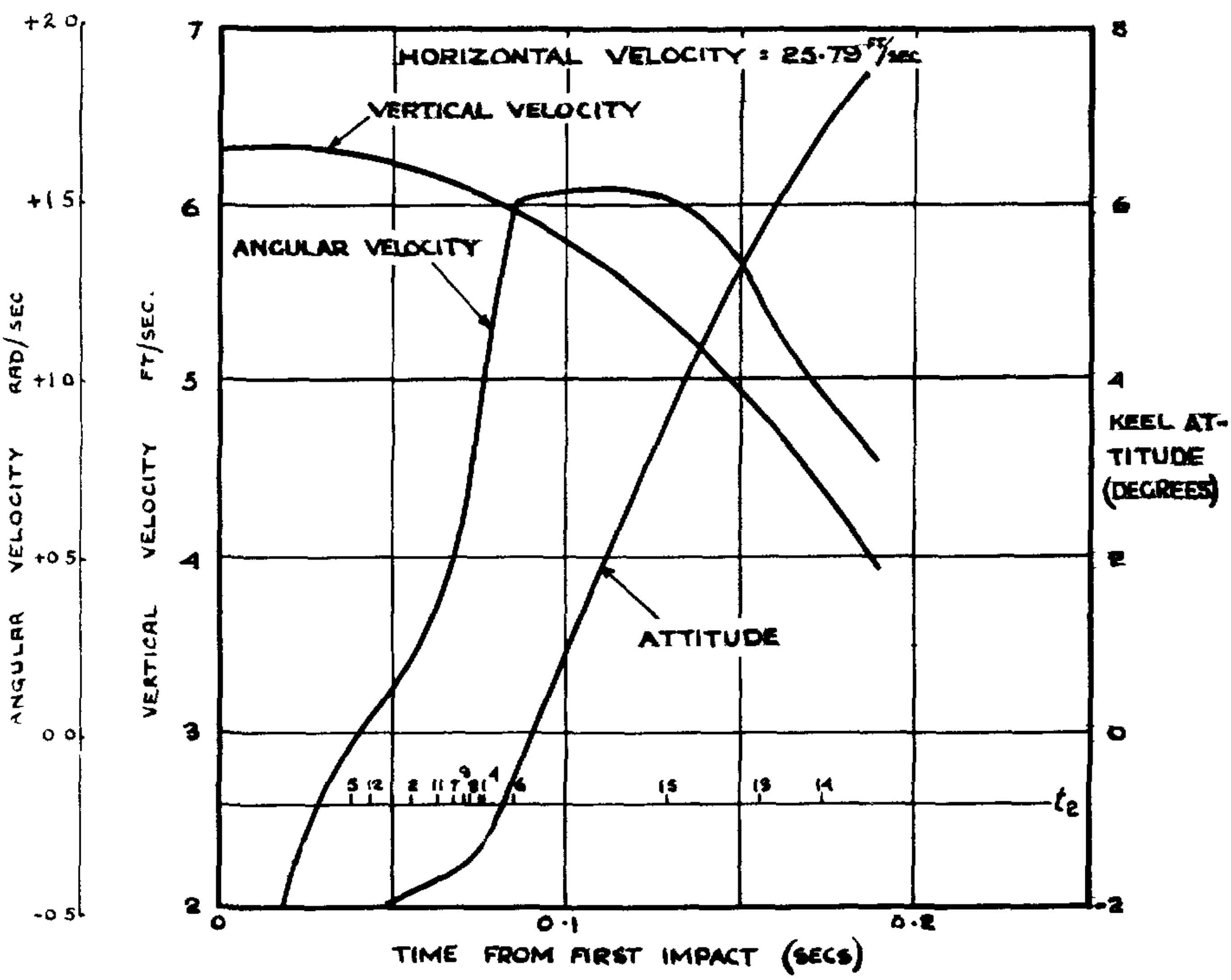

FIG. 24

ACCELERATION DUE TO GRAVITY = 2·1 FT/SEC²

DIAPHRAGM	$P_{MAX.}$	INITIAL CONDITIONS			LOCAL IMPACT CONDITIONS		
		V_H	V_V	α	V_H	V_V	α
1	1·68	32·10	10·34	8·85	31·60	10·73	7·50
2							
3							
4	1·30	32·30	9·42	4·85	33·0	− 2·42	3·90
5							
6	0·97	32·20	8·22	2·10	33·60	− 0·13	3·60
7	2·00	32·00	7·05	0·35	32·90	5·50	− 1·44
8	1·10	32·10	7·05	0·35	32·90	5·50	− 1·40
9	3·25	32·20	7·05	0·35	32·80	5·20	− 1·40
10	2·20	32·00	6·72	0·35	32·90	4·37	− 1·33
11	2·20	32·10	6·73	0·35	32·90	5·50	− 1·44
12	1·80	32·20	7·34	0·35	31·90	7·08	− 1·15
13	1·45	32·30	3·98	−6·65	33·70	7·40	− 6·70
14							
15	3·85	32·30	1·63	− 6·65	33·30	10·43	− 4·55

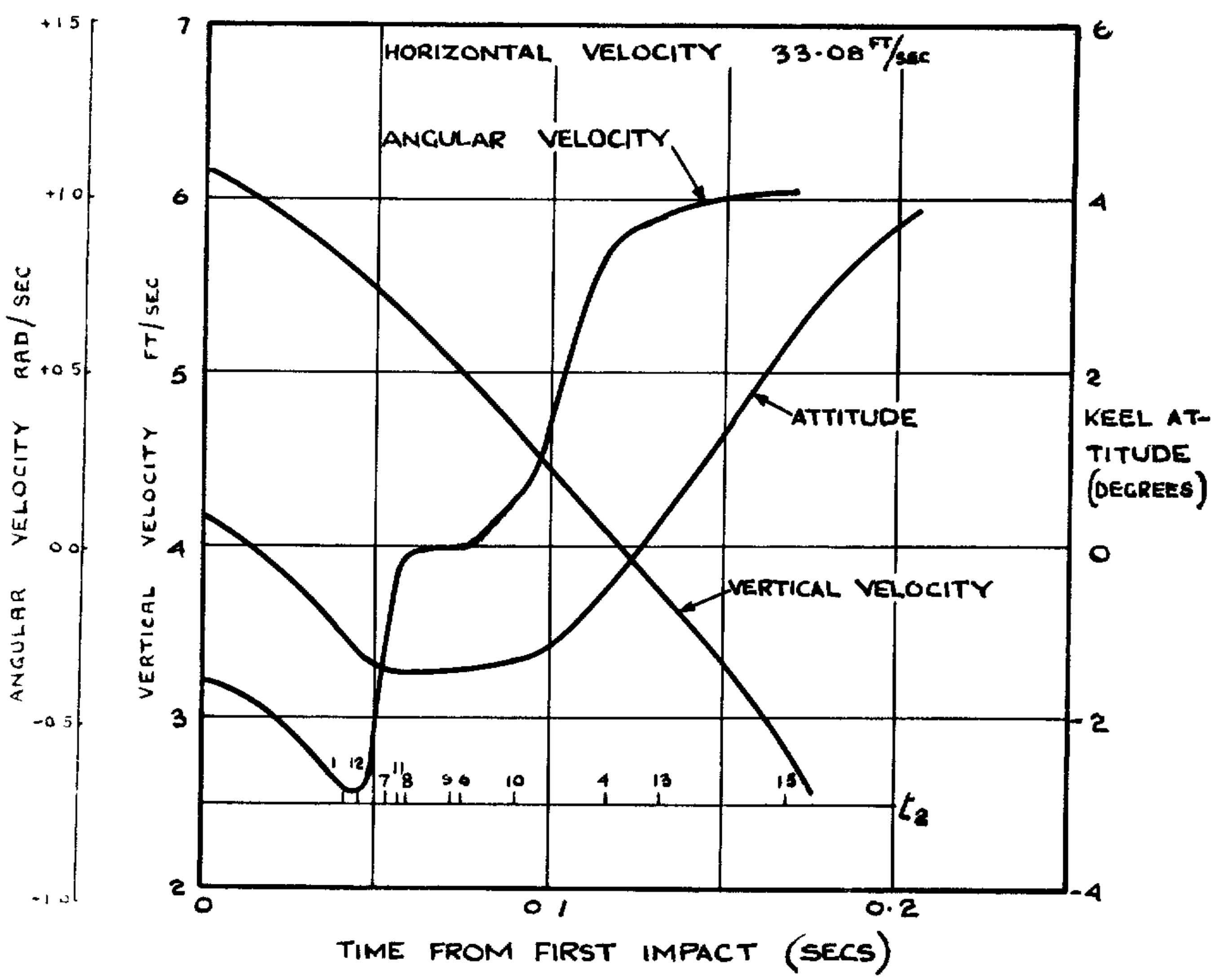

FIG. 25

ACCELERATION DUE TO GRAVITY = 2·1 FT/SEC²							
DIAPHRAGM	$P_{MAX.}$	INITIAL CONDITIONS			LOCAL IMPACT CONDITIONS		
		V_H	V_V	α	V_H	V_V	α
1							
2							
3							
4							
5	3·80	40·39	3·74	7·25	39·47	4·43	7·80
6	1·85	40·29	3·71	7·25	40·15	3·81	7·55
7							
8	2·00	40·41	4·47	5·50	39 59	4·56	6 10
9	2·65	40·33	4·47	5·50	39·26	4·06	6·05
10	2·55	40·51	4·67	5·50	39 36	4·49	6·10
11	3·90	40·38	4·67	5·50	39·97	4·45	5·97
12	2·85	40·28	4·30	5·50	39·13	4·27	6·05
13							
14							
15	1·70	40·48	7·90	− 1·50	40·09	6·25	−0·93

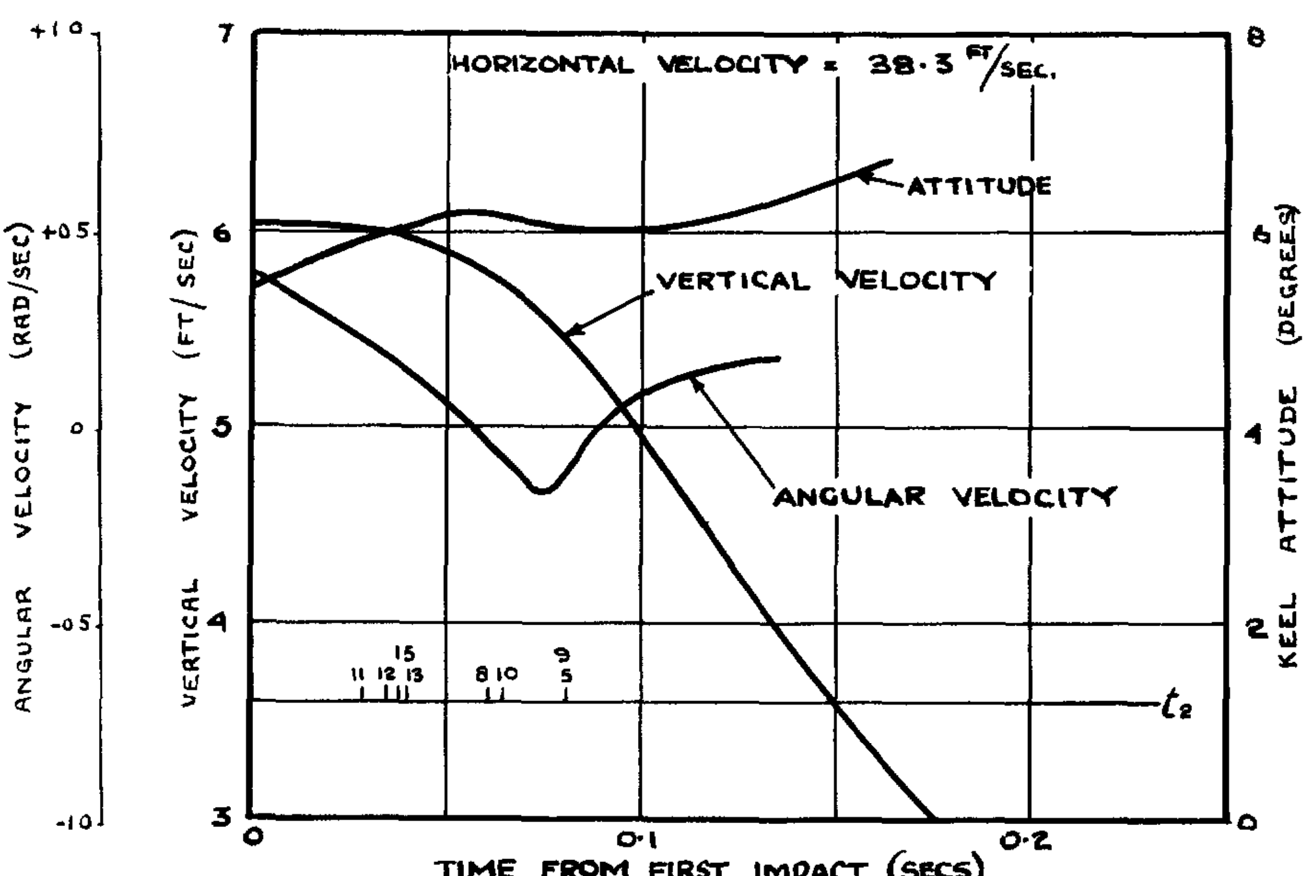

FIG 26.

ACCELERATION DUE TO GRAVITY = 2·1 FT/SEC²

DIAPHRAGM	P_{MAX}	INITIAL CONDITIONS			LOCAL IMPACT CONDITIONS		
		V_H	V_V	α	V_H	V_V	α
1							
2							
3							
4							
5							
6	1·30	40·4	5·01	10·85	38·5	1·62	8·55
7	4·40	40·6	5·80	9·10	38·7	4·69	9·45
8	2·80	40·6	5·81	9·10	38·7	3·74	7·98
9	3·20	40·5	5·82	9·10	38·1	4·19	7·47
10	3·30	40·7	6·02	9·10	38·0	4·48	8·30
11	4·00	40·6	6·04	9·10	37·8	5·10	9·00
12	3·50	40·4	5·62	9·10	38·5	6·01	8·20
13	1·80	40·7	7·95	2·10	40·6	7·21	3·05
14							
15	4·95	40·9	9·64	2·10	38·6	1·97	1·05

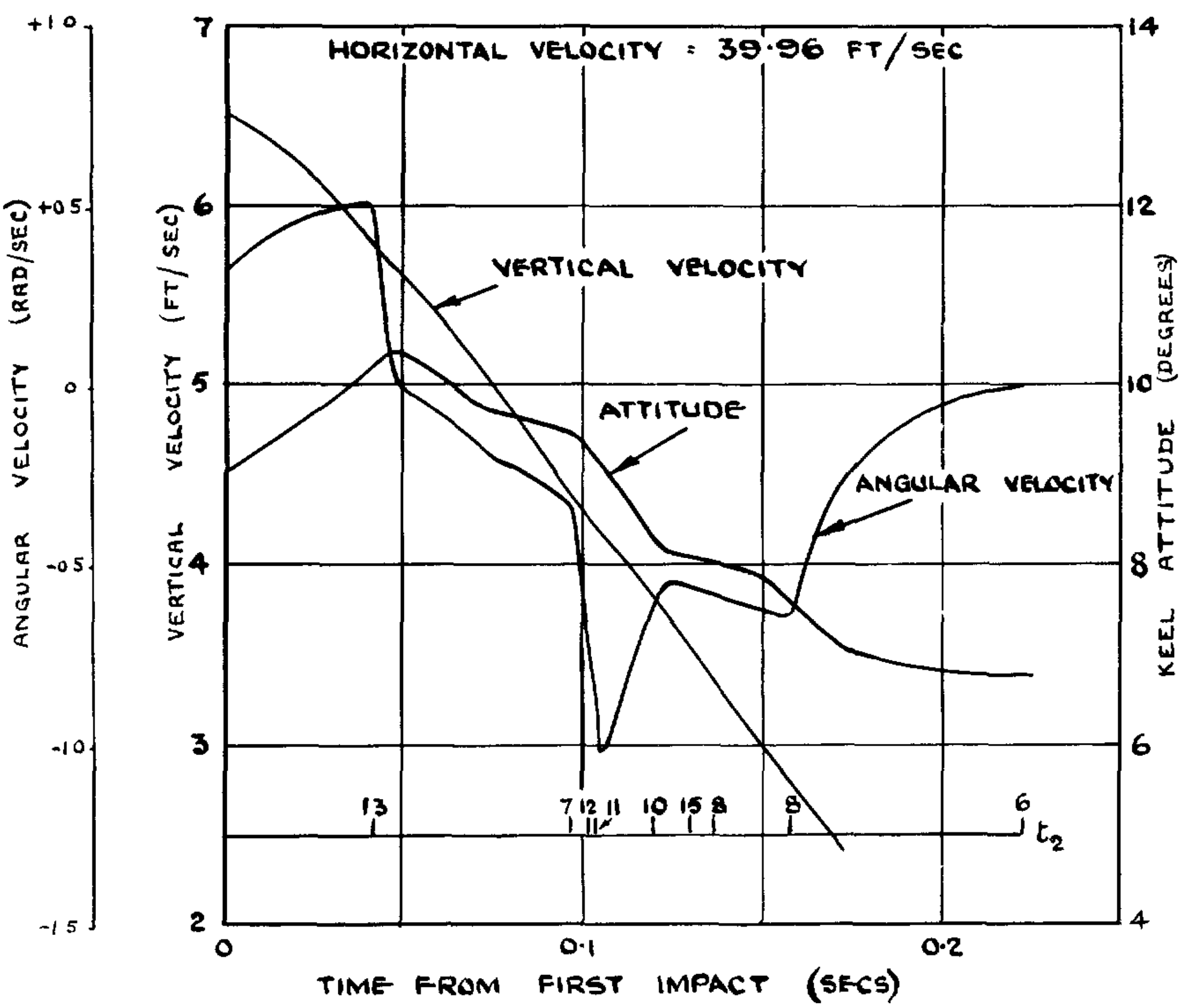

FIG 27

ACCELERATION DUE TO GRAVITY : 2·1 FT/SEC^2							
DIAPHRAGM	P_{MAX}	INITIAL CONDITIONS			LOCAL IMPACT CONDITIONS		
		V_H	V_V	α	V_H	V_V	α
1							
2	2·65	37·05	8·81	7·75	36·29	7·78	6·10
3	2·75	37·13	8·81	7·75	37·61	1·68	6·40
4							
5							
6	1·40	37·07	7·96	4·10	37·73	3·28	3·15
7	1·90	36·91	7·14	2·35	37·57	5·85	2·30
8	2·20	36·98	7·13	2·35	37·50	4·31	1·32
9	1·80	37·07	7·14	2·35	37·63	3·91	1·55
10	2·50	36·89	6·91	2·35	37·90	4·28	1·44
11							
12	2·30	37·12	7·34	2·35	37·63	5·97	2·28
13							
14							
15							

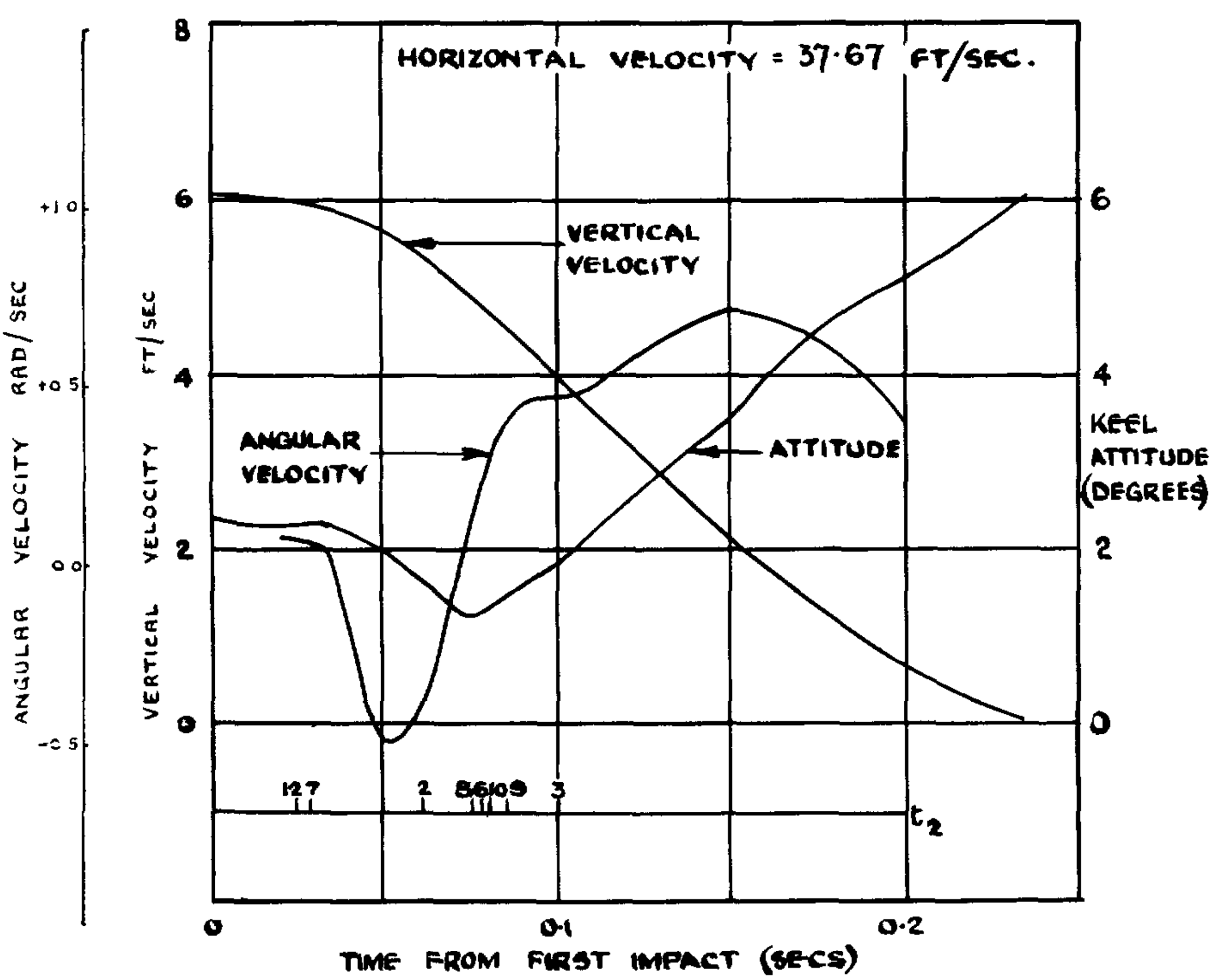

FIG. 28.

ACCELERATION DUE TO GRAVITY = 2·1 FT/SEC²							
DIAPHRAGM	P_{MAX}	INITIAL CONDITIONS			LOCAL IMPACT CONDITIONS.		
		V_H	V_V	α	V_H	V_V	α
1							
2	1·55	37·2	6·89	9·32	37·4	1·25	7·45
3	1·58	37·2	6·89	9 32	37·2	1·05	7·86
4							
5	2·25	37·1	6·20	6·57	37·0	5·73	4·23
6	1·88	37·2	6·19	6·57	37·1	5·78	4·25
7							
8	1·80	37·1	5·53	4·82	36·9	5·33	2·70
9	1·40	37·1	5·48	4·82	36·7	4·75	1·70
10	2·40	37·0	5·35	4·82	36·9	4·96	2·50
11	2·70	37·1	5·34	4·82	36·8	5·52	2·95
12	1·88	37·2	5·69	4·82	36·8	6·32	3·55
13							
14							
15							

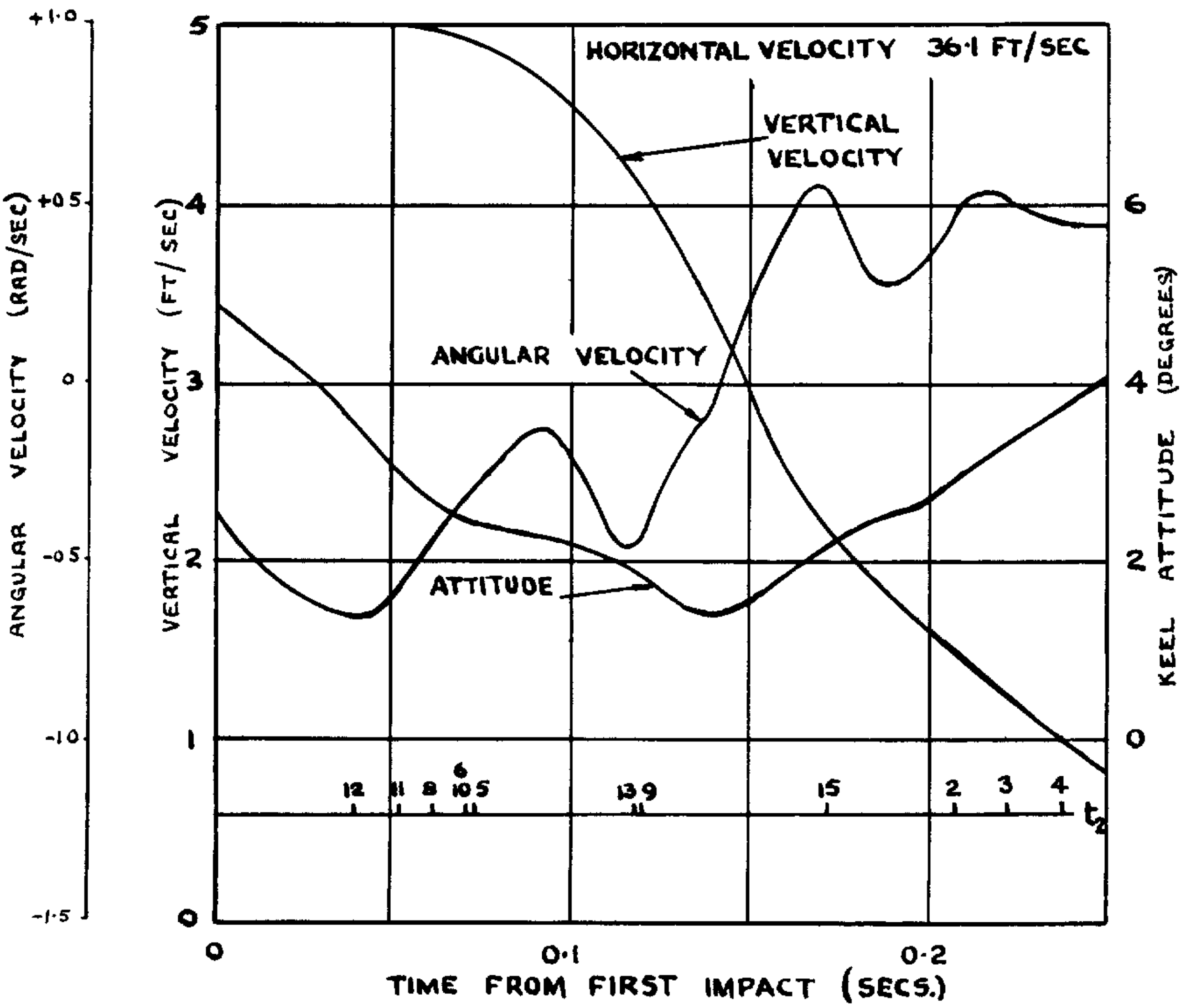

FIG 29

DIAPHRAGM	P_{MAX}	INITIAL CONDITIONS V_H	V_V	α	LOCAL IMPACT CONDITIONS V_H	V_V	α
ACCELERATION DUE TO GRAVITY = 2·1 FT/SEC²							
1	1·6	35·8	6·14	2·58	36·6	5·96	2·10
1a	1·85	35·8	6·17	8·58	36·6	5·84	8·10
1b	2·70	35·8	6·14	2·58	36·8	4·08	2·55
2	0·65	35·8	6·11	-1·42	36·9	7·00	-1·80
3	1·08	35·8	6·11	-1·42	36·6	5·84	-1·80
4							
5	0·70	35·8	6·07	-4·17	36·9	2·62	0·25
6	1·00	35·8	6·07	-4·17	37·0	1·91	1·00
7							
8	1·80	35·8	6·03	-5·92	36·9	5·53	-1·50
9	0·55	35·8	6·03	-5·92	36·9	4·71	-4·40
10	2·40	35·8	6·01	-5·92	37·2	3·38	1·20
11	1·40	35·8	6·02	-5·92	36·6	2·88	3·15
12	1·90	35·8	6·04	-5·92	36·8	2·51	1·95
15	3·90	35·8	5·83	-12·92	35·8	3·89	-1·05

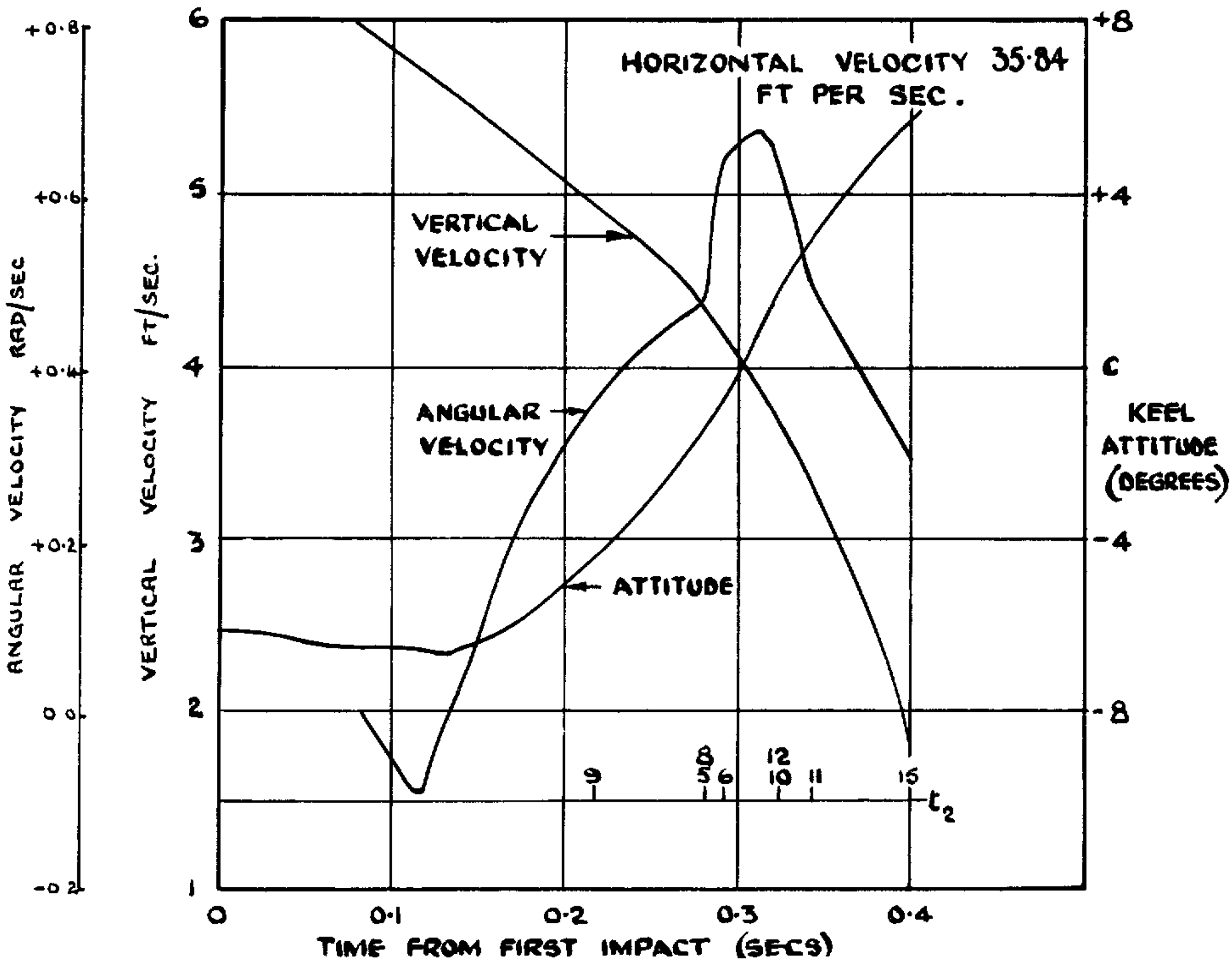

FIG. 30.

ACCELERATION DUE TO GRAVITY = 2·1 FT/SEC^2							
DIAPHRAGM	P. MAX	INITIAL CONDITIONS			LOCAL IMPACT CONDITIONS		
		V_H	V_V	α	V_H	V_V	α
1	1·9	36·13	7·22	10·84	35·74	4·02	11·0
2							
3	3·67	36·10	7·30	6·84	35·55	3·78	7·15
4	1·70	36·09	7·30	6·84	33·60	10·05	5·65
5							
6	1·10	36·13	7·41	4·09	33·34	7·83	3·02
7	1·70	36·15	7·52	2·34	35·45	5·99	2·30
8	1·20	36·14	7·52	2·34	33·92	4·34	0·72
9	3·25	36·13	7·52	2·34	34·55	0·29	− 0·90
10	1·70	36·15	7·55	2·34	32·73	5·09	1·60
11	2·30	36·14	7·55	2·34	35·66	4·96	2·60
12	1·60	36·12	7·60	2·34	35·74	4·93	2·67
13							
14							
15							

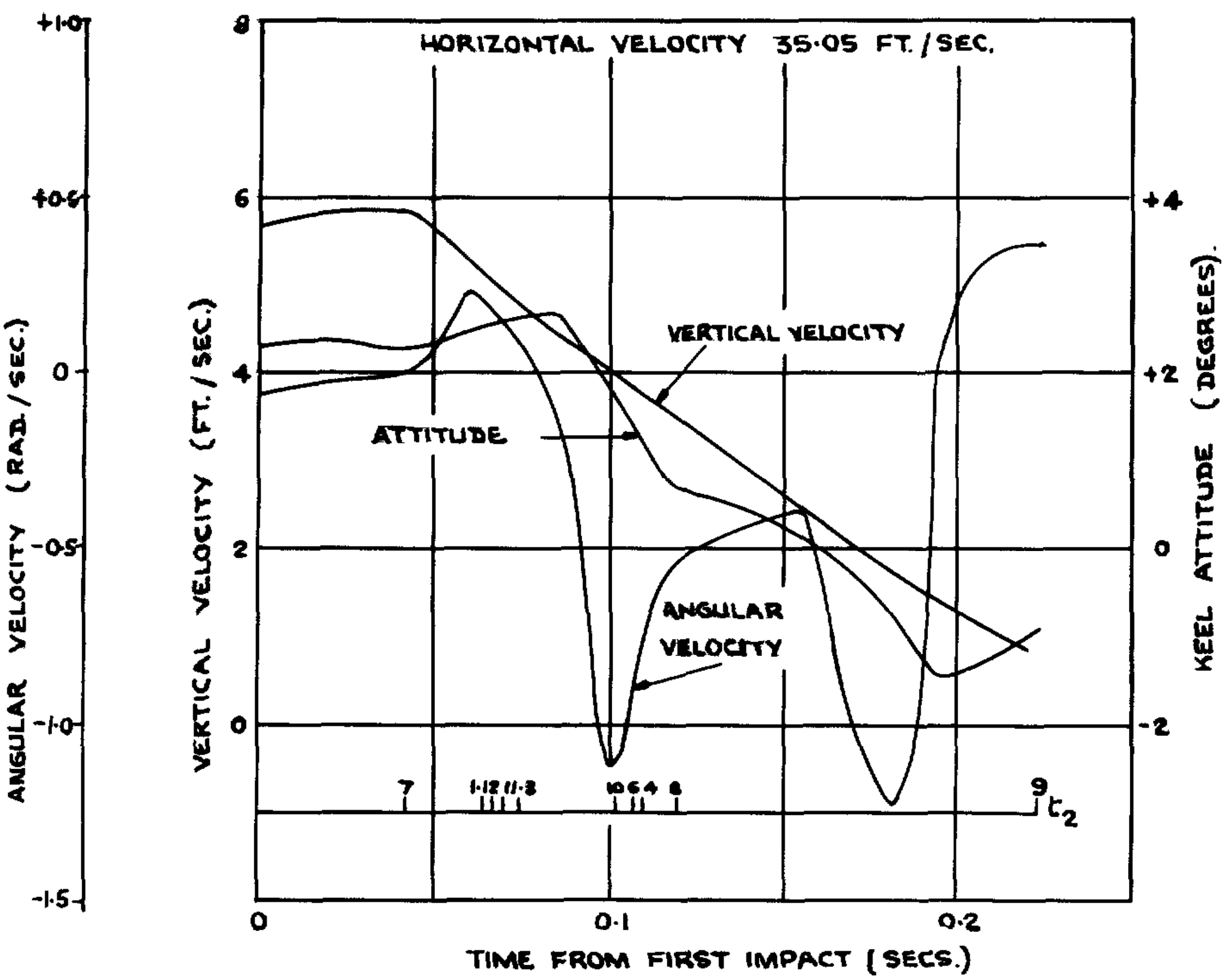

FIG. 31.

ACCELERATION DUE TO GRAVITY = ZERO

DIAPHRAGM	P_{MAX}	INITIAL CONDITIONS			LOCAL IMPACT CONDITIONS		
		V_H	V_V	α	V_H	V_V	α
1	/	/	/	/	/	/	/
2	/	/	/	/	/	/	/
3	2.95	38.1	3.30	9.68	35.7	4.73	10.07
4	/	/	/	/	/	/	/
5	/	/	/	/	/	/	/
6	1.57	38.2	4.55	6.93	36.5	4.08	6.90
7	3.08	38.5	5.74	5.18	37.9	5.18	6.15
8	2.65	38.3	5.74	5.18	37.4	4.67	6.60
9	4.60	38.3	5.75	5.18	35.4	2.83	5.10
10	2.90	38.5	6.07	5.18	37.3	4.46	6.70
11	3.90	38.4	6.08	5.18	37.3	4.82	6.65
12	2.85	38.2	5.48	5.18	37.3	4.56	6.50
13	1.45	38.5	8.91	−1.82	36.1	2.12	−0.2
14	/	/	/	/	/	/	/
15	/	/	/	/	/	/	/

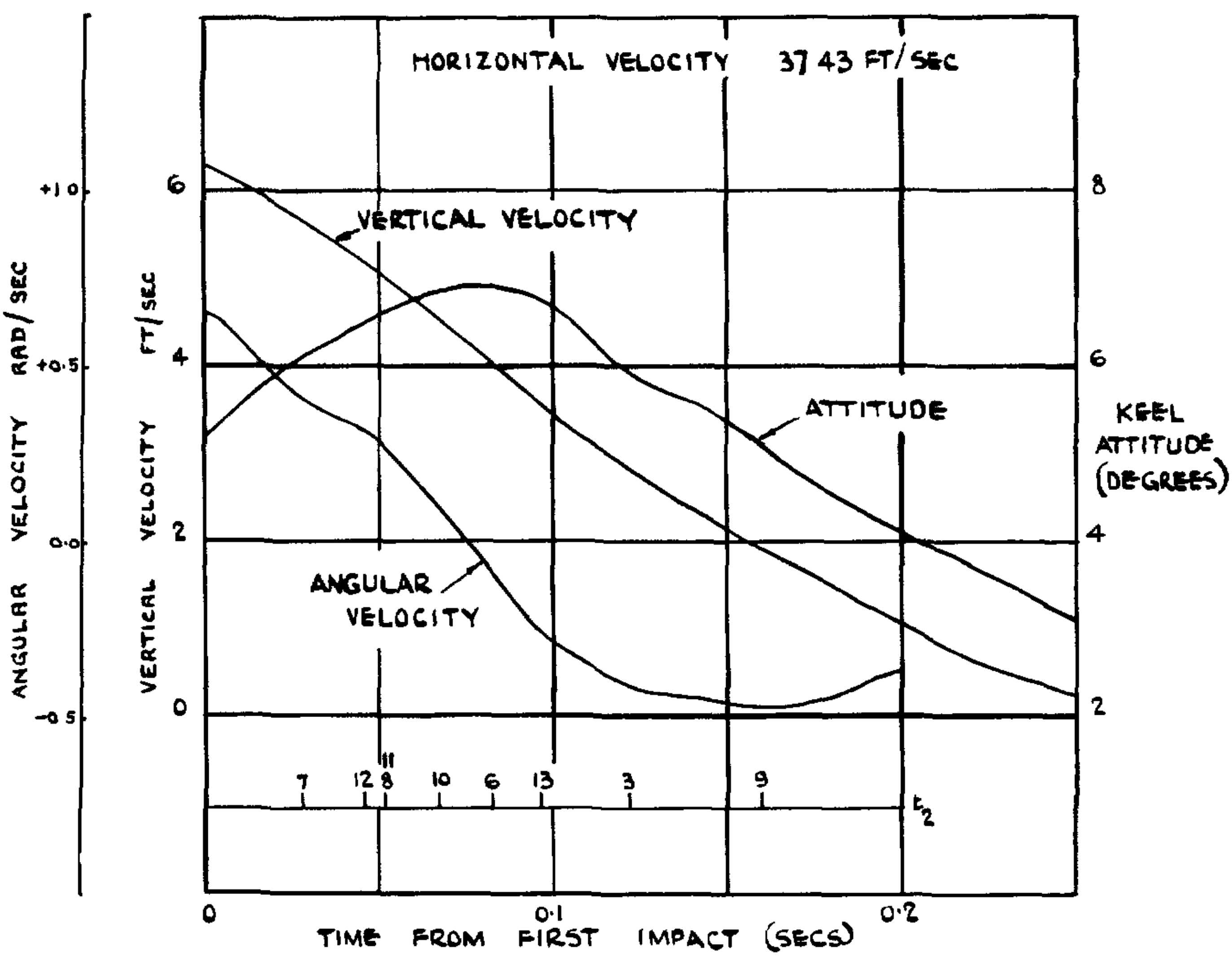

ACCELERATION DUE TO GRAVITY = ZERO

DIAPHRAGM	P_{MAX}	INITIAL CONDITIONS V_H	V_V	α	LOCAL IMPACT CONDITIONS V_H	V_V	α
1	/	/	/	/	/	/	/
2	/	/	/	/	/	/	/
3	/	/	/	/	/	/	/
4	/	/	/	/	/	/	/
5	/	/	/	/	/	/	/
6	1·25	37·65	9·04	12·20	36·21	5·11	6·97
7	3·60	37·50	8·60	10·45	36·43	6·42	6·90
8	3·75	37·54	8·59	10·45	36·65	6·24	6 95
9	4·00	37·59	8·59	10·45	35·99	5·98	6·15
10	3·30	37·47	8·48	10·45	36·09	5·61	6·40
11	4·15	37·56	8·47	10·45	36·47	6·49	7·15
12	3 30	37·63	8·69	10·45	36 56	7·20	7·30
13	0·90	37·41	7·41	3·45	36·68	5·40	1·50
14	/	/	/	/	/	/	/
15	1·25	37·32	6 47	3·45	36·15	2 33	2 18

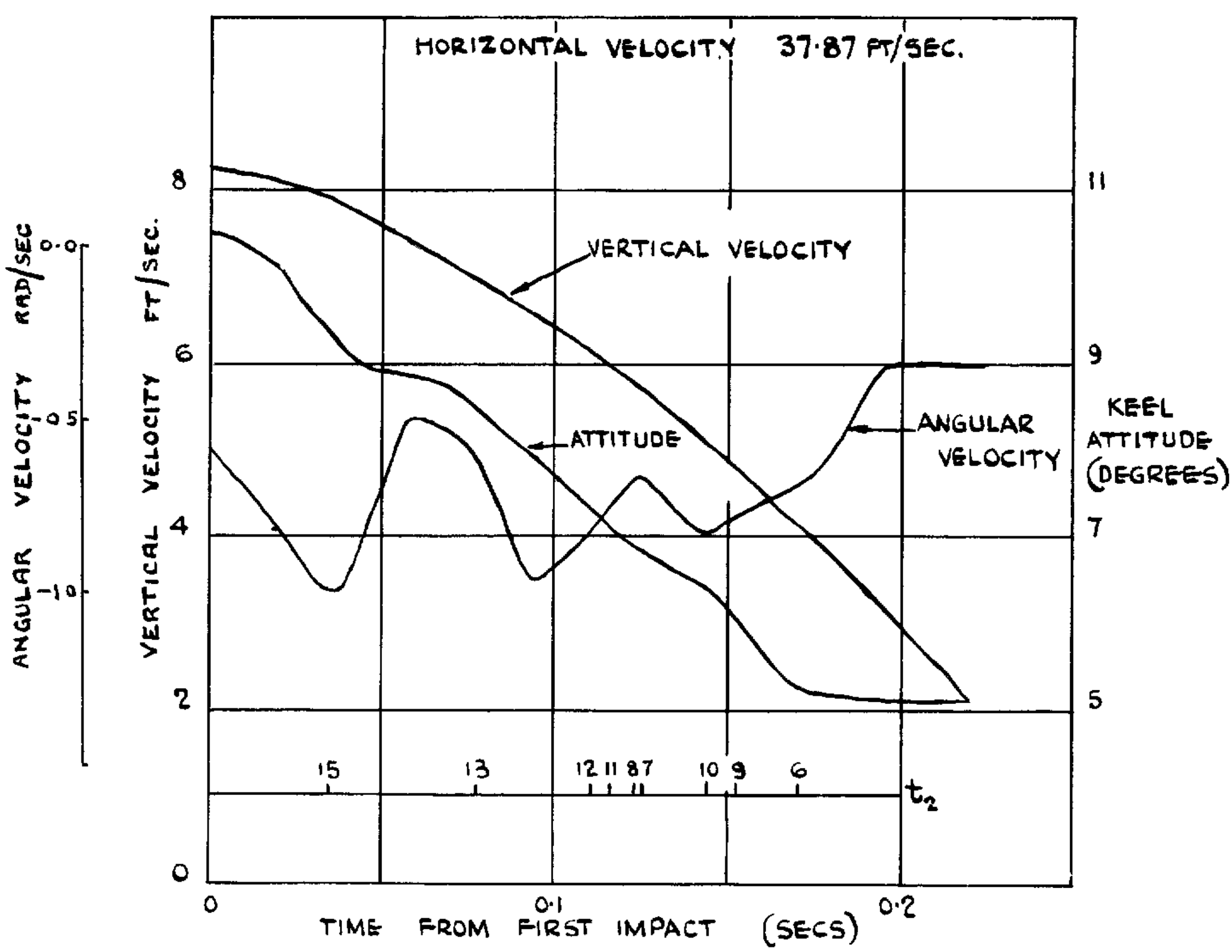

FIG.33.

ACCELERATION DUE TO GRAVITY = 4·2 FT/SEC^2

DIAPHRAGM	P_{MAX}	INITIAL CONDITIONS			LOCAL IMPACT CONDITIONS		
		V_H	V_V	α	V_H	V_V	α
1	/	/	/	/	/	/	/
2	/	/	/	/	/	/	/
3	/	/	/	/	/	/	/
4	/	/	/	/	/	/	/
5	/	/	/	/	/	/	/
6	1·05	40·4	5·91	3·30	38·9	1·70	7·10
7	1·98	40·5	6·45	1·55	39·9	5·26	1·75
8	1·75	40·5	6·45	1·55	39·9	4·99	1·90
9	2·80	40·4	6·45	1·55	39·7	2·25	4·60
10	3·10	40·2	6·60	1·55	38·8	4·30	2·35
11	3·35	40·2	6·60	1·55	39·8	4·38	2·24
12	2·20	40·3	6·31	1·55	39·8	4·99	1·80
13	/	/	/	/	/	/	/
14	/	/	/	/	/	/	/
15	/	/	/	/	/	/	/

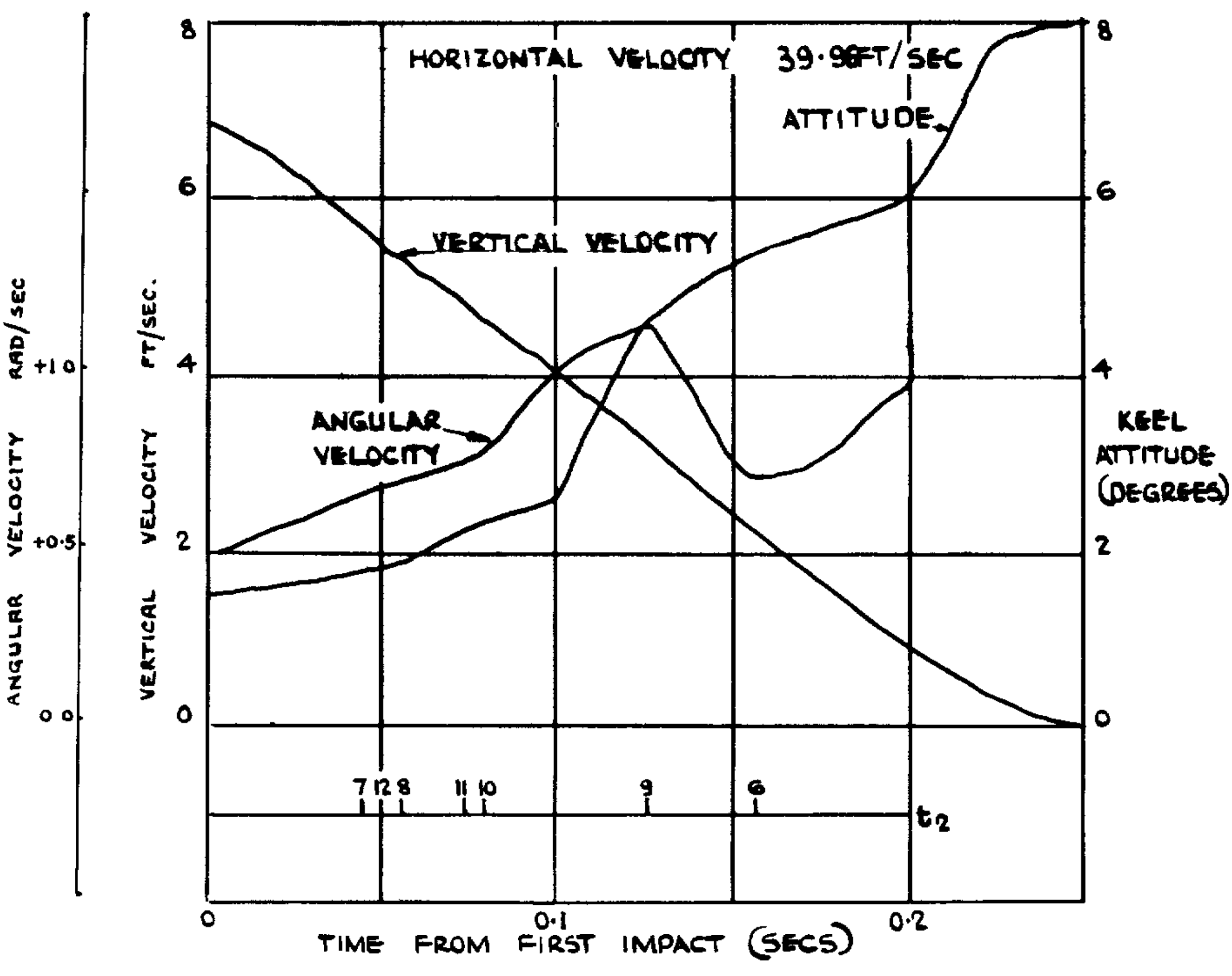

FIG. 34

ACCELERATION DUE TO GRAVITY = 4·2 FT/SEC^2

DIAPHRAGM	P_{MAX}	INITIAL CONDITIONS			LOCAL IMPACT CONDITIONS		
		V_H	V_V	α	V_H	V_V	α
1	0·57	39·66	10·27	9·30	40·01	7·24	7·37
2	/	/	/	/	/	/	/
3	3·20	39·68	9·34	5·30	40·45	5·50	3·35
4	1·25	39·83	9·32	5·30	41·14	−2·04	5·60
5	/	/	/	/	/	/	/
6	0·88	39·68	8·08	2·55	40·83	4·66	0·62
7	1·70	39·48	6·88	0·80	39·76	6·13	0·37
8	1·10	39·58	6·88	0·80	39·12	6·43	−0·68
9	1·36	39·71	6·89	0·80	40·89	4·62	−0·96
10	2·20	39·46	6·55	0·80	41·13	4·88	−1·04
11	2·30	39·66	6·55	0·80	39·75	6·18	0·08
12	1·95	39·77	7·18	0·80	39·70	6·75	−0·20
13	/	/	/	/	/	/	/
14	/	/	/	/	/	/	/
15	2·90	39·94	1·21	−6·20	40·43	7·62	−4·20

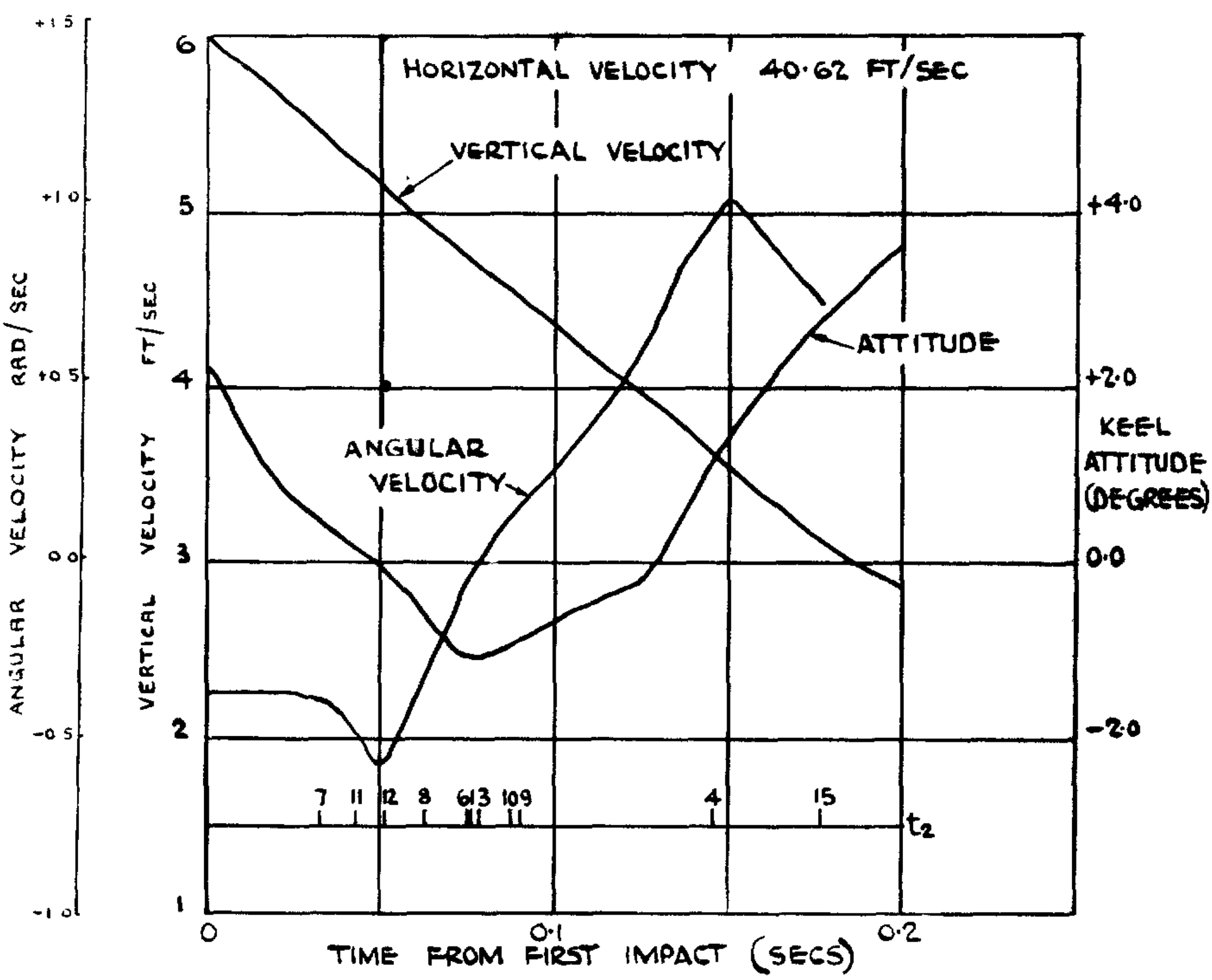

FIG. 35.

ACCELERATION DUE TO GRAVITY = 63 FT/SEC²

DIAPHRAGM	P_{MAX}	INITIAL CONDITIONS			LOCAL IMPACT CONDITIONS		
		V_H	V_V	α	V_H	V_V	α
1	/	/	/	/	/	/	/
2	/	/	/	/	/	/	/
3	/	/	/	/	/	/	/
4	/	/	/	/	/	/	/
5	/	/	/	/	/	/	/
6	1·30	40·4	5·23	6·15	38·5	2·69	8·13
7	3·80	40·6	5·76	4·40	41·0	4·35	4·96
8	3·62	40·5	5·76	4·40	39·6	4·67	6·50
9	2·30	40·5	5·76	4·40	40·5	5·04	4·73
10	3·40	40·6	5·80	4·40	39·2	4·93	6·45
11	3·60	40·5	5·81	4·40	41·0	4·04	5·70
12	3·00	40·4	5·74	4·40	40·4	3·66	6·14
13	2·40	40·5	7·17	−2·6	40·7	7·10	−0·86
14	/	/	/	/	/	/	/
15	3·10	40·5	8·28	−2·6	39·1	2·57	−0·55

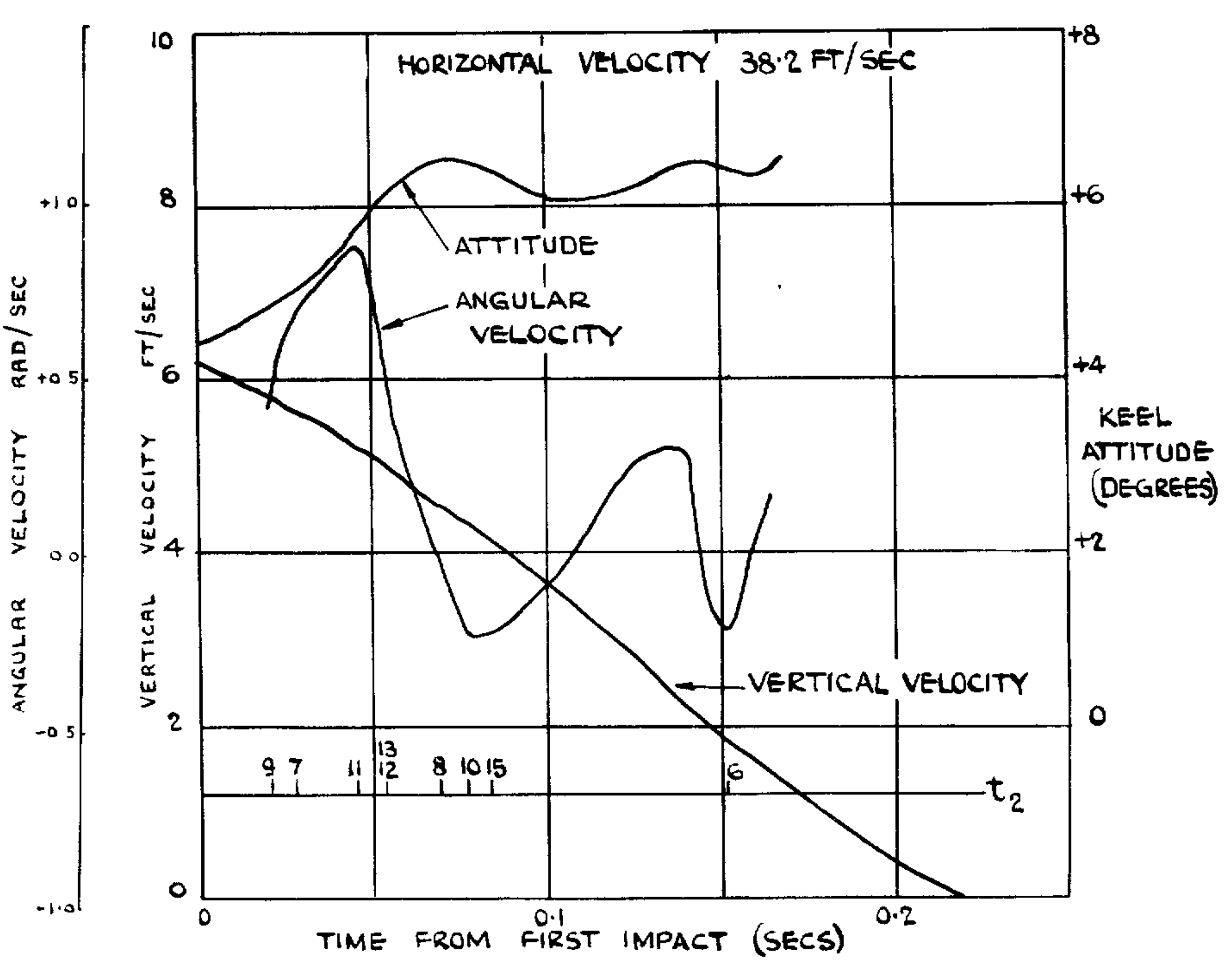

FIG. 36.

ACCELERATION DUE TO GRAVITY = 6·3 FT/SEC^2

DIAPHRAGM	P_{MAX}	INITIAL CONDITIONS V_H	V_V	α	LOCAL IMPACT CONDITIONS V_H	V_V	α
1	/	/	/	/	/	/	/
2	/	/	/	/	/	/	/
3	/	/	/	/	/	/	/
4	/	/	/	/	/	/	/
5	3·25	38·46	4·87	3·97	37·32	3·18	7·30
6	1·92	38·32	4·87	3·97	37·62	4·48	5·55
7	/	/	/	/	/	/	/
8	2 66	38·43	5·86	2·22	38·01	3·92	4 75
9	3·60	38·31	5·84	2·22	36·79	2·77	5·75
10	3·66	38·53	6·11	2·22	39·10	4·15	4·90
11	3·80	38·38	6·13	2·22	37·71	5·21	3 85
12	2 70	38 27	5·62	2 22	37 79	4 42	4·15
13	2·40	38·34	8·46	−4·78	38·61	9·98	−3·92
14	/	/	/	/	/	/	/
15	/	/	/	/	/	/	/

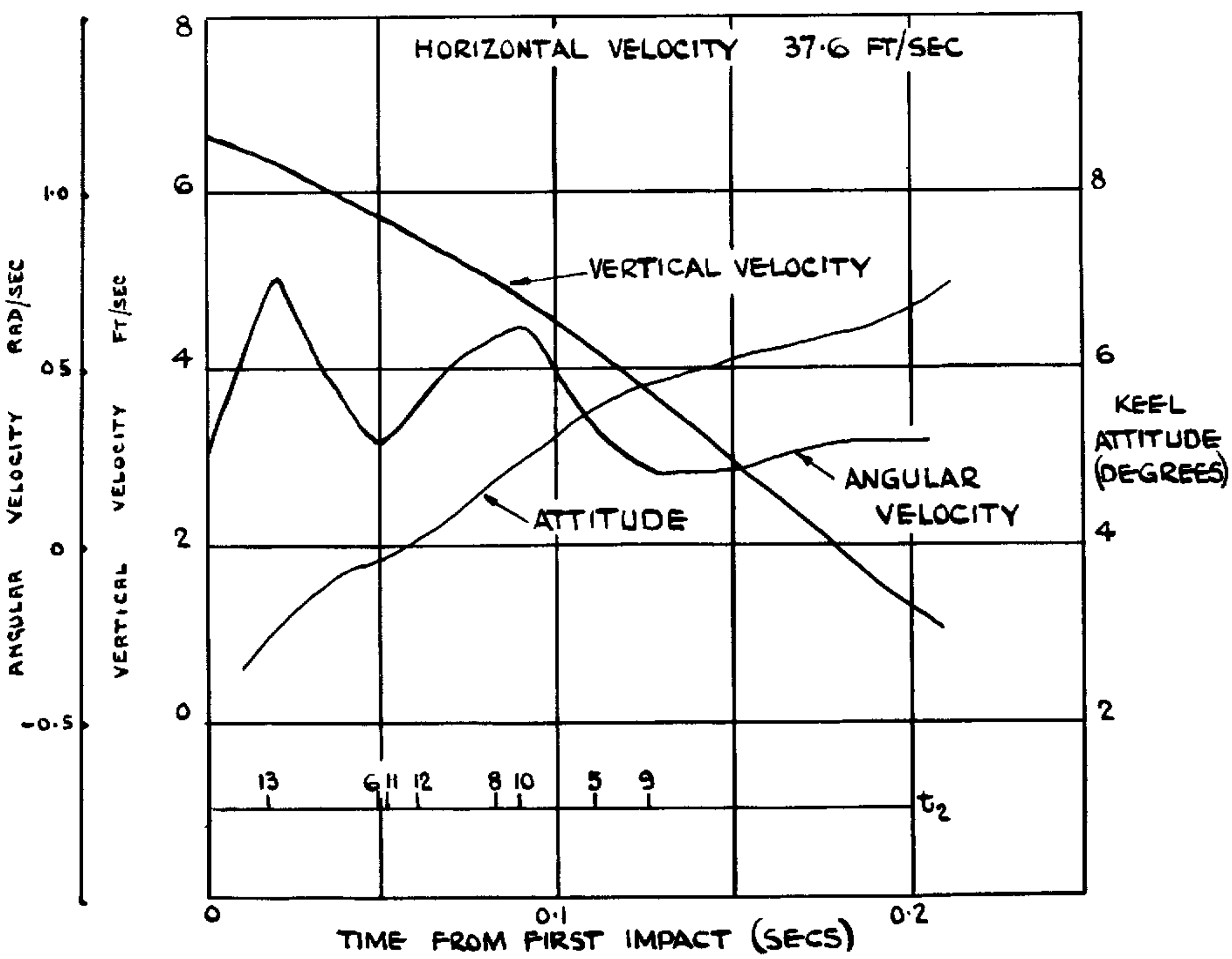

FIG. 37.

ACCELERATION DUE TO GRAVITY = 2·1 FT/SEC.² DAMPER $\frac{2}{3}$.							
DIAPHRAGM	P MAX.	INITIAL CONDITIONS			LOCAL IMPACT CONDITIONS		
		V_H	V_V	∝	V_H	V_V	∝
1	—	—	—	—	—	—	—
2	—	—	—	—	—	—	—
3	—	—	—	—	—	—	—
4	—	—	—	—	—	—	—
5	4·7	32·29	6·38	1·95	31·83	4·10	1 90
6	3·0	32·30	6·38	1·95	32 67	0·76	2 45
7	—	—	—	—	—	—	—
8	12·0	32·20	6·23	1·95	33·07	1·255	3·03
9	6·5	32·30	6·23	1·95	31·95	4 50	1·88
10	12·7	32·28	6·17	1 95	32·34	3·206	2·08
11	14·0	32·29	6·17	1·95	32·30	3·206	2·08
12	—	—	—	—	—	—	—
13	2·7	32·33	5·80	-4·65	32·91	6·60	-3·70
14	—	—	—	—	—	—	—
15	—	—	—	—	—	—	—

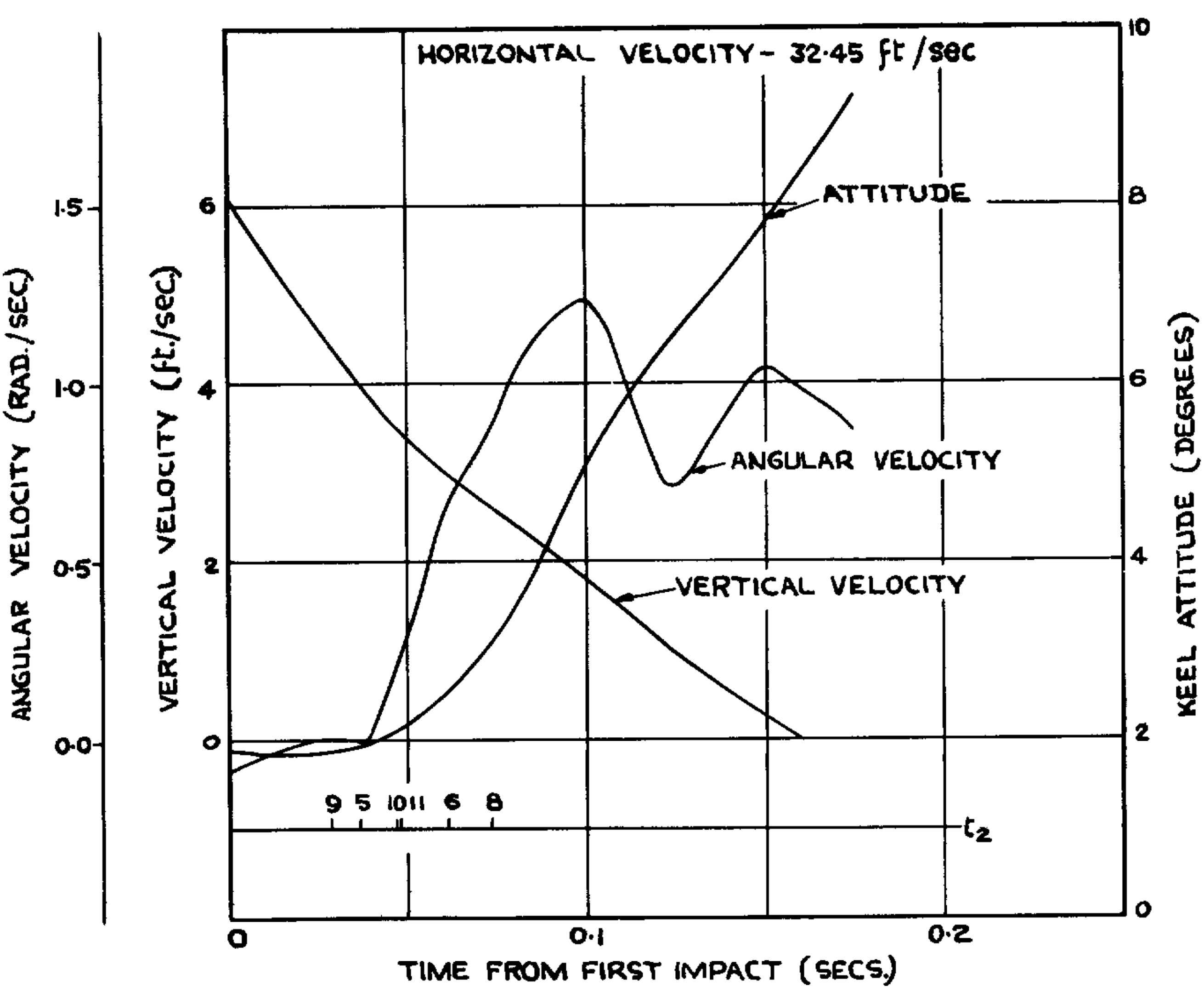

FIG. 38.

ACCELERATION DUE TO GRAVITY = 21 FT/SEC². DAMPER $\frac{2}{3}$							
DIAPHRAGM	P MAX.	INITIAL CONDITIONS			LOCAL IMPACT CONDITIONS		
		V_H	V_V	α	V_H	V_V	α
1	—	—	—	—	—	—	—
2	—	—	—	—	—	—	—
3	—	—	—	—	—	—	—
4	—	—	—	—	—	—	—
5	9.0	32.2	5.69	6.75	31.0	2.32	7.08
6	3.7	32.2	5.70	6.75	31.4	-1.04	7.42
7	—	—	—	—	—	—	—
8	10.4	32.2	5.85	6.75	31.2	3.23	7.02
9	6.5	32.2	5.86	6.75	31.8	5.00	6.72
10	17.0	32.2	5.91	6.75	31.7	4.68	6.92
11	19.5	32.2	5.91	6.75	31.2	3.13	7.03
12	—	—	—	—	—	—	—
13	—	—	—	—	—	—	—
14	—	—	—	—	—	—	—
15	—	—	—	—	—	—	—

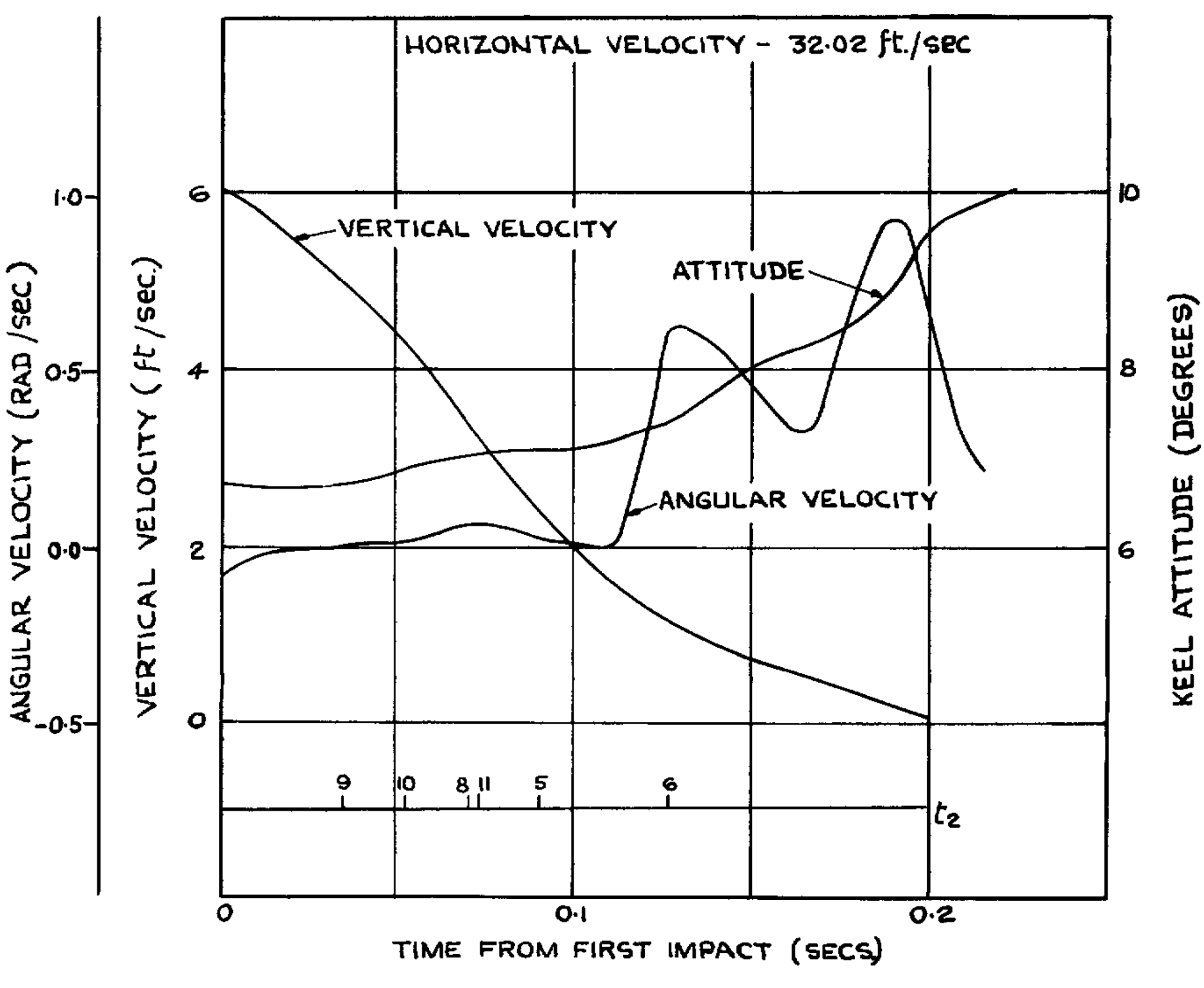

FIG. 39.

ACCELERATION DUE TO GRAVITY = 2·1FT / SEC.² DAMPER $\frac{1}{3}$.							
DIAPHRAGM	PMAX.	INITIAL CONDITIONS			LOCAL IMPACT CONDITIONS		
		V_H	V_V	α	V_H	V_V	α
1	—	—	—	—	—	—	—
2	—	—	—	—	—	—	—
3	—	—	—	—	—	—	—
4	—	—	—	—	—	—	—
5	4·8	33·5	5·85	0·8	33·2	5·02	0·8
6	—	—	—	—	—	—	—
7	—	—	—	—	—	—	—
8	5·8	33·5	5·85	0·8	34·2	2·45	1·95
9	—	—	—	—	—	—	—
10	9·65	33·5	5·85	0·8	34·2	2·85	2·10
11	12·0	33·5	5·85	0·8	34·6	3·01	1·60
12	—	—	—	—	—	—	—
13	2·9	33·5	5·85	-5·8	34·3	7·55	-2·05
14	—	—	—	—	—	—	—
15	—	—	—	—	—	—	—

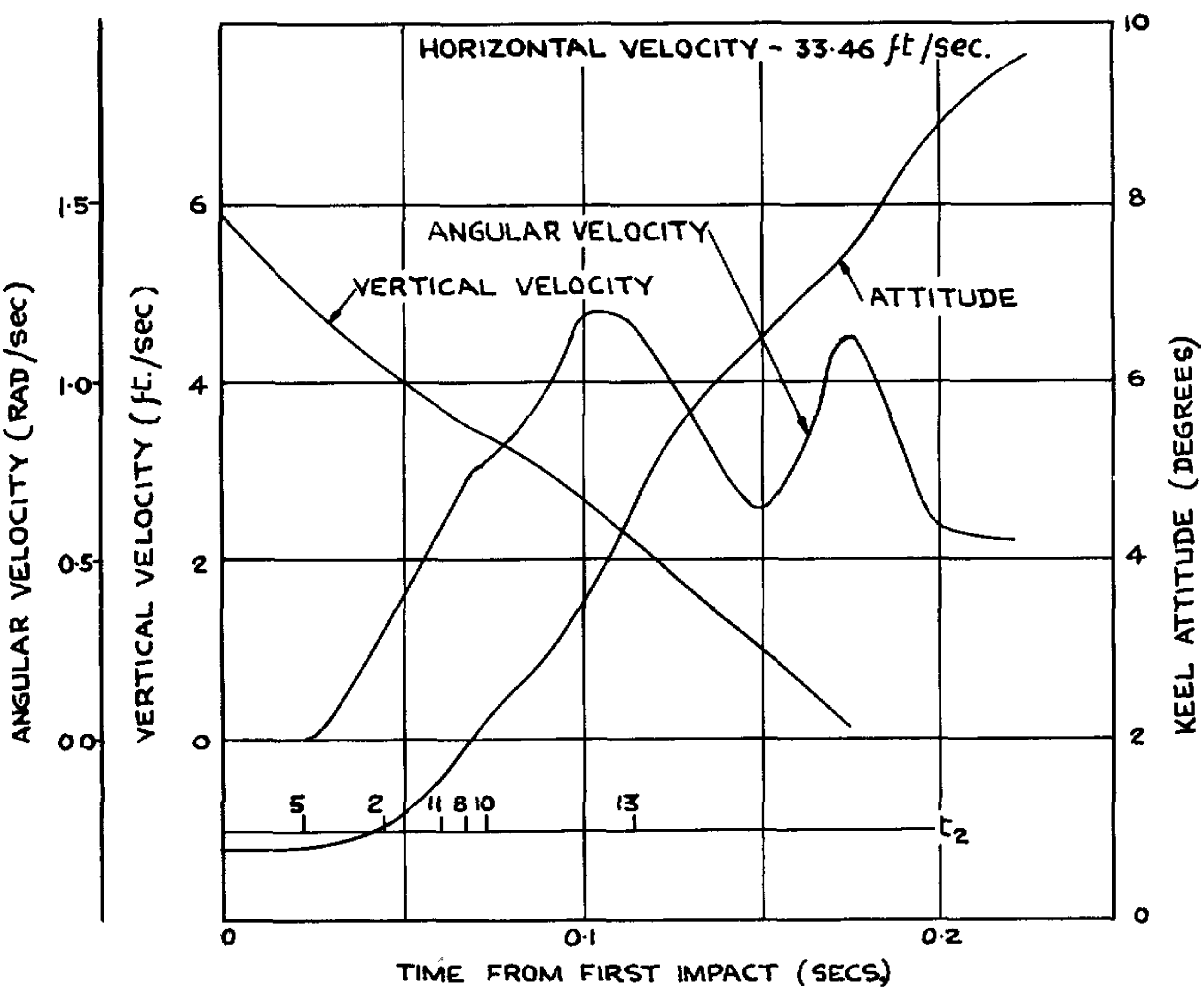

FIG. 40.

ACCELERATION DUE TO GRAVITY = 2·1 ft/sec². DAMPER 1/3.							
DIAPHRAGM	P. MAX.	INITIAL CONDITIONS			LOCAL IMPACT CONDITIONS		
		V_H	V_V'	α	V_H	V_V	α
1	—	—	—	—	—	—	—
2	—	—	—	—	—	—	—
3	—	—	—	—	—	—	—
4	—	—	—	—	—	—	—
5	9·7	33·75	6·1	6·7	33 06	2·09	6·83
6	—	—	—	—	—	—	—
7	—	—	—	—	—	—	—
8	11·0	33·75	6·1	6·7	33 77	5·78	6·73
9	—	—	—	—	—	—	—
10	18·5	33·75	6·1	6·7	33·13	4·05	6·80
11	9·7	33·75	6·1	6·7	32·91	3·76	6·77
12	—	—	—	—	—	—	—
13	1·3	33 75	6·1	0·1	33·28	3·72	0·43
14	—	—	—	—	—	—	—
15	—	—	—	—	—	—	—

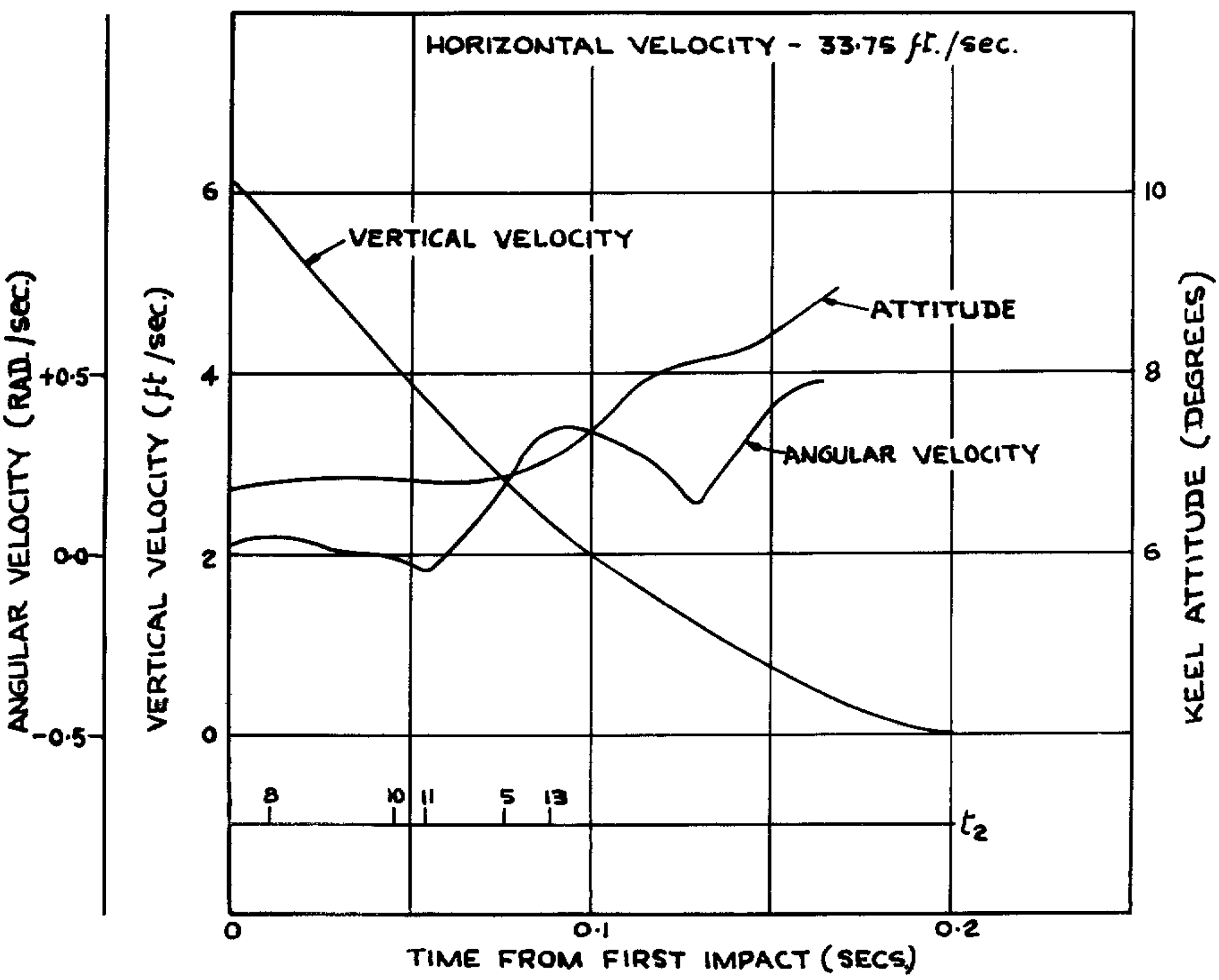

ACCELERATION DUE TO GRAVITY = 21 ft/sec² DAMPER 3/3.								
DIAPHRAGM	P. MAX.	INITIAL CONDITIONS			LOCAL IMPACT CONDITIONS			
		V_H	V_V	α	V_H	V_V	α
1	—	—	—	—	—	—	—
2	—	—	—	—	—	—	—
3	—	—	—	—	—	—	—
4	—	—	—	—	—	—	—
5	8·6	34·0	5·60	7·6	33·0	2·35	7·8
6	3·9	34·0	5·60	7·6	33·0	0·67	8·02
7	—	—	—	—	—	—	—
8	—	—	—	—	—	—	—
9	—	—	—	—	—	—	—
10	17·5	34·0	5·60	7·6	33·5	3·86	7·85
11	19·0	34·0	5·60	7·6	34·3	6·36	7·64
12	—	—	—	—	—	—	—
13	1·90	34·0	5·60	1·0	34·0	5·08	1·15
14	—	—	—	—	—	—	—
15	4·60	34·0	5·60	1·0	33·5	3·86	1·25

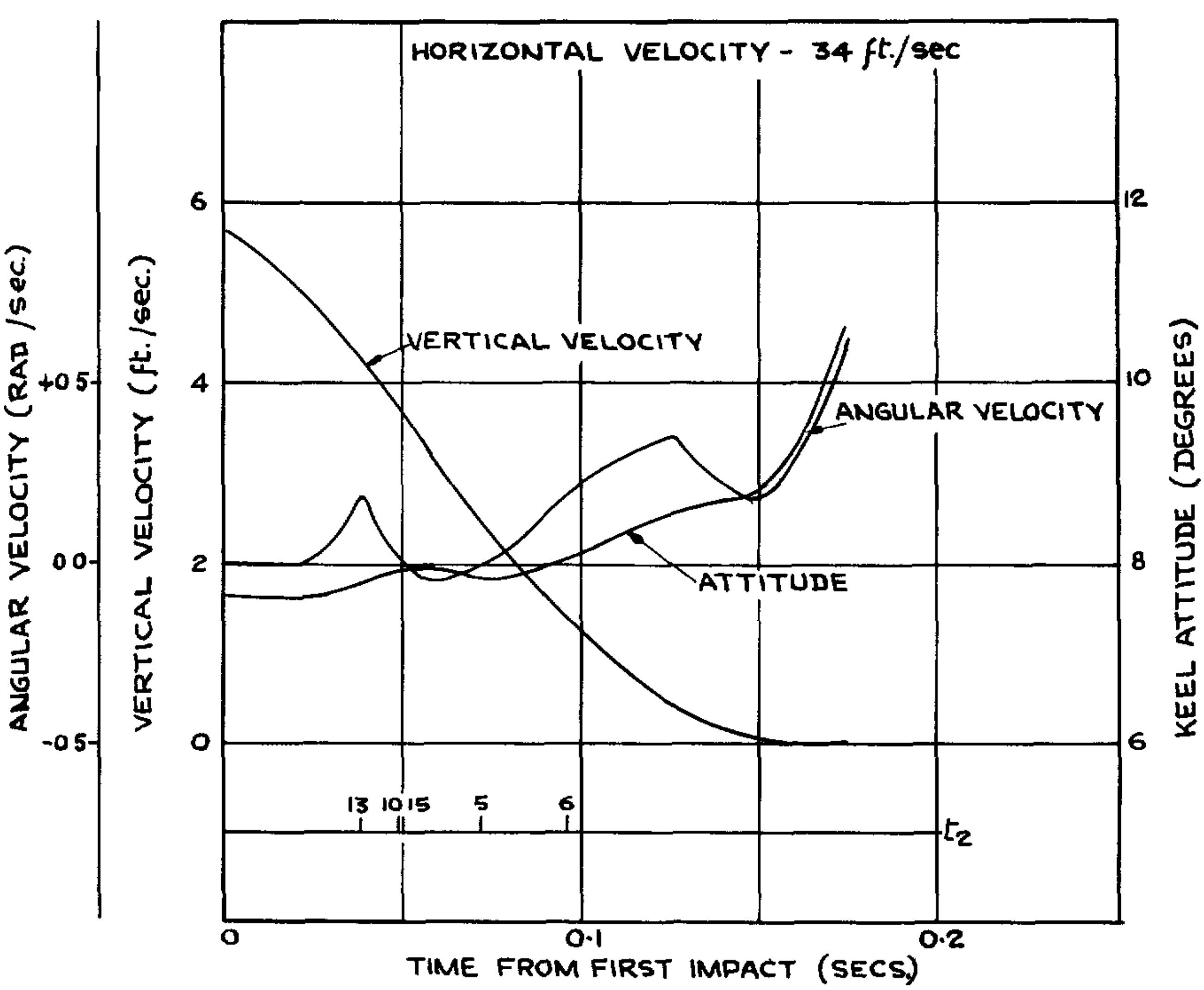

FIG. 42.

ACCELERATION DUE TO GRAVITY = 21 ft/sec.² DAMPER $\frac{1}{3}$							
DIAPHRAGM	P. MAX.	INITIAL CONDITIONS			LOCAL IMPACT CONDITIONS		
		V_H	V_V	α	V_H	V_V	α
1	2·1	33·11	5·5	7·0	32·92	5 0	7·0
2	6·8	33·11	5·5	2·2	33·93	2·34	2·5
3	5·8	33·11	5·5	2·2	32 94	5·1	2·2
4	6 0	33·11	5·5	2·2	33 84	2·29	2 7
5	1 8	33 11	5·5	- 3 2	32 93	5·05	- 3·2
6	11	33·11	5·5	- 3·2	33·55	3 92	- 3·1
7	——	——	——	——	——	——	——
8	3·6	33·11	5·5	- 3·2	33·95	4·05	- 2·6
9	2·3	33·11	5·5	- 3·2	34 02	3 78	- 1 95
10	4·0	33 11	5·5	- 3·2	33 86	4·52	- 2 8
11	4·15	33 11	5·5	- 3·2	33 99	4 13	- 1·8
12	——	——	——	——	——	——	——
13	2·3	33·11	5·5	- 9·2	33·90	5·98	-1·0
14	——	——	——	——	——	——	——
15	——	——	——	——	——	——	——

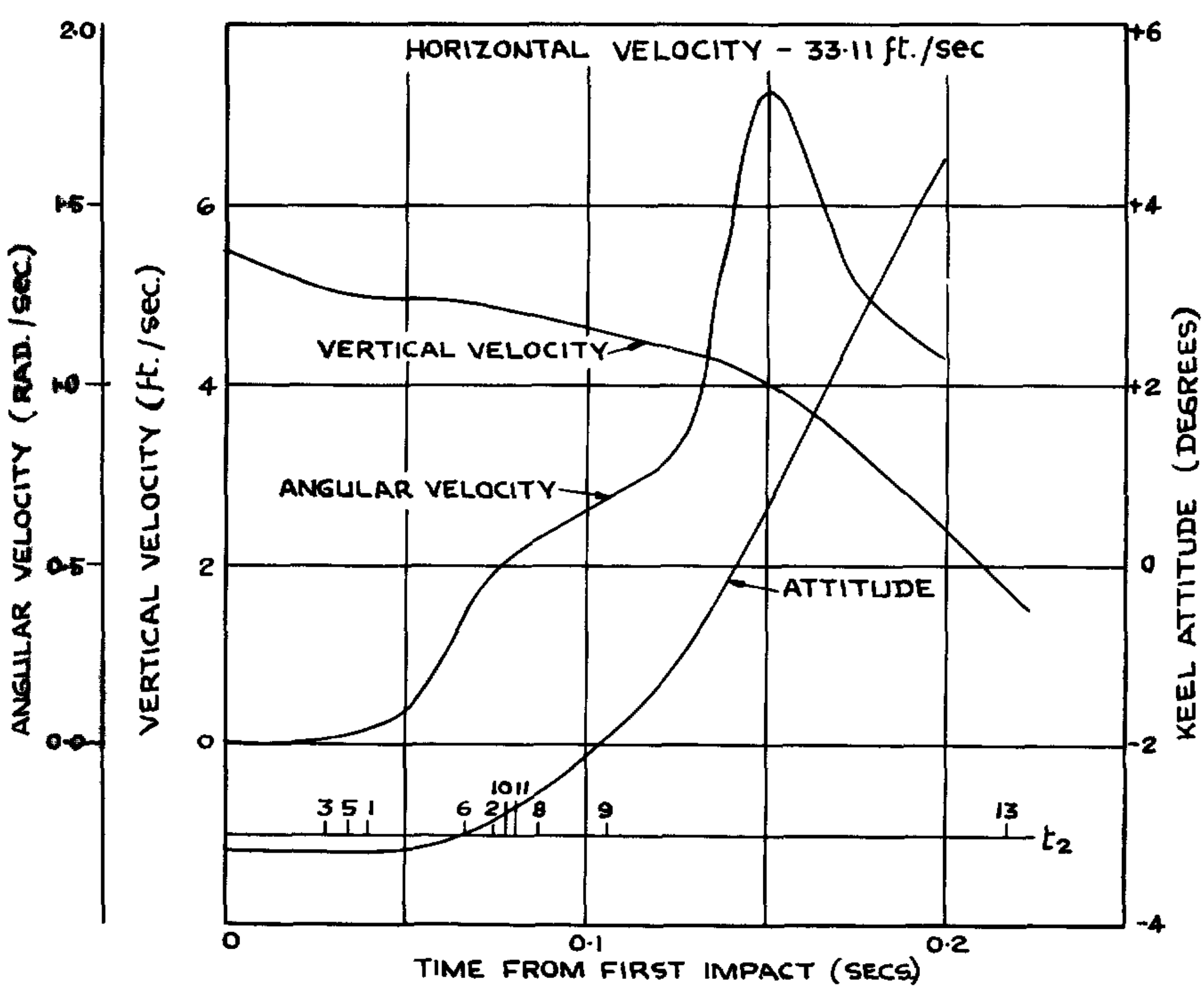

ACCELERATION DUE TO GRAVITY = 2·1 FT/SEC.

FIG. 43.

DAMPER 2/3.

DIAPHRAGM	$P_{MAX.}$	INITIAL CONDITIONS			LOCAL IMPACT CONDITIONS.		
		V_H	V_V	α	V_H	V_V	α
1	5·0	33·6	8·13	7·3	34·0	6·9	7·5
2	7·5	33·5	7·83	2·5	33·5	7·99	2·8
3	5·5	33·6	7·84	2·5	34·0	6·8	2·7
4	5·1	33·6	7·84	2·5	33·8	4·97	2·77
5	3·1	33·5	7·46	−2·9	34·0	6·8	2·7
6	4·7	33·6	7·46	−2·9	33·7	6·0	−2·7
7							
8	1·8	33·6	7·11	−2·9	33·7	6·0	−2·7
9							
10	2·5	33·6	6·98	−2·9	35·9	5·37	−2·6
11	5·7	33·6	6·98	−2·9	33·7	6·0	−2·7
12							
13							
14							
15							

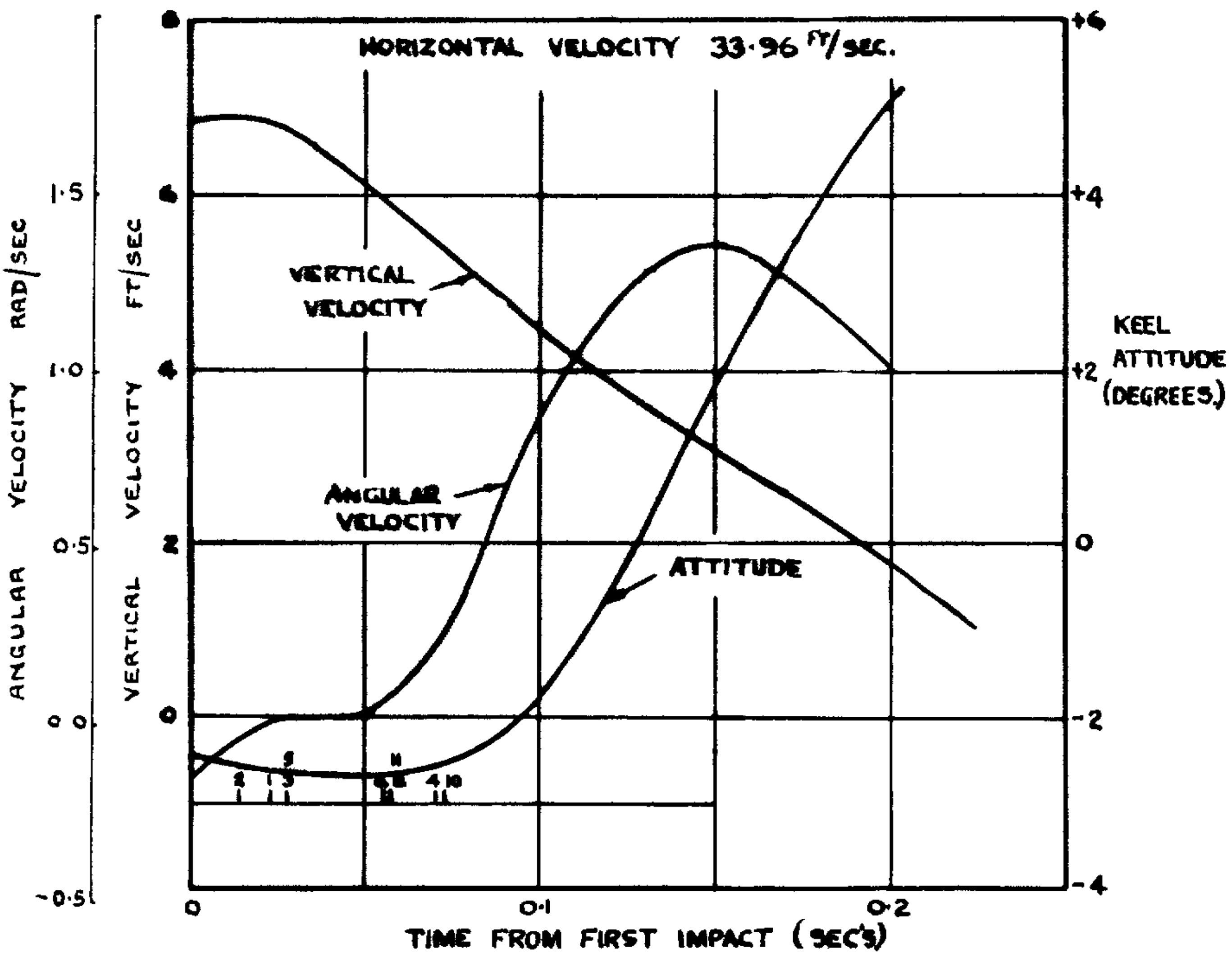

FIG.44.

ACCELERATION DUE TO GRAVITY 2·1 FT/SEC^2

DAMPER 0

DIAPHRAGM	P MAX	INTIALS CONDITIONS			LOCAL IMPACT CONDITIONS		
		V_H	V_V	∝	V_H	V_V	∝
1	2·35	32·13	5·4	2·8	32·99	3·44	3·1
1a	0·95	32·13	5·4	3·36	32·08	6·22	4·16
1b	1·30	32·13	5·4	9·2	33·0	2·56	10·02
2	2·70	32·13	5·4	-2·0	32·90	4·06	-1·4
3	3·60	32·13	5·4	-2·0	32·79	4·21	-1·3
4	2·10	32·13	5·4	-2·0	32·13	6·40	-1·2
5							
6							
7							
8							
9							
10							
11							
12							
13							

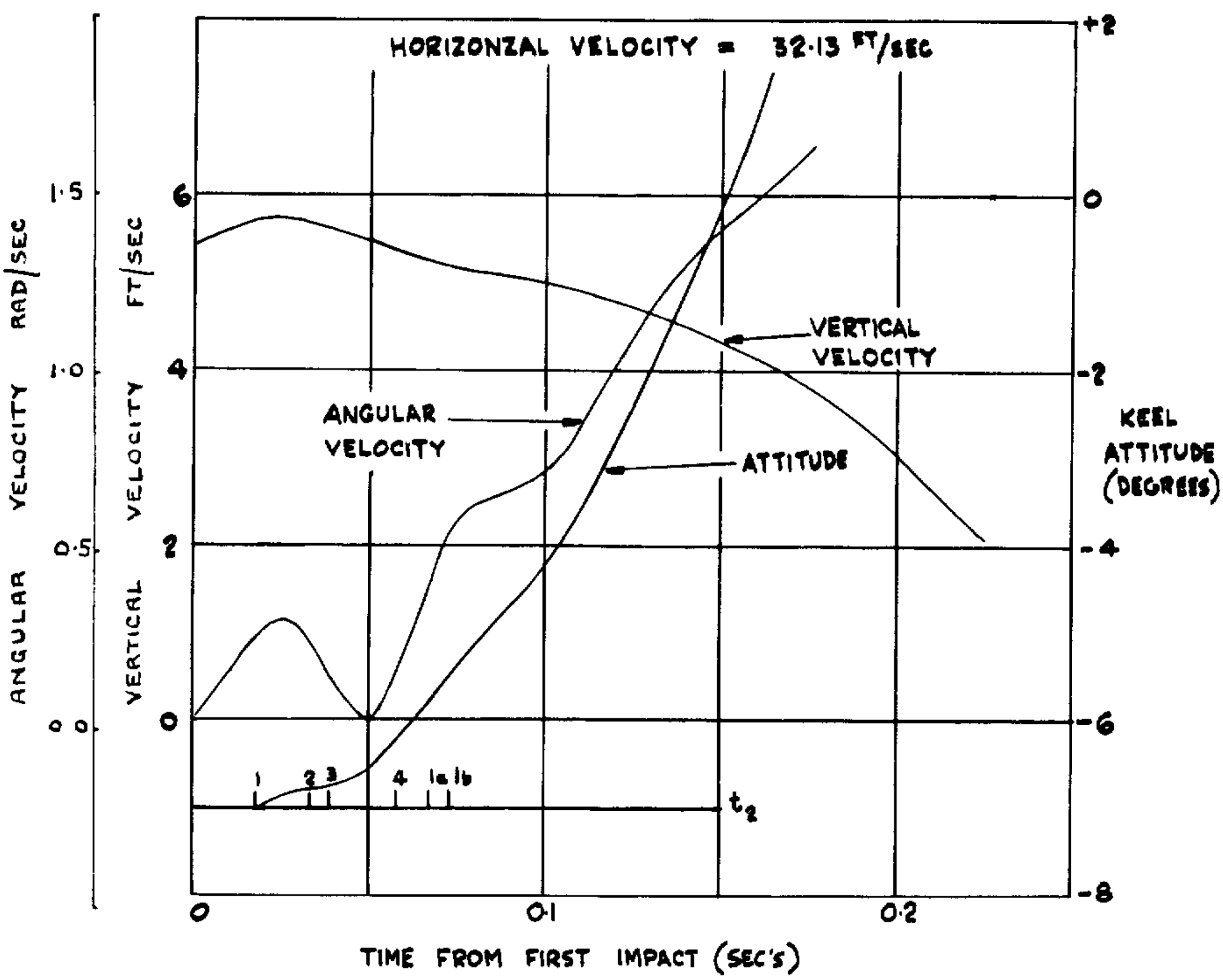

FIG 45.

ACCELERATION DUE TO GRAVITY = 2·1 FT/SEC^2 DAMPER 3/3.							
DIAPHRAGM	P_{MAX}	INITIAL CONDITIONS			LOCAL IMPACT CONDITIONS		
		V_H	V_V	α	V_H	V_V	α
1	5·5	32·4	4·95	4·2	32·4	5·1	4·2
1a	4·2	32·4	4·95	4·75	32·4	5·1	4·75
1b	1·6	32·4	4·95	10·6	32·4	5·1	10·6
2	>5·0	32·4	4·95	-0·6	32·4	5·1	-0·6
3	4·0	32·4	4·95	-0·6	32·4	5·1	-0·6
4	2·35	32·4	4·95	-0·6	32·4	5·1	-0·6
5							
6							
7							
8							
9							
10							
11							
12							
13							

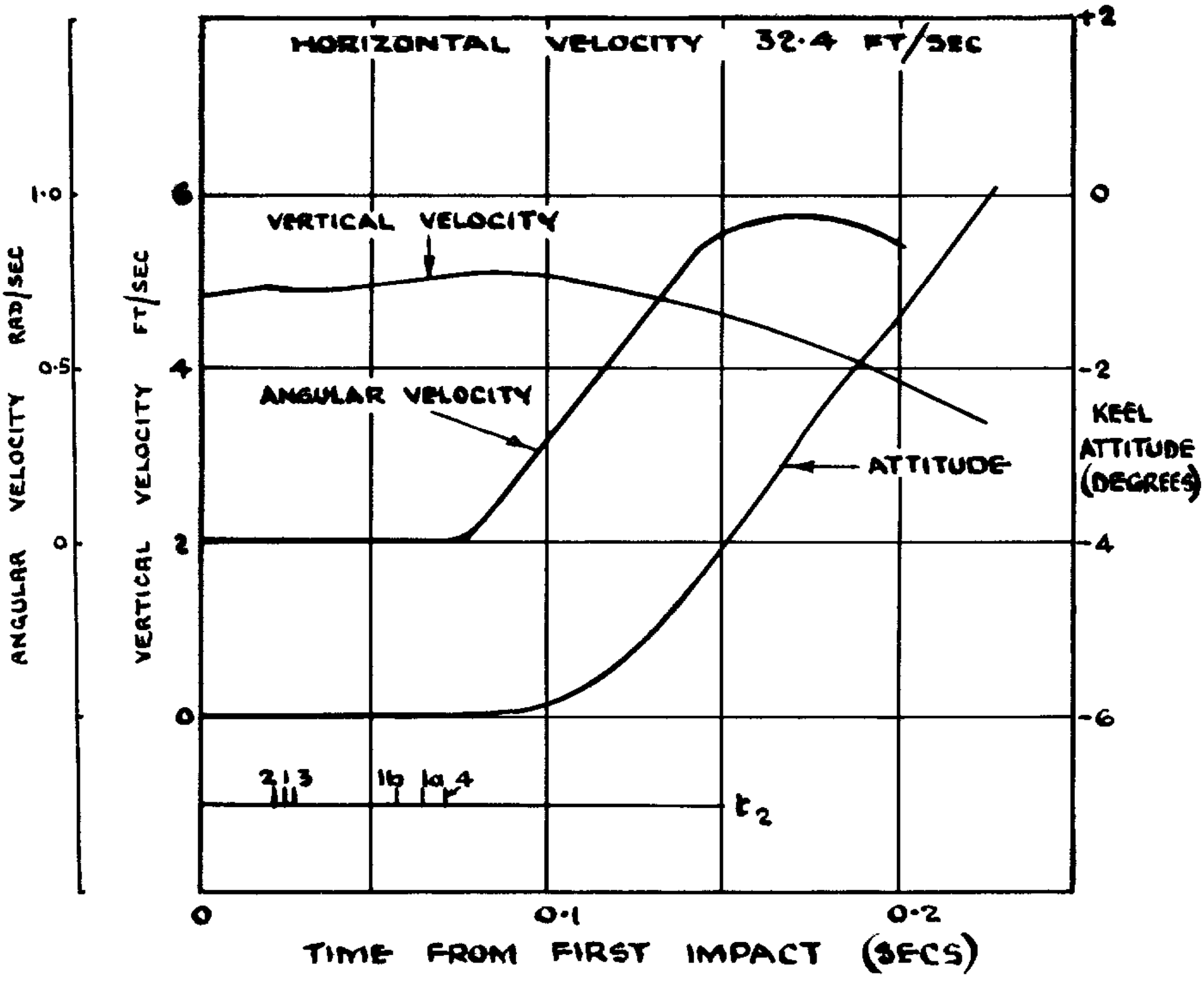

ACCELERATION DUE TO GRAVITY = 21 FT/SEC

FIG 46

DAMPER 2/3

DIAPHRAGM	PMAX	INITIAL VELOCITY			LOCAL IMPACT CONDITIONS		
		V_H	V_V	α	V_H	V_V	α
1							
1a	6·1	33·22	6·7	2·75	33·39	4·56	3·3
1b	1·35	33·22	6·7	8·60	33·61	3·49	9·2
2	5·0	33·22	6·7	-2·60	33·54	6·19	-2·6
3	8·0	33·22	6·7	-2·60	33·63	5·57	-2·4
4	22·8	33·22	6·7	-2·60	33·56	5·41	-2·25
5							
6							
7							
8							
9							
10							
11							
12							
13							
14							
15							

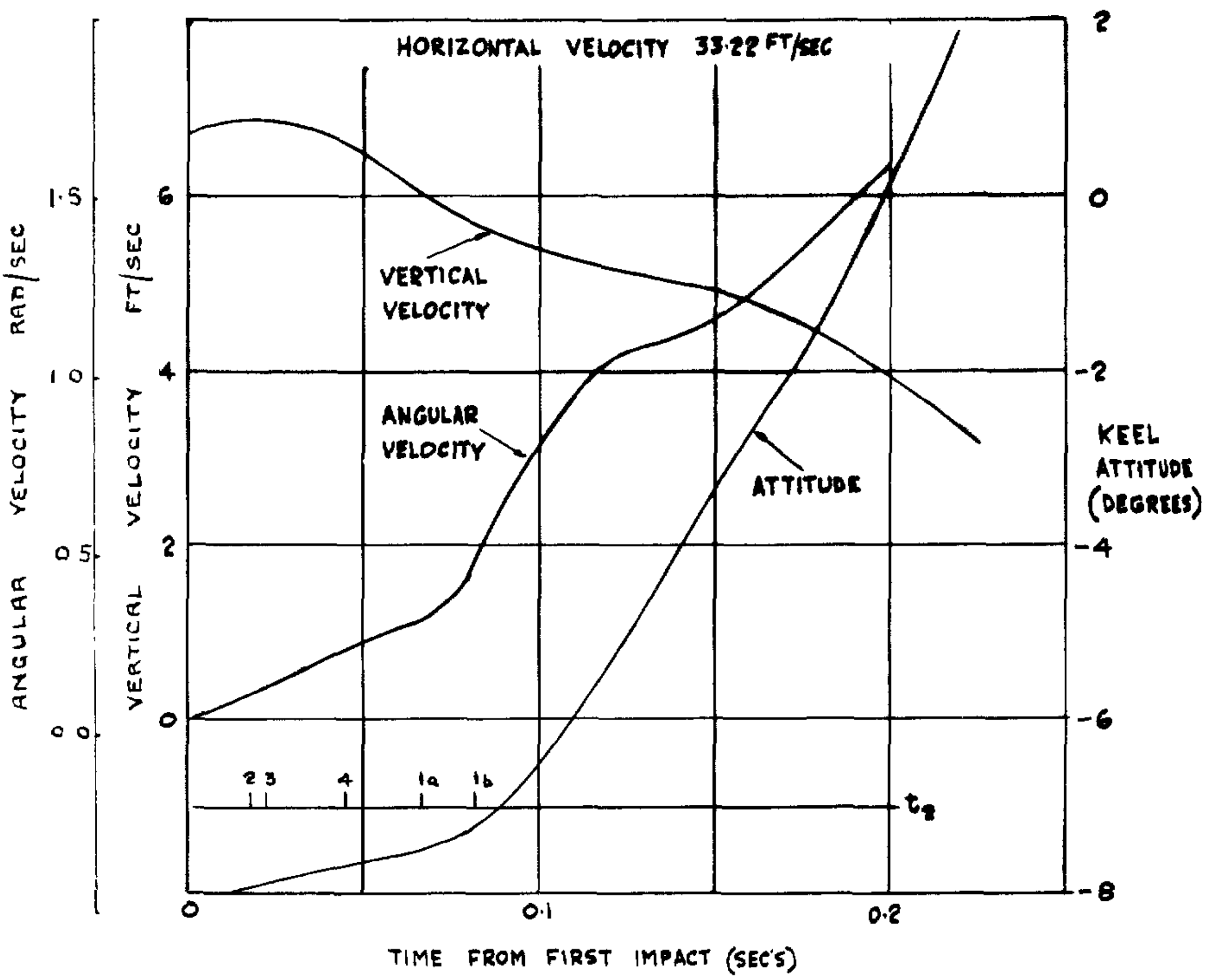

ACCELERATION DUE TO GRAVITY = 21 FT/SEC² — FIG. 47.

DAMPER 3/3

DIAPHRAGM	P MAX	INITIAL CONDITIONS			LOCAL IMPACT CONDITIONS		
		V_H	V_V	α	V_H	V_V	α
1	3·5	30·8	6·15	8·1	31·2	3·72	8·15
2	9·0	30 8	6·15	3·3	31·2	4·15	3·35
3	8·0	30·8	6 15	3·3	31·2	4·23	3·20
4	2 4	30 8	6·15	3·3	32 2	-0·43	4·40
5	2·9	30·8	6·15	- 2·1	30·7	5·84	- 2·26
6	2·2	30·8	6·15	- 2·1	30·9	-0·08	4·5
7							
8	2·3	30·8	6·15	-2·1	30·7	5·92	-2·2
9							
10	2·45	30·8	6·15	-2·1	31·2	5·47	-2·2
11	7·0	30·8	6·15	-2·1	30·7	5·92	-2·2
12							
13							
14							
15							

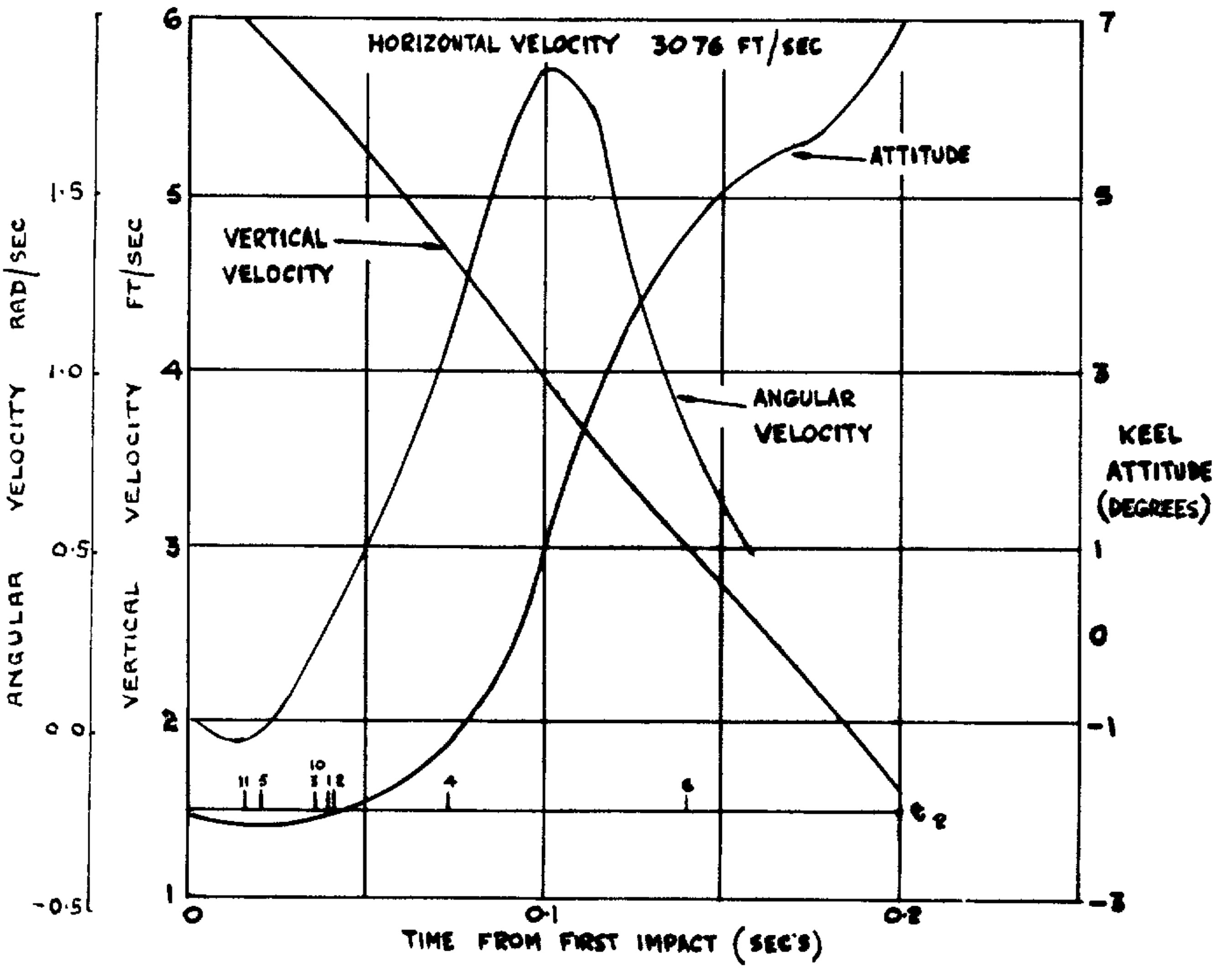

ACCELERATION DUE TO GRAVITY = 2·1 FT/SEC² **FIG 48**

DAMPER 3/3

DIAPHRAGM	P MAX	INITIAL CONDITIONS			LOCAL IMPACT CONDITIONS		
		V_H	V_V	α	V_H	V_V	α
1	3·4	35·38	6·05	7·5	36·28	2·14	8·15
2	8 0	35·38	6·05	2·7	35·43	6·2	2·7
3	6·7	35 38	6·05	2 7	35·78	4 86	2·9
4							
5	3 3	35 38	6·05	-2·7	35 62	5·61	-2·6
6	2·04	35 38	6 05	-2 7	35·93	4·89	-2·37
7							
8							
9							
10	3·0	35 38	6 05	-2 7	36 16	5·40	-2 2
11	6·2	35·38	6·05	-2·7	36·47	4·92	-1 7
12							
13							
14							
15							

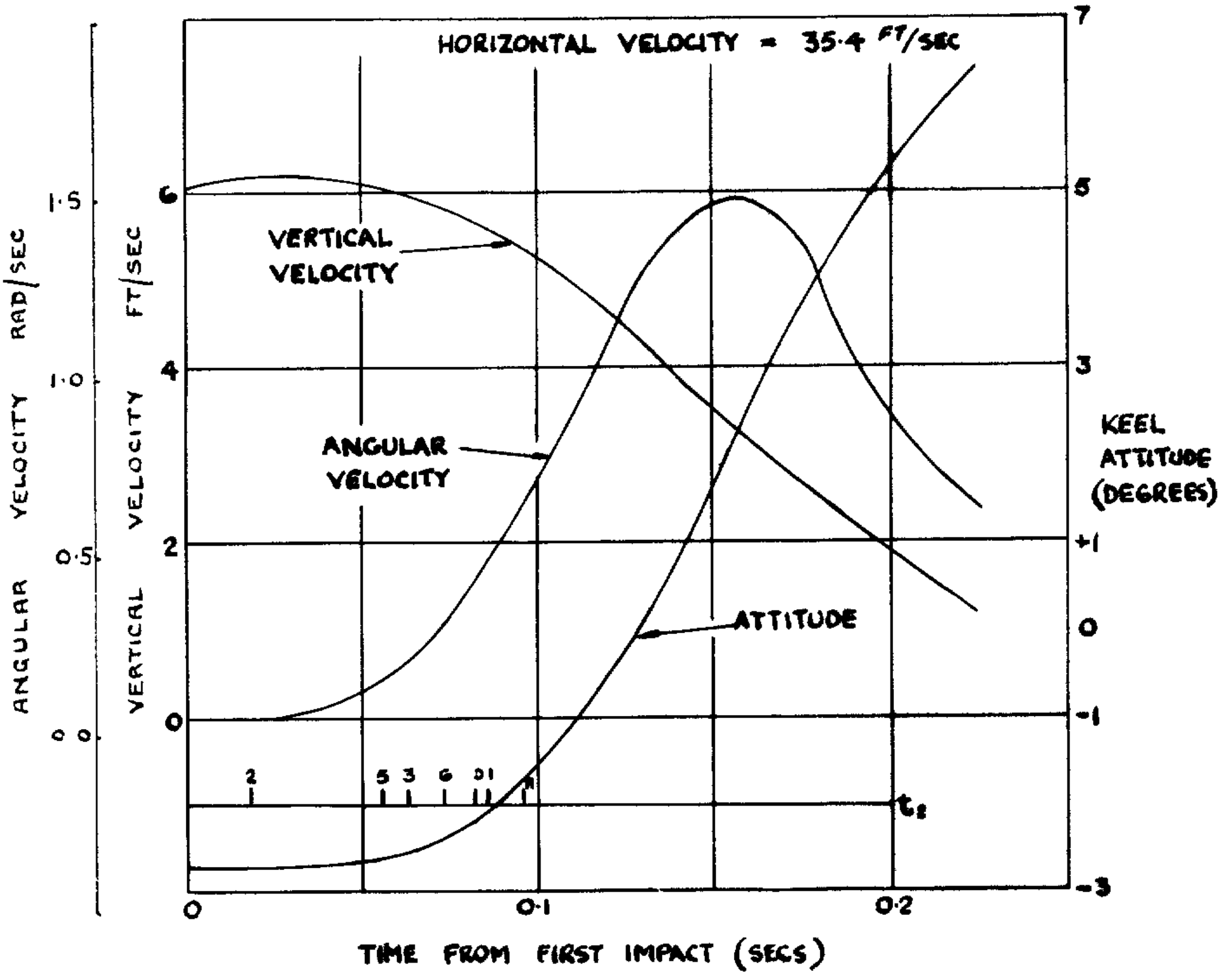

ACCELERATION DUE TO GRAVITY - ZERO
DAMPER 2/3

DIAPHRAGM	P_{MAX}	INITIAL CONDITIONS			LOCAL IMPACT CONDITIONS		
		V_H	V_V	α	V_H	V_V	α
1	4·9	33·0	5·9	7·2	33·2	4·37	7·3
2	7·0	33·0	5·9	2·4	33·0	5·85	2·4
3	3·35	33·0	5·9	2·4	34·0	1·44	3·3
4	3·7	33·0	5·9	2·4	33·9	1·42	3·3
5	3·4	33·0	5·9	−3·0	32·9	5·75	−3·0
6	1·1	33·0	5·9	−3·0	34·0	2·91	−2·2
7							
8							
9							
10	3·1	33·0	5·9	−3·0	34·0	4·52	−2·3
11	3·6	33·0	5·9	−3·0	34·0	4·07	−1·7
12							
13							
14							
15							

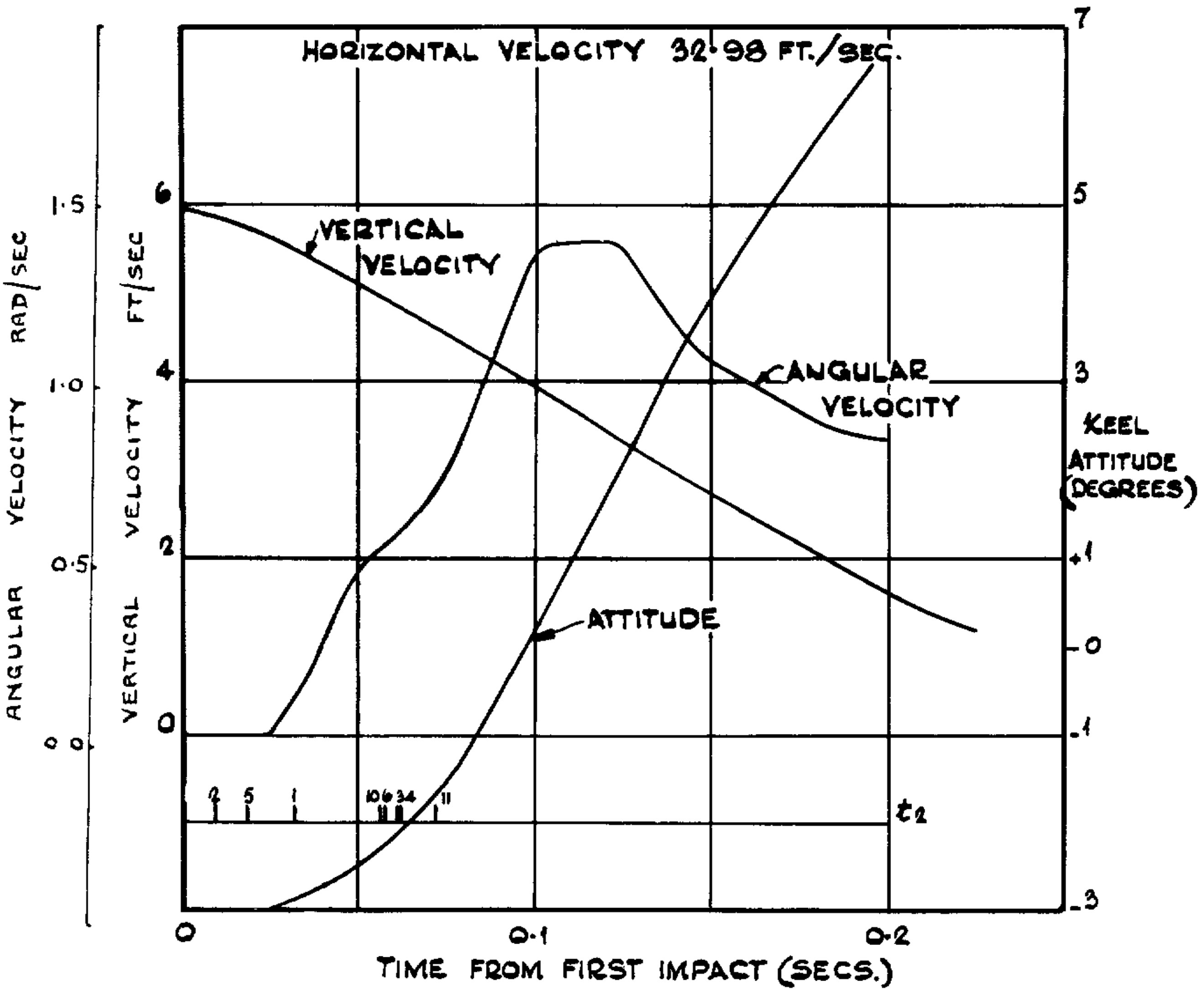

FIG 50

ACCELERATION DUE TO GRAVITY 4·2 FT/SEC²
DAMPER 2/3

DIAPHRAGM	$P_{MAX.}$	INITIAL CONDITIONS			LOCAL IMPACT CONDITIONS		
		V_H	V_V	α	V_H	V_V	α
1							
2							
3							
4							
5	4·6	32·4	6·2	2·2	32·3	5·82	2·12
6	3·1	32·4	6·2	2·2	32·3	6·00	2·1
7	5·4	32·4	6·2	2·2			
8	9·6	32·4	6·2	2·2	33·1	·52	5·7
9							
10	10·5	32·4	6·2	2·2	32·9	4·87	2·28
11	15·0	32·4	6·2	2·2	33·4	3·62	2·8
12							
13	2·55	32·4	6·2	−4·4	33·4	7·98	−3·15
14							
15							

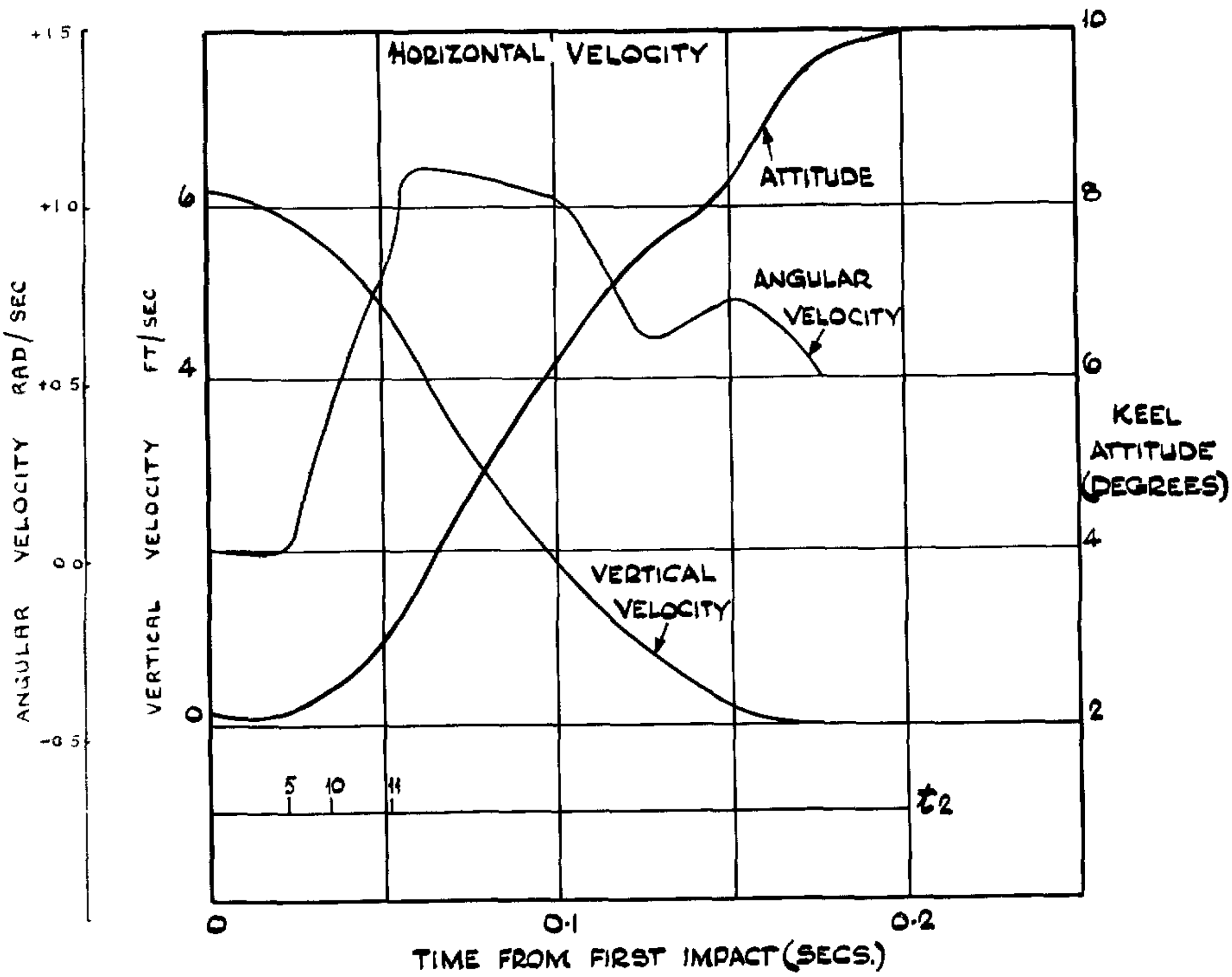

FIG. 51

ACCELERATION DUE TO GRAVITY 4·2 FT./SEC²
DAMPER 2/3.

DIAPHRAGM	P_{MAX}	INITIAL CONDITIONS			LOCAL IMPACT CONDITIONS		
		V_H	V_V	α	V_H	V_V	α
1	2·5	36·4	5·8	7·8	36·9	3·91	8·0
2	>5	36·4	5·8	3·0	37·3	2·27	3·85
3	8·3	36·4	5·8	3·0	37·3	4·34	3·2
4	4·5	36·4	5·8	3·0	36·5	4·15	4·05
5	3·4	36·4	5·8	− 2·4	36·7	5·60	− 2·3
6	1·35	36·4	5·8	− 2·4	37·4	4·14	− 2·0
7							
8	2·6	36·4	5·8	− 2·4	37·4	5·09	− 1·95
9							
10	2·3	36·4	5·8	− 2·4	37·4	5·44	− 1·90
11							
12							
13							
14							
15							

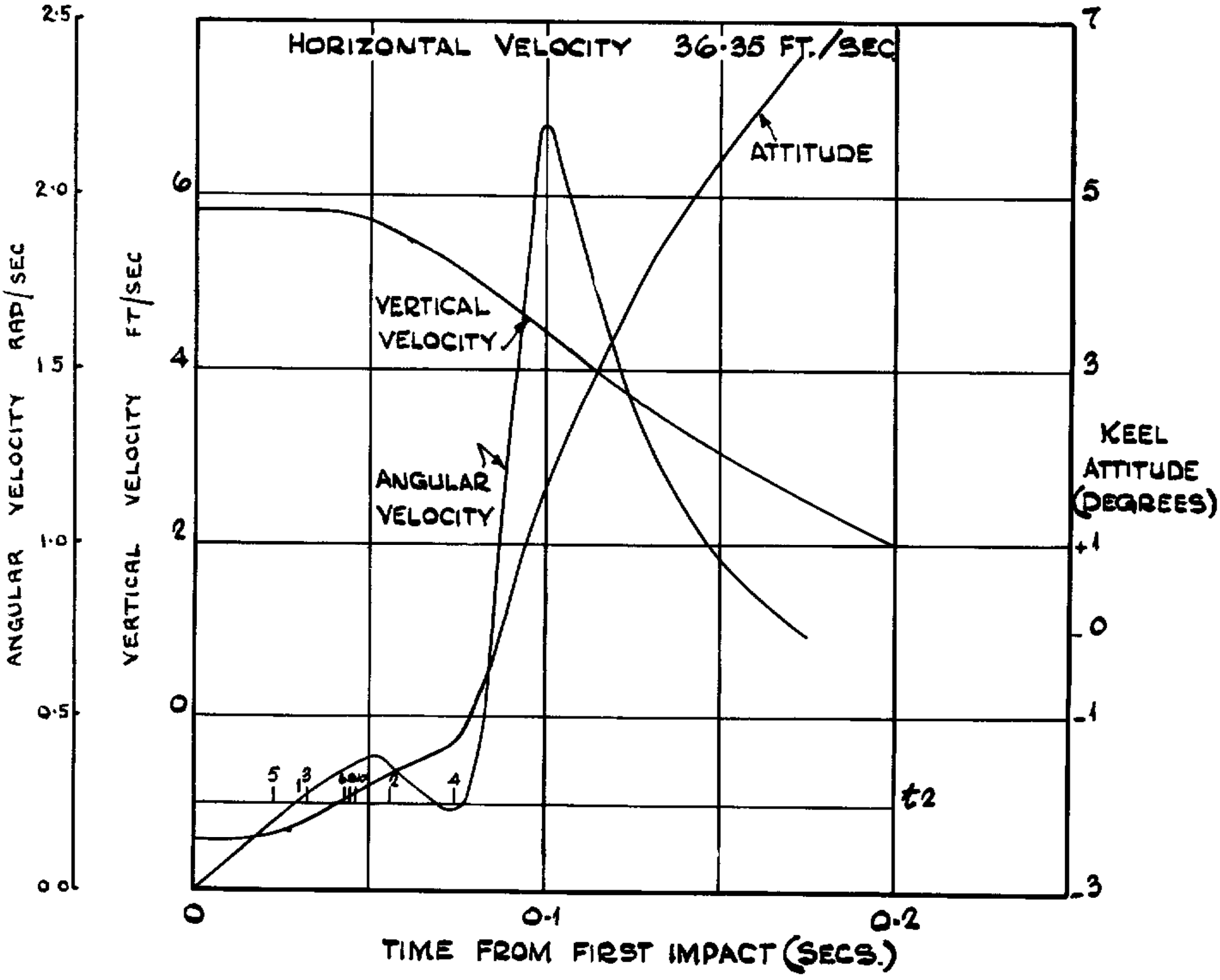

ACCELERATION DUE TO GRAVITY 6·3 FT./SEC.²
DAMPER 2/3

DIAPHRAGM	P_{MAX}	INITIAL CONDITIONS			LOCAL IMPACT CONDITIONS		
		V_H	V_V	α	V_H	V_V	α
1	3·35	34·4	6·6	7·5	34·25	4·06	7·64
2	8·0	34·4	6·6	2·7	34·26	5·06	2·82
3	5·0	34·4	6·6	2·7	34·30	5·24	2·77
4	4·5	34·4	6·6	2·7	34·69	5·01	3·15
5	3·1	34·4	6·6	−2·7	34·31	5·42	−2·61
6	3·7	34·4	6·6	−2·7	34·29	5·37	−2·60
7							
8	3·6	34·4	6·6	−2·7	34·23	5·33	−2·55
9							
10	2·7	34·4	6·6	−2·7	34·23	5·40	−2·55
11							
12							
13							
14							
15							

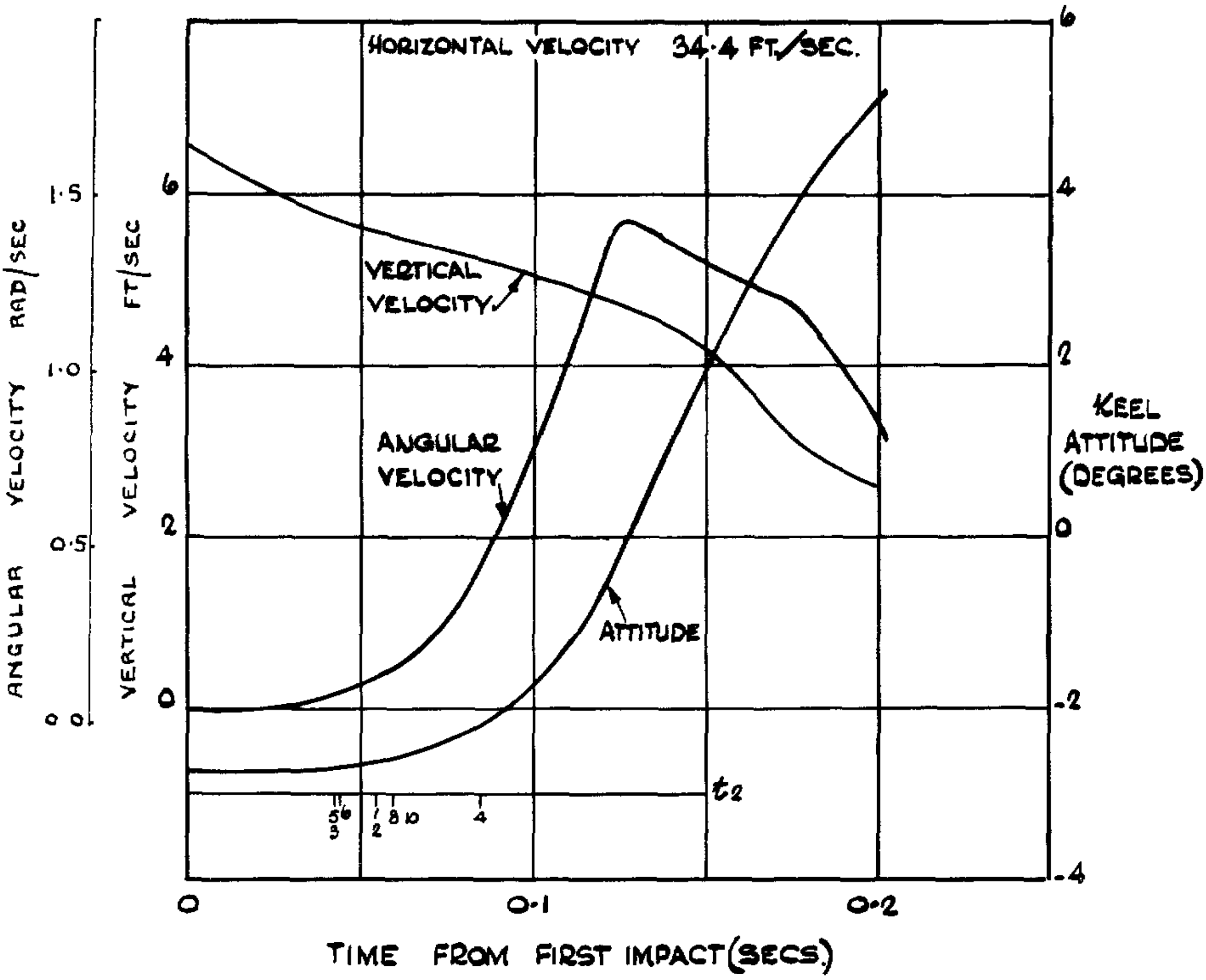

ACCELERATION DUE TO GRAVITY 6·3 FT/SEC²
DAMPER 2/3.

DIAPHRAGM	P_{MAX}	INITIAL CONDITIONS			LOCAL IMPACT CONDITIONS		
		V_H	V_V	α	V_H	V_V	α
1							
2							
3							
4							
5	5·1	36·4	5·55	2·3	36·5	3·96	2·35
6	1·9	36·4	5·55	2·3	37·1	0·77	3·5
7							
8	4·3	36·4	5·55	2·3	36·2	5·15	2·26
9							
10	9·0	36·4	5·55	2·3	36·8	4·15	2·6
11							
12							
13	1·65	36·4	5·55	−4·3	37·0	6·09	− 1·55
14							
15	5·8	36·4	5·55	−4·3	36·98	9·21	−0·85

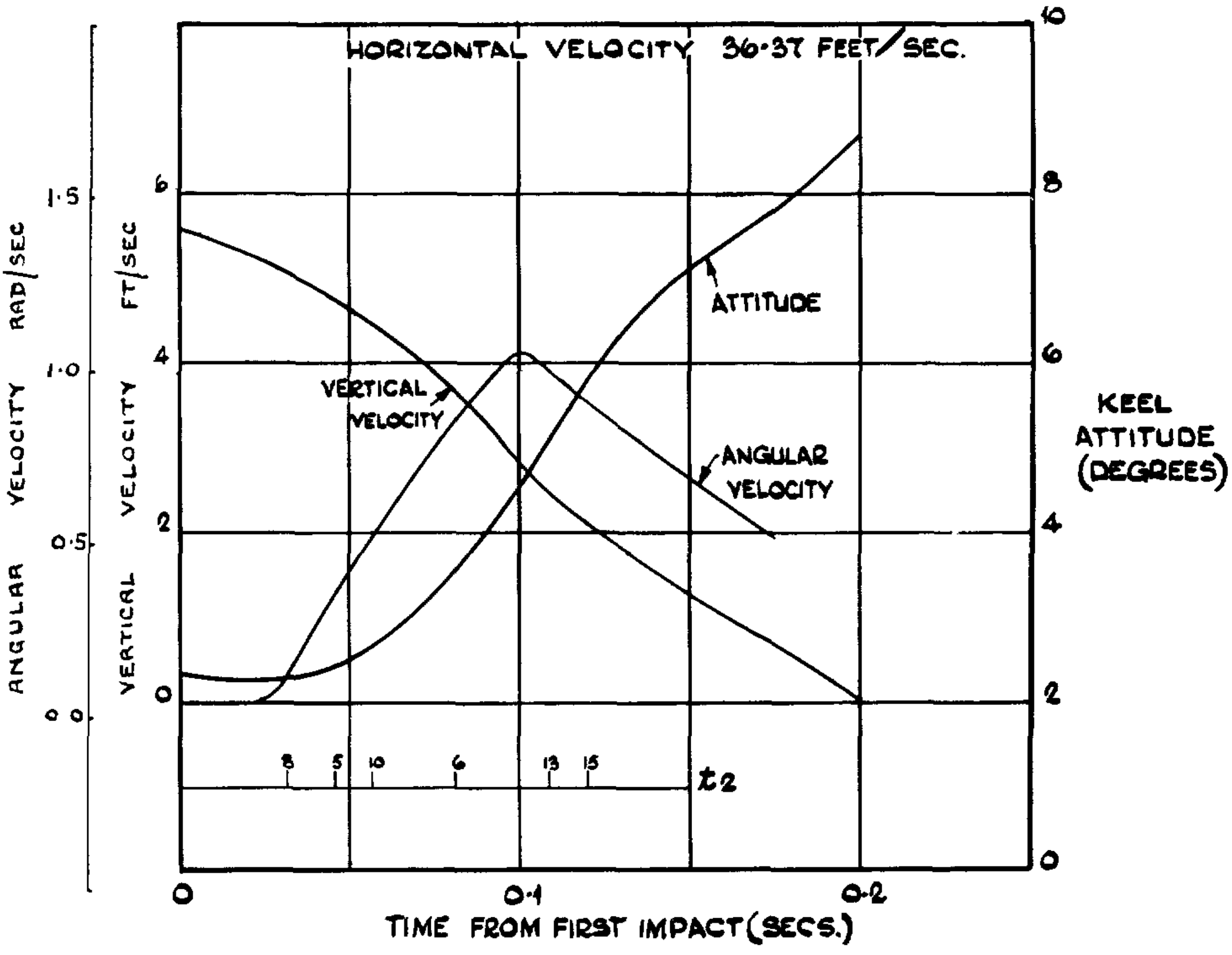

FIG. 54

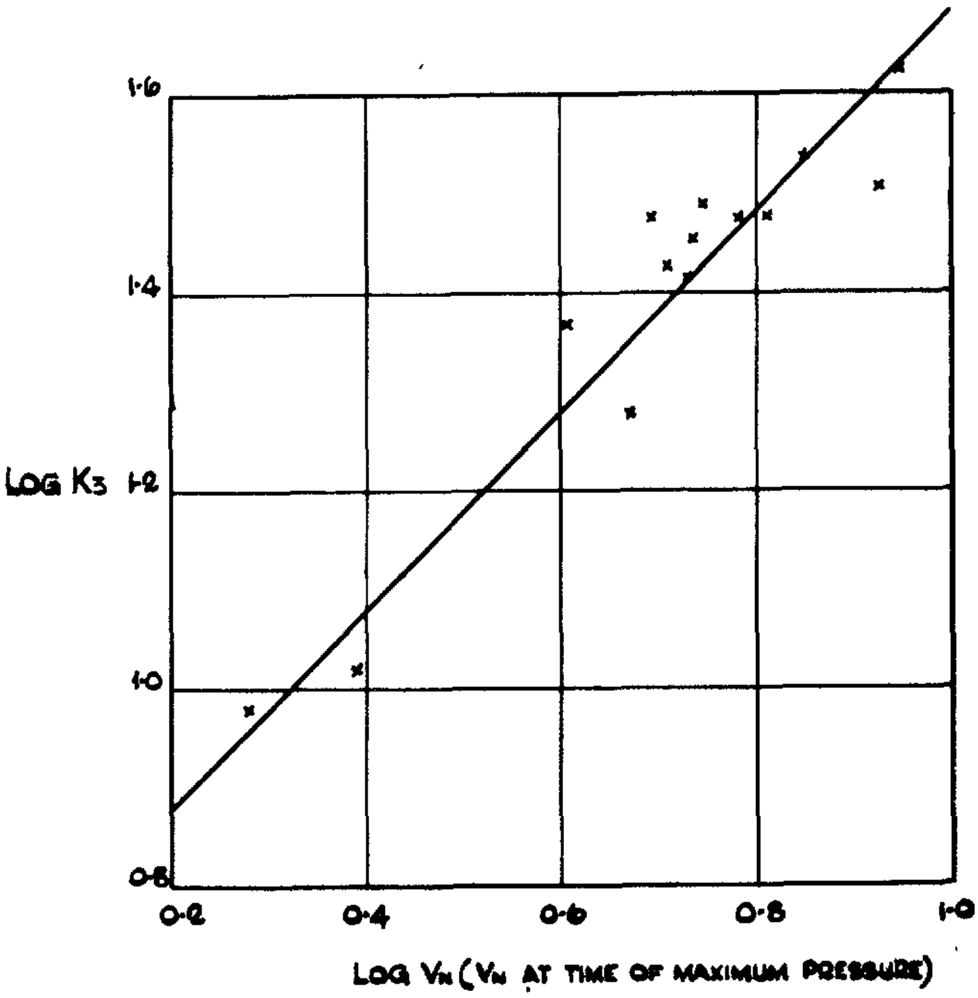

VARIATION OF K3 WITH VN FOR RATES OF DESCENT OF 4 TO 6 FT./SEC

(POINTS FROM POSITION 9)

FIG. 55

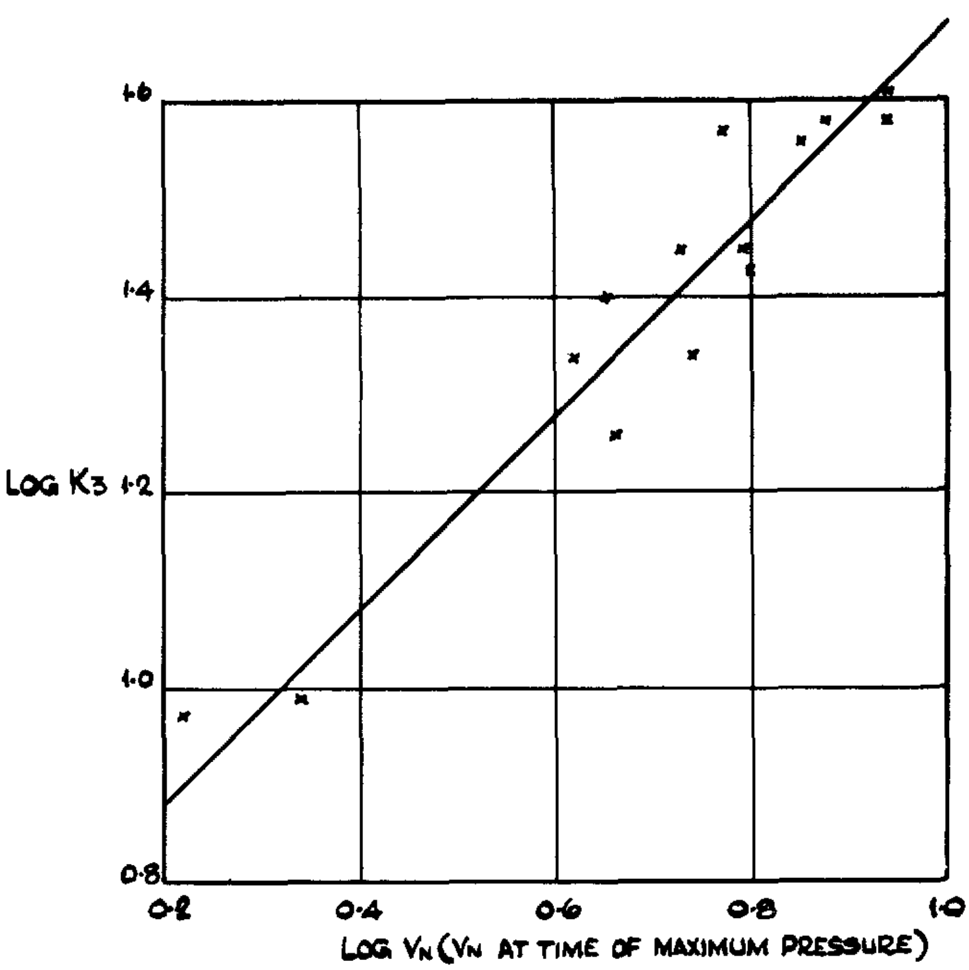

VARIATION OF K3 WITH VN FOR RATES OF DESCENT OF 4 TO 6 FT./SEC.

(POINTS FROM POSITION 10)

FIG. 56

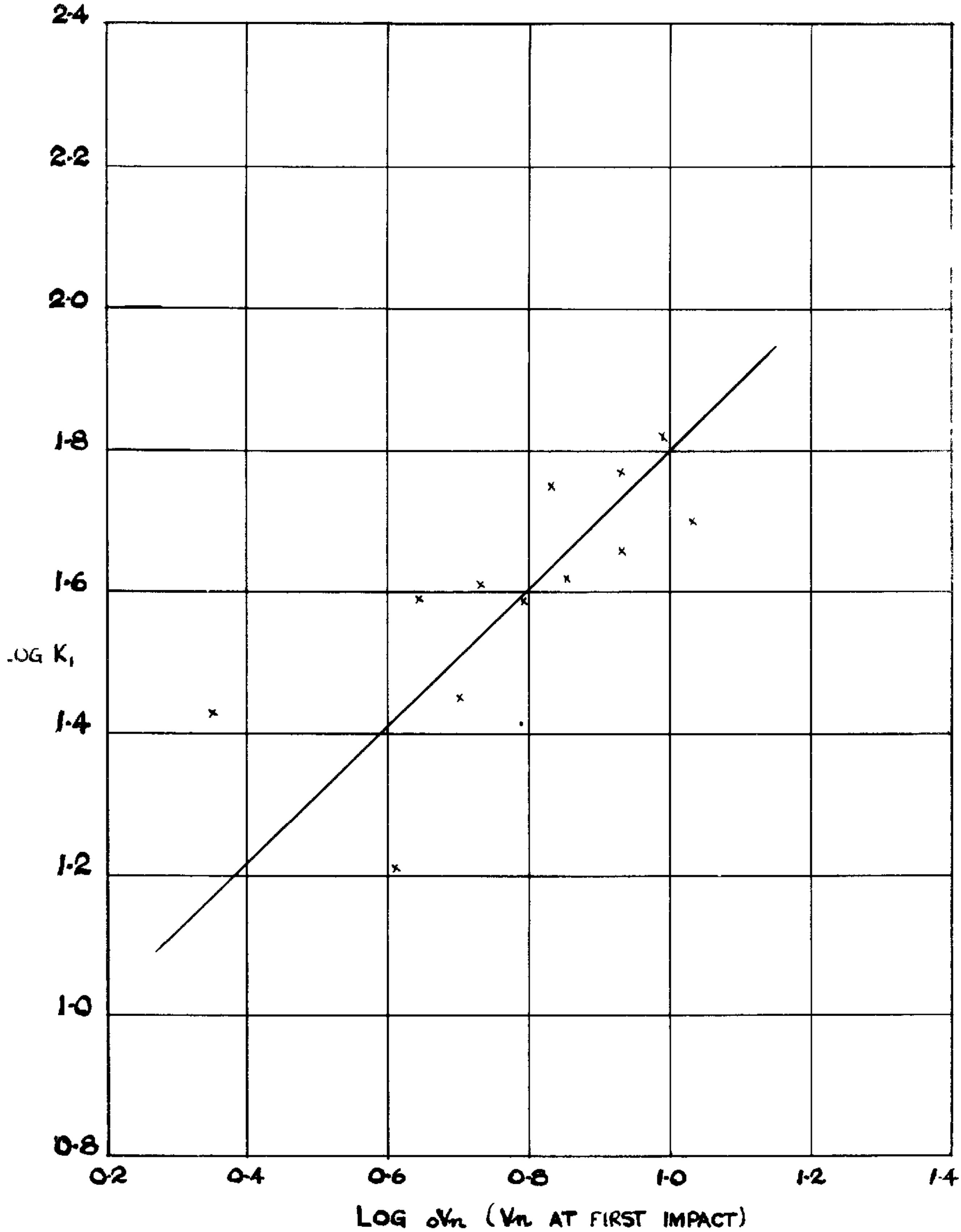

VARIATION OF K_1 WITH $_oV_n$ FOR A RATE OF DESCENT OF 4 TO 6 FT/SEC
(POINTS FROM POSITION 9)

FIG 57.

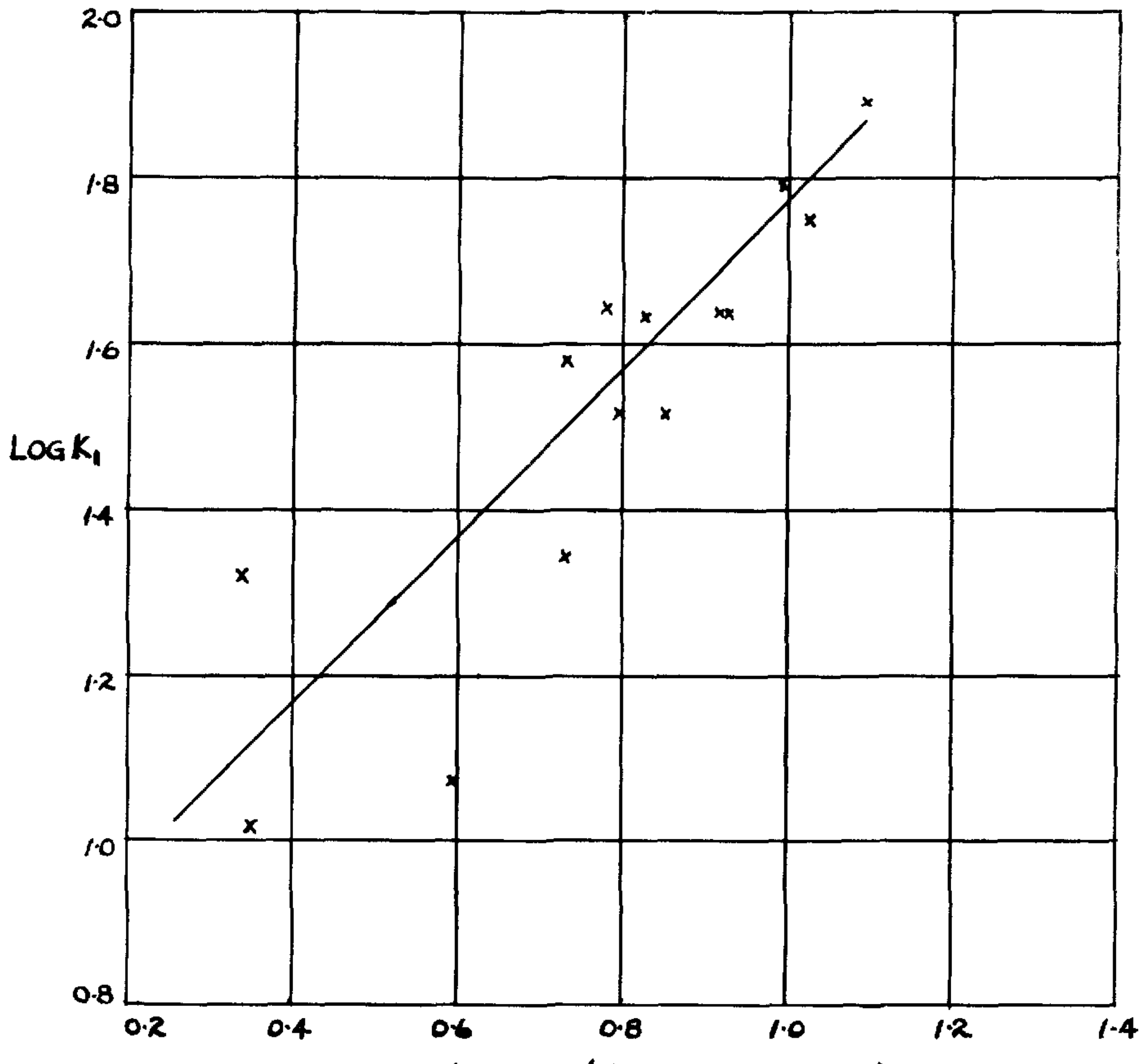

VARIATION OF K_1 WITH $_0V_n$ FOR RATES OF DESCENT OF 4 TO 6 FT/SEC.
(POINTS FROM POSITION 10)

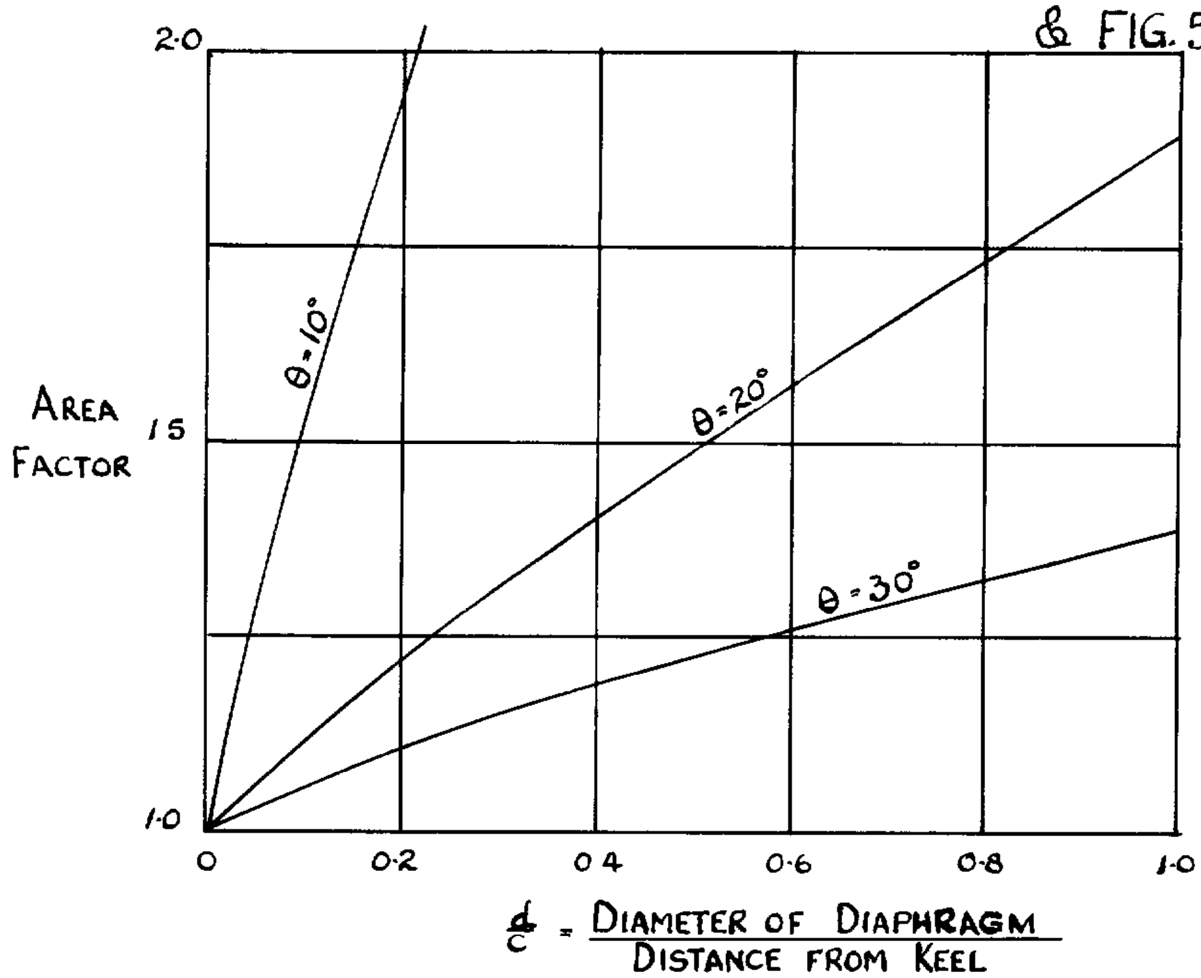

VARIATION OF AREA FACTOR WITH DEAD RISE – θ AND RATIO $\frac{d}{c}$ FOR CIRCULAR DIAPHRAGMS.

FIG. 59.

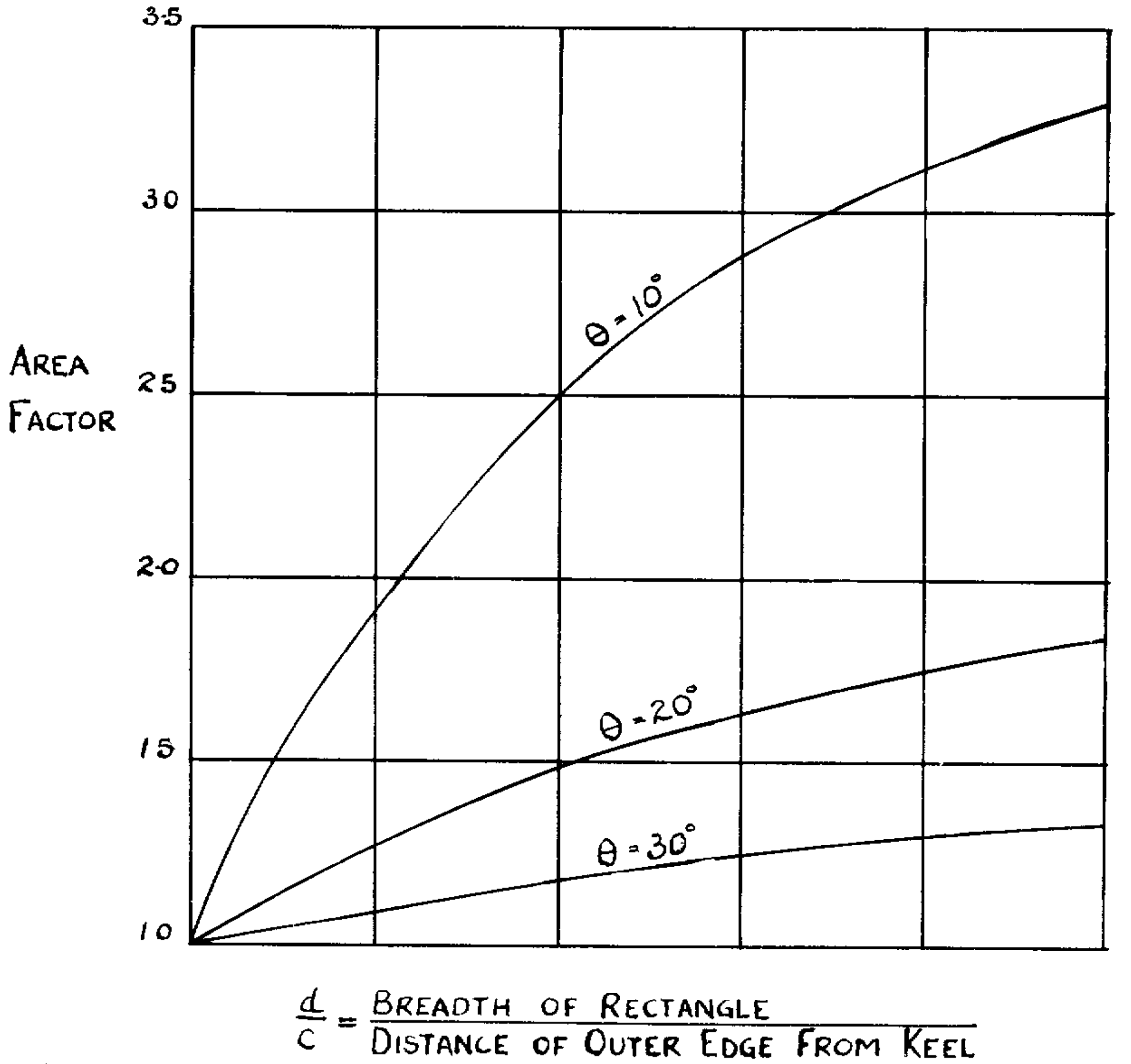

VARIATION OF AREA FACTOR WITH DEAD RISE AND RATIO $\frac{d}{c}$ FOR RECTANGULAR DIAPHRAGMS

FIG 61
& FIG 60

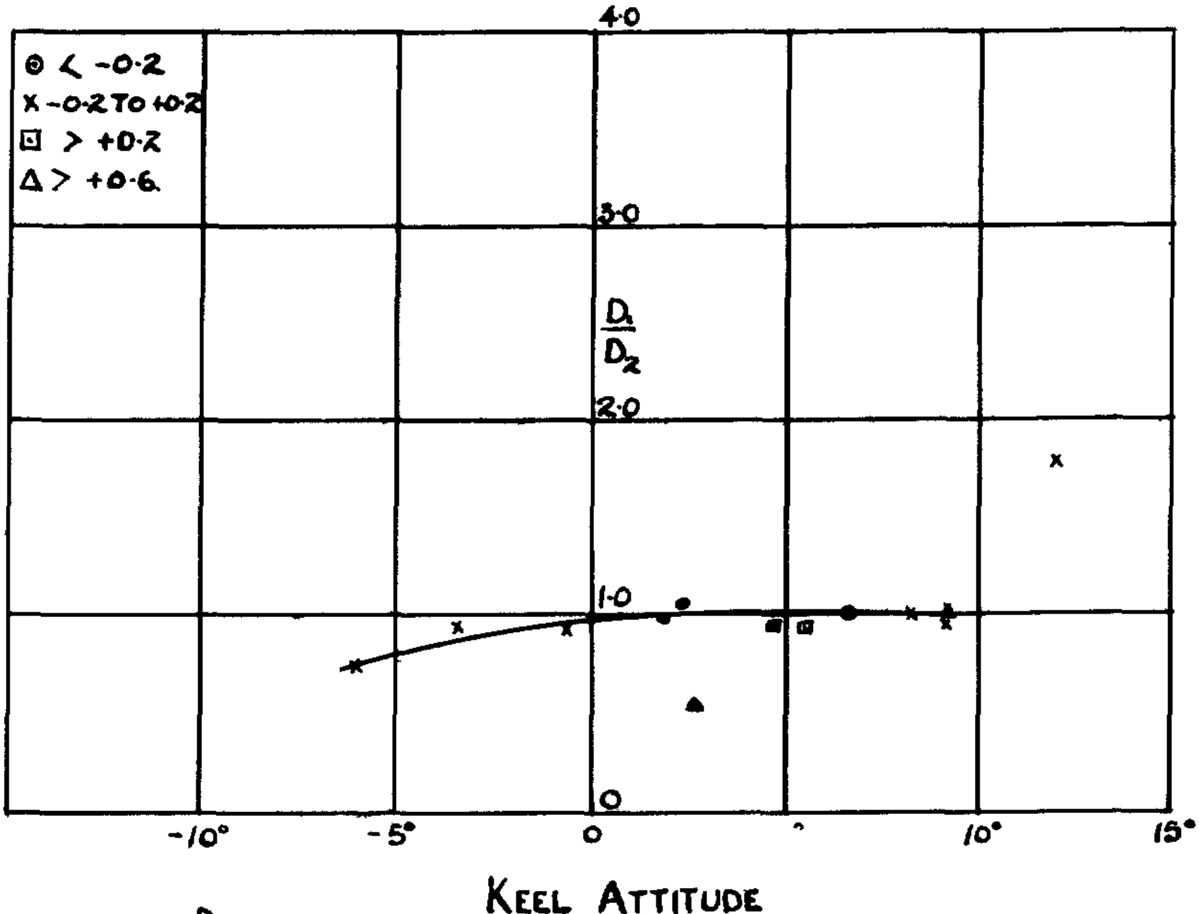

Variation of $\frac{D_1}{D_2}$ with initial keel attitude and angular velocity for diaphragm 10.

FIG 60.

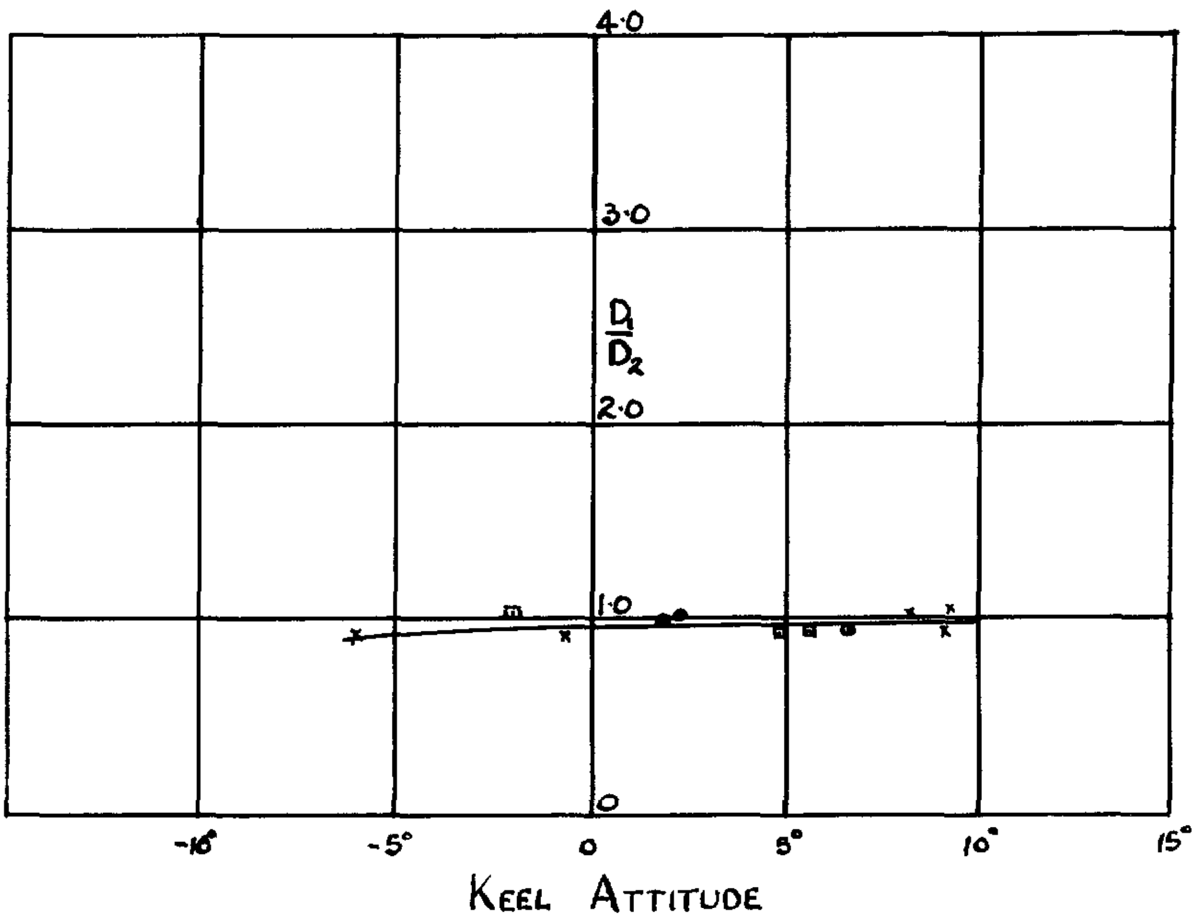

Variation of $\frac{D_1}{D_2}$ with Initial Keel Attitude and Angular Velocity For Diaphragm 5.

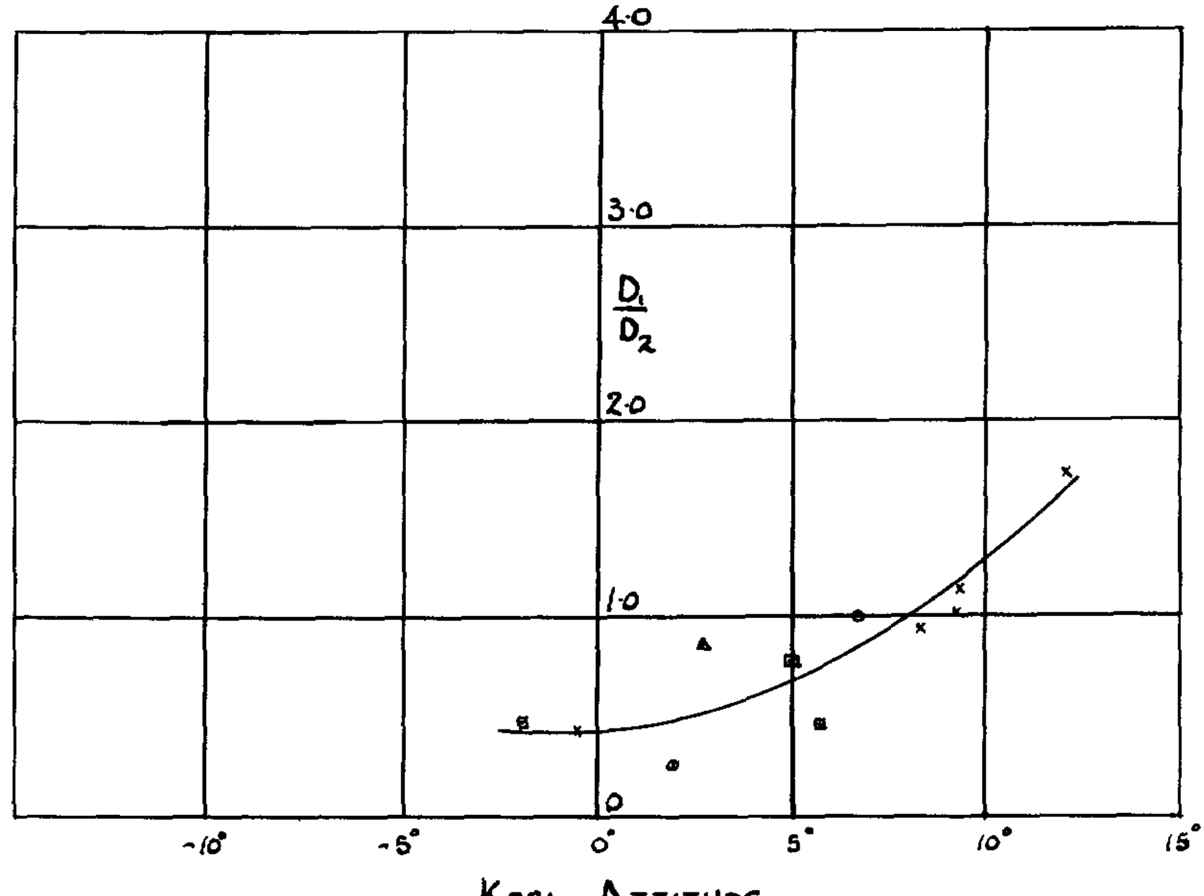

VARIATION OF $\frac{D_1}{D_2}$ WITH INITIAL KEEL ATTITUDE AND ANGULAR VELOCITY FOR DIAPHRAGM 15.

FIG. 63.
& FIG. 64

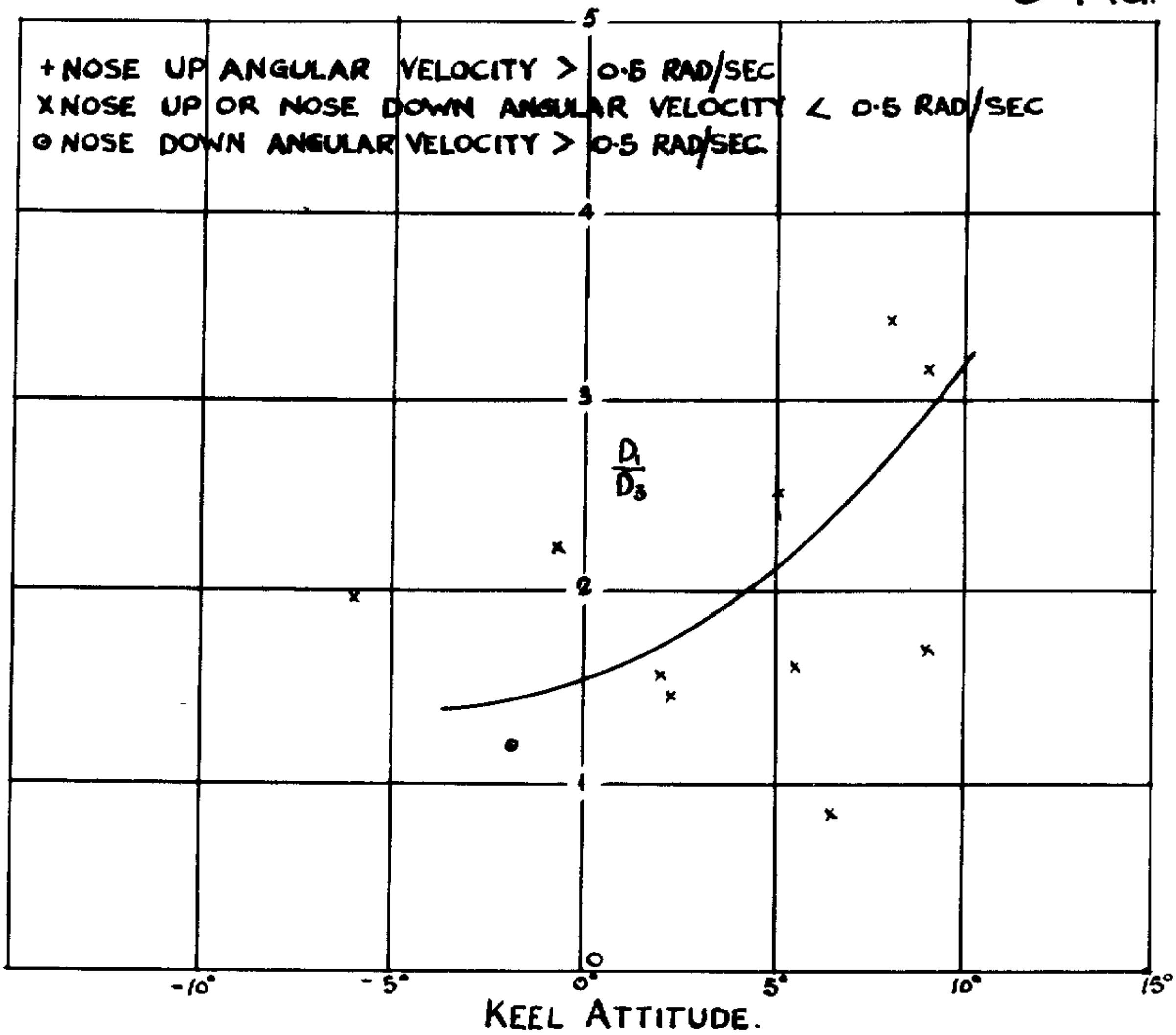

VARIATION OF $\frac{D_1}{D_3}$ WITH KEEL ATTITUDE AND ANGULAR VELOCITY AT FIRST IMPACT (DIAPHRAGM 5) ($\frac{2c}{b}$ = 0·36)

FIG 64.

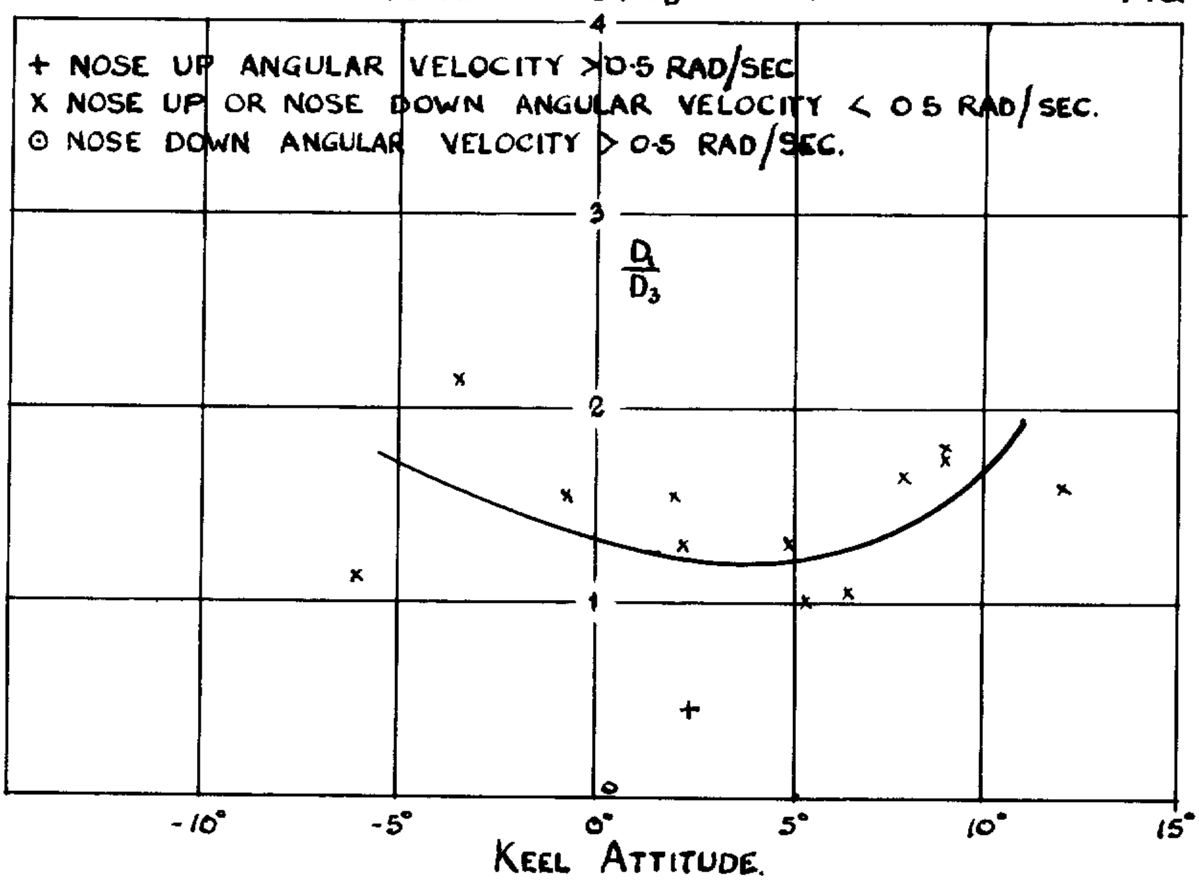

VARIATION OF $\frac{D_1}{D_3}$ WITH KEEL ATTITUDE AND ANGULAR VELOCITY AT FIRST IMPACT (DIAPHRAGM 10) ($\frac{2c}{b}$ = 0·33)

FIG 65

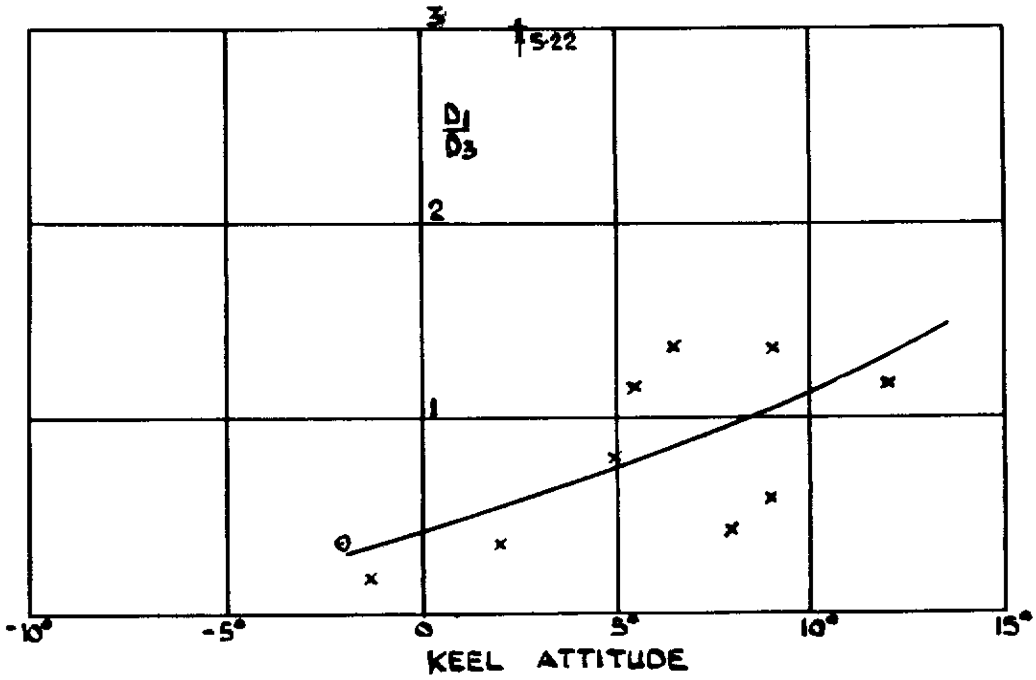

VARIATION OF $\frac{D_1}{D_3}$ WITH KEEL ATTITUDE AND ANGULAR VELOCITY AT FIRST IMPACT

(DIAPHRAGM 15) $\left(\frac{2c}{b} = 0{\cdot}27\right)$

FIG. 66.

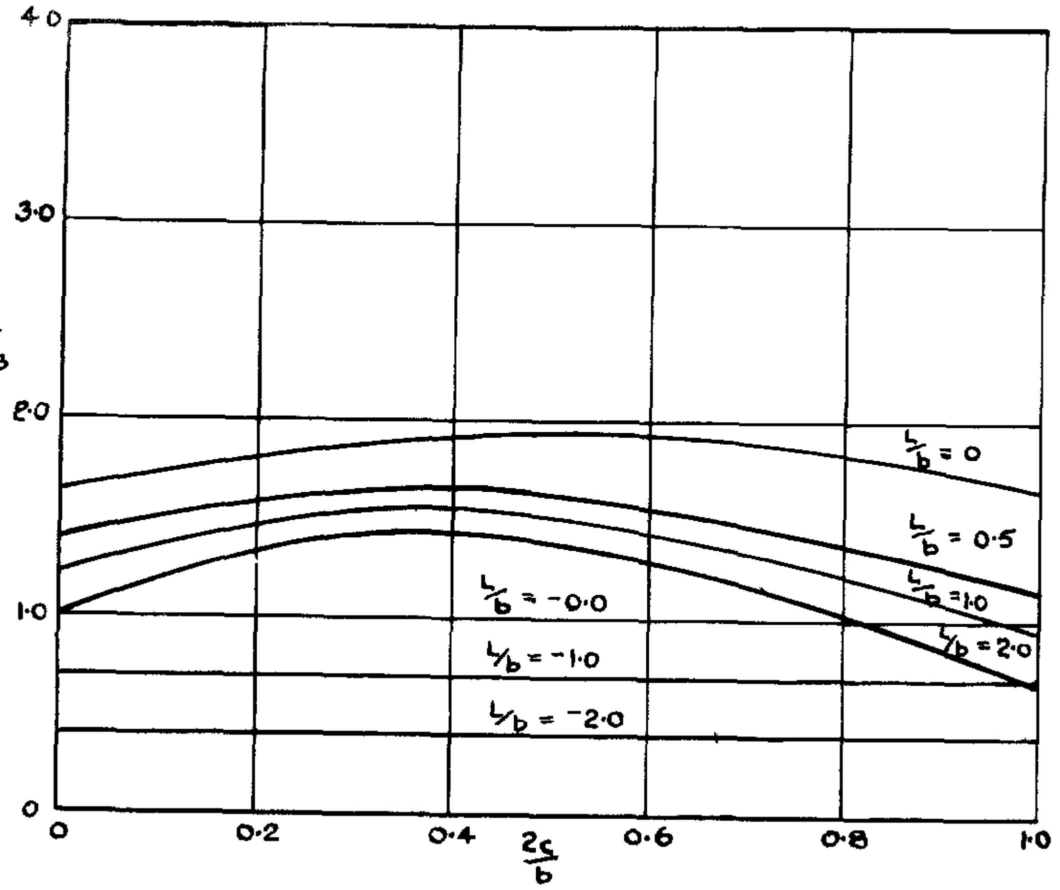

VARIATION OF $\frac{D_1}{D_3}$ WITH RATIOS $\frac{\text{WETTED BEAM}}{\text{BEAM AT STEP}}$ AND $\frac{\text{DISTANCE FOR}^{\text{D}}\text{ OF C.G}}{\text{BEAM AT STEP}}$ FOR $\alpha = 5°$

FIG. 67.

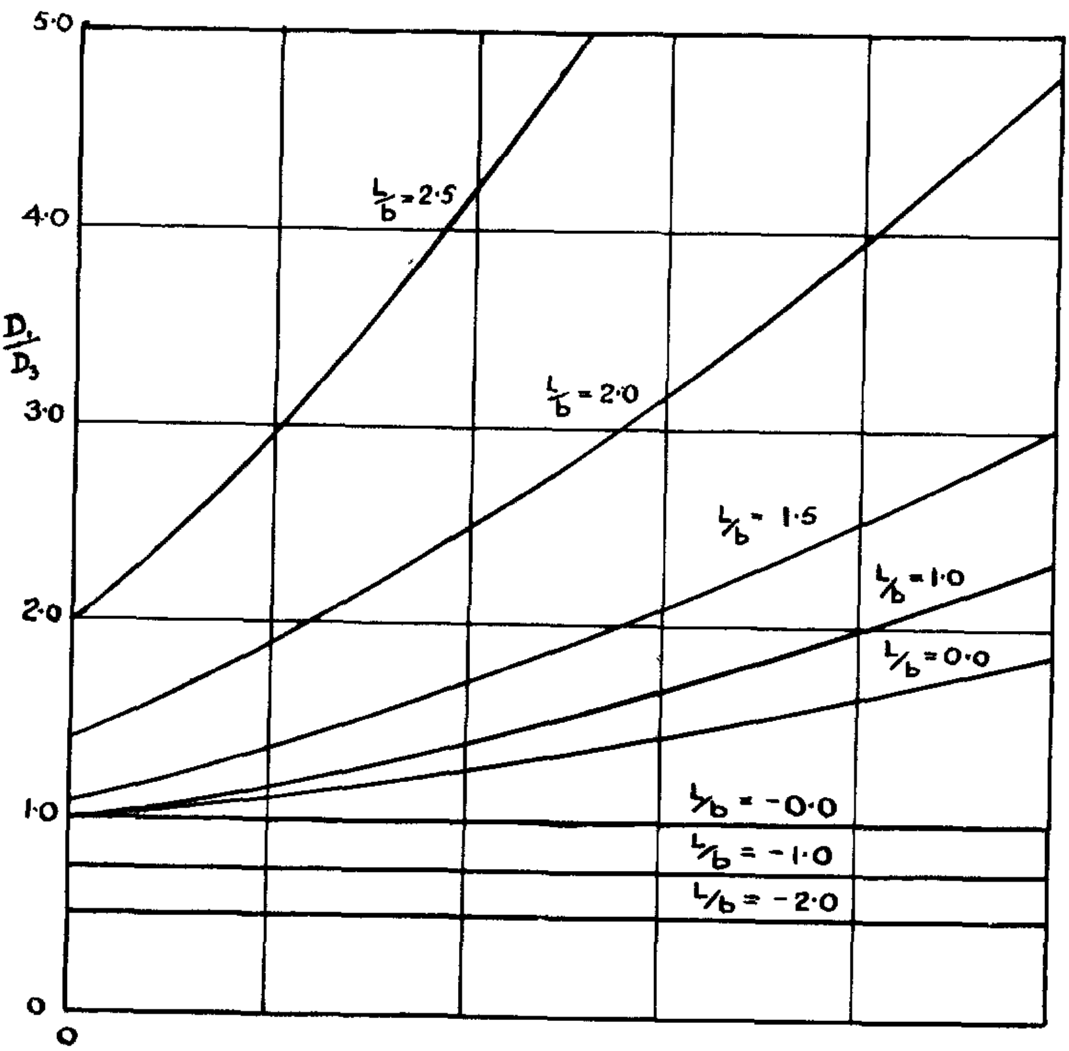

VARIATION OF $\frac{D_1}{D_3}$ WITH RATIOS $\frac{\text{WETTED BEAM}}{\text{BEAM AT STEP}}$ AND $\frac{\text{DISTANCE FOR}^{\text{D}}\text{ OF C.G.}}{\text{BEAM AT STEP}}$ FOR $\alpha = 0°$

FIG. 68.

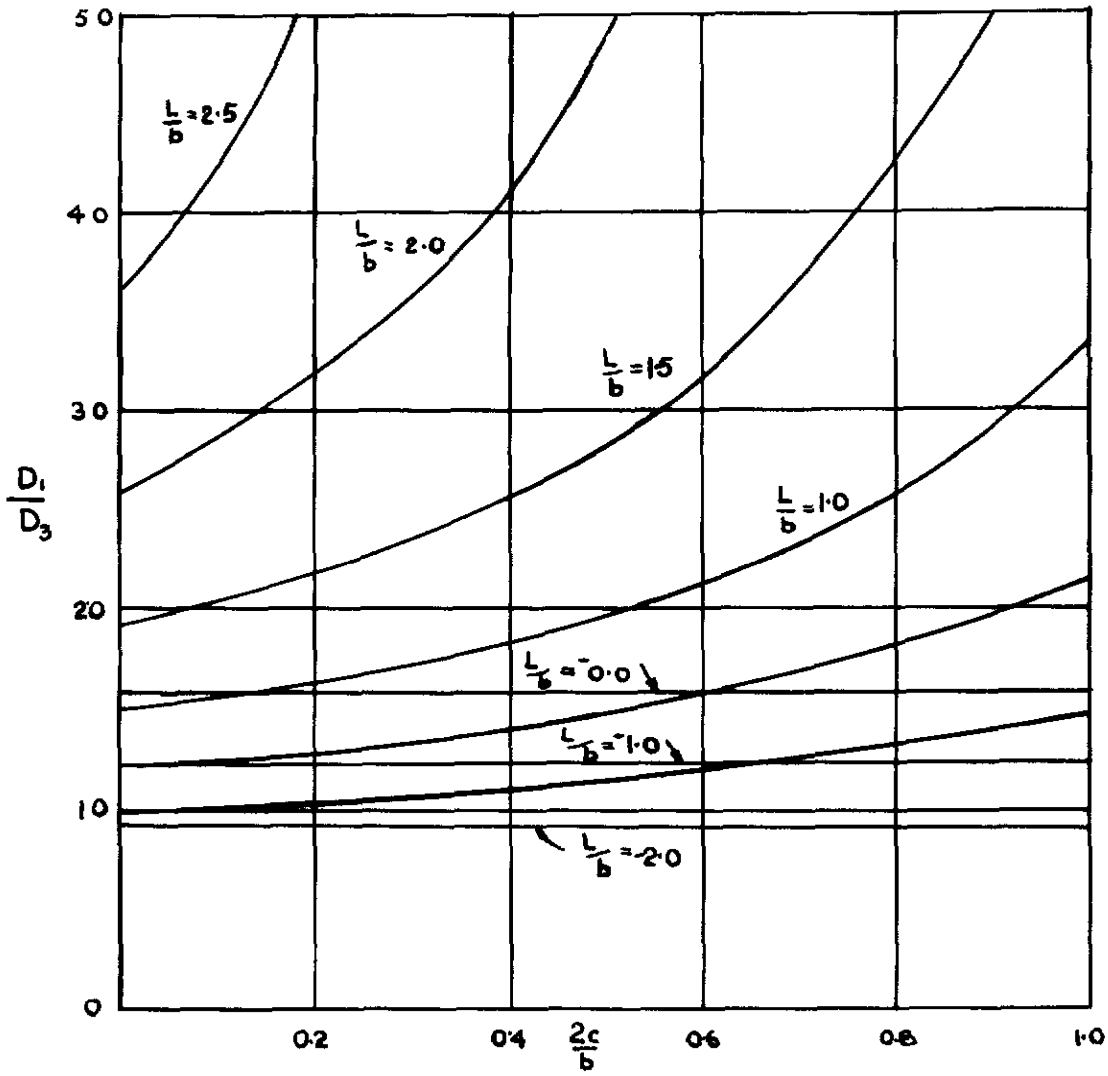

VARIATION OF $\frac{D_1}{D_3}$ WITH RATIOS $\frac{\text{WETTED BEAM}}{\text{BEAM AT STEP}}$ AND $\frac{\text{DISTANCE FOR}^{D}\text{ OF C.G.}}{\text{BEAM AT STEP}}$ FOR $\alpha = 5$.

FIG. 69.

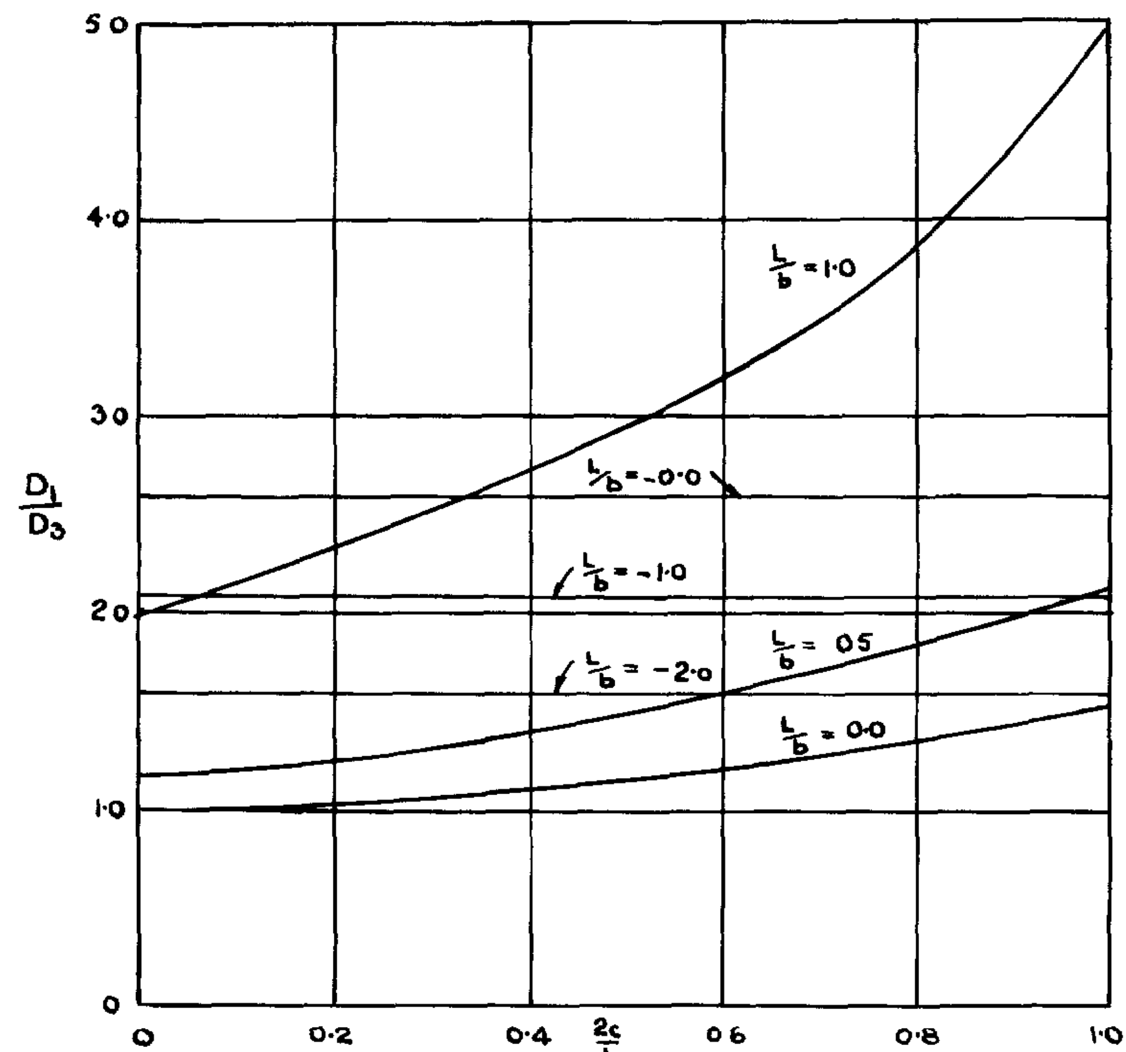

VARIATION OF $\frac{D_1}{D_3}$ WITH RATIOS $\frac{\text{WETTED BEAM}}{\text{BEAM AT STEP}}$ AND $\frac{\text{DISTANCE FOR}^{D}\text{ OF C.G}}{\text{BEAM AT STEP}}$ FOR $\alpha = 10$

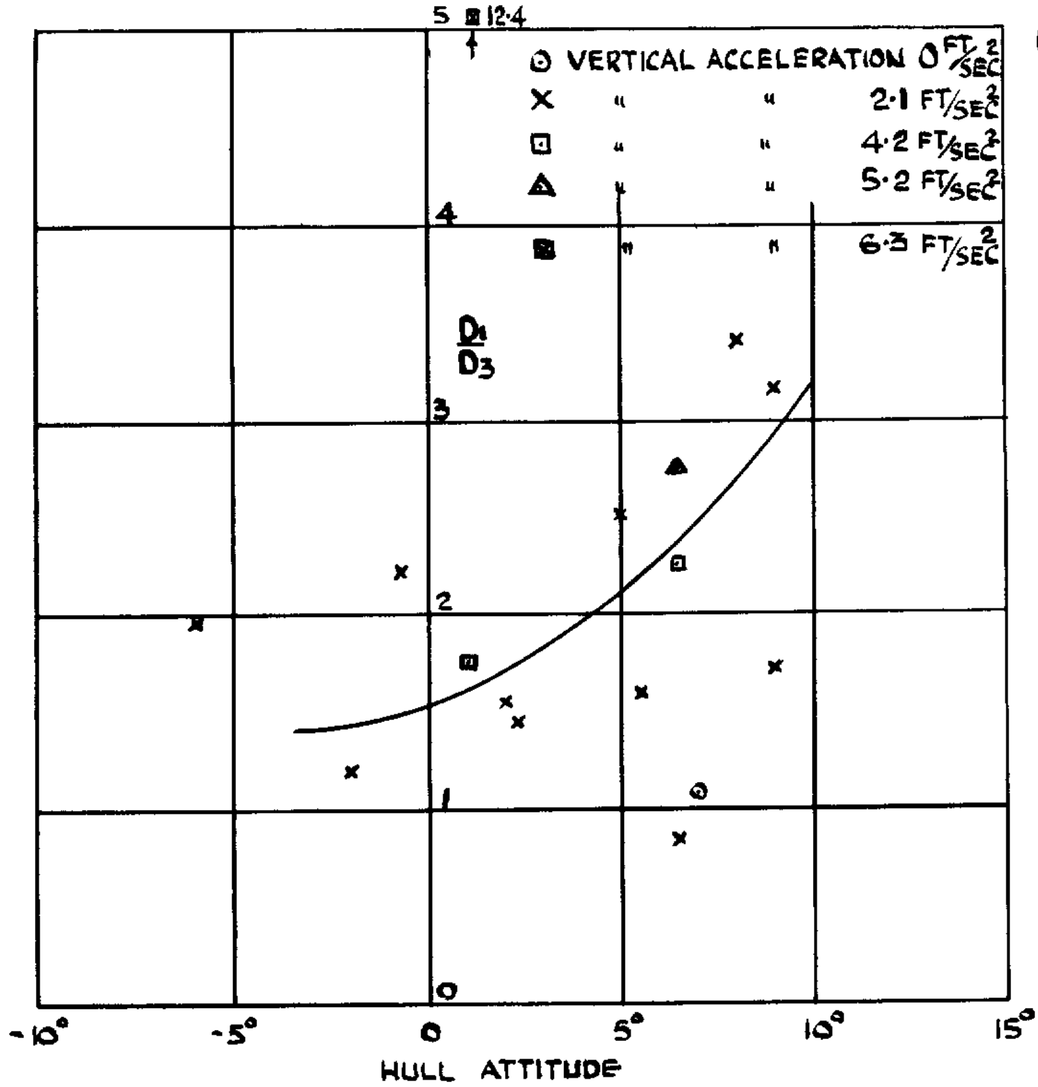

FIG 70

VARIATION OF $\frac{D_1}{D_3}$ WITH KEEL ATTITUDE AND VERTICAL ACCELERATION DUE TO GRAVITY (DIAPHRAGM 5) $\left(\frac{2c}{b} = 0{\cdot}36\right)$

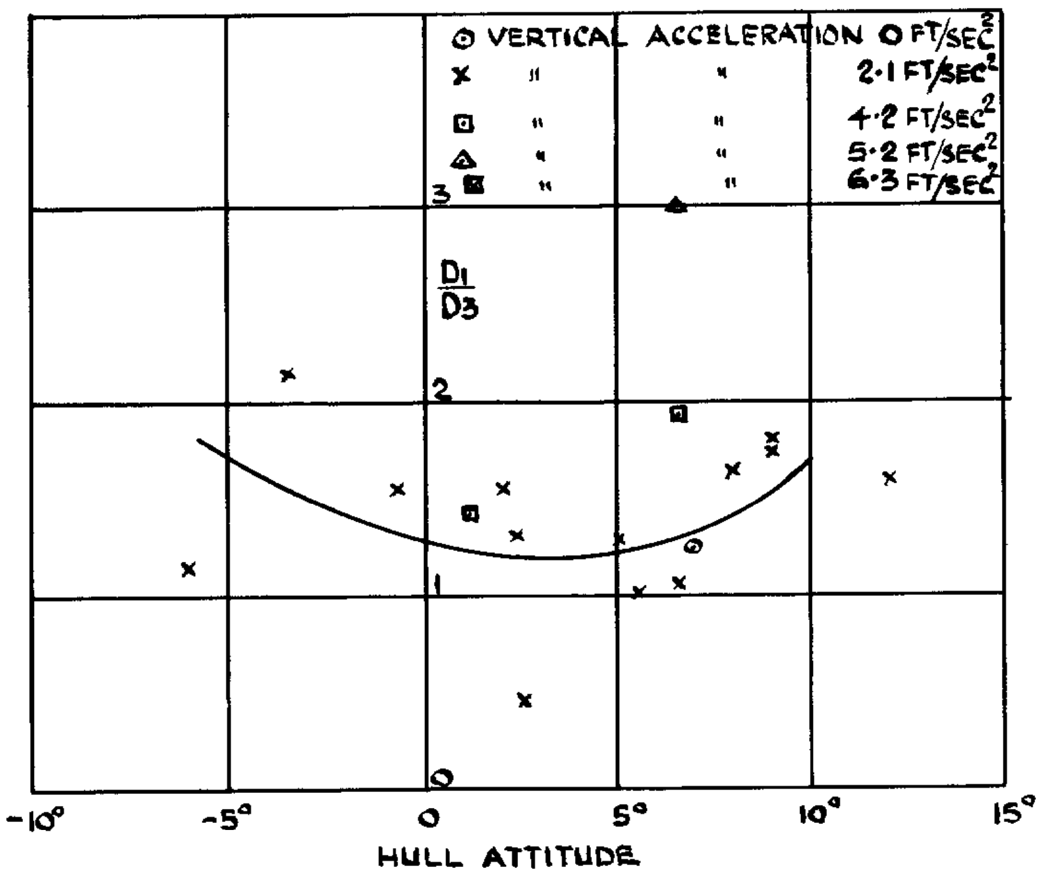

FIG 71

VARIATION OF $\frac{D_1}{D_3}$ WITH KEEL ATTITUDE AND VERTICAL ACCELERATION DUE TO GRAVITY (DIAPHRAGM 10) $\left(\frac{2c}{b} = 0{\cdot}33\right)$

FIG 72

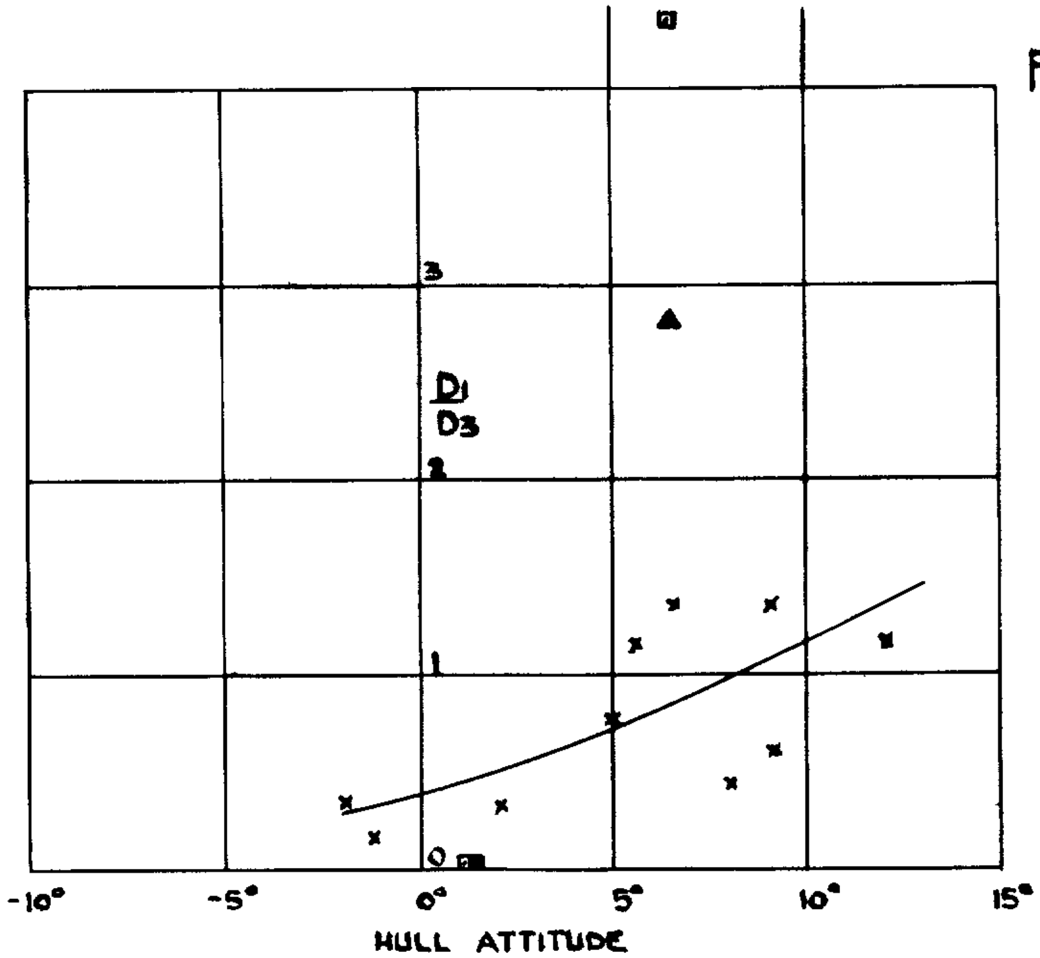

VARIATION OF $\frac{D_1}{D_3}$ WITH KEEL ATTITUDE AND VERTICAL ACCELERATION DUE TO GRAVITY

(DIAPHRAGM 15) $\left(\frac{2c}{b} = 0{\cdot}27\right)$

⊙	VERTICAL	ACCELERATION	0 FT/SEC^2
×	"	"	2·1 FT/SEC^2
⊡	"	"	4·2 FT/SEC^2
▲	"	"	5·2 FT/SEC^2
⊠	"	"	6·3 FT/SEC^2

FIG 73

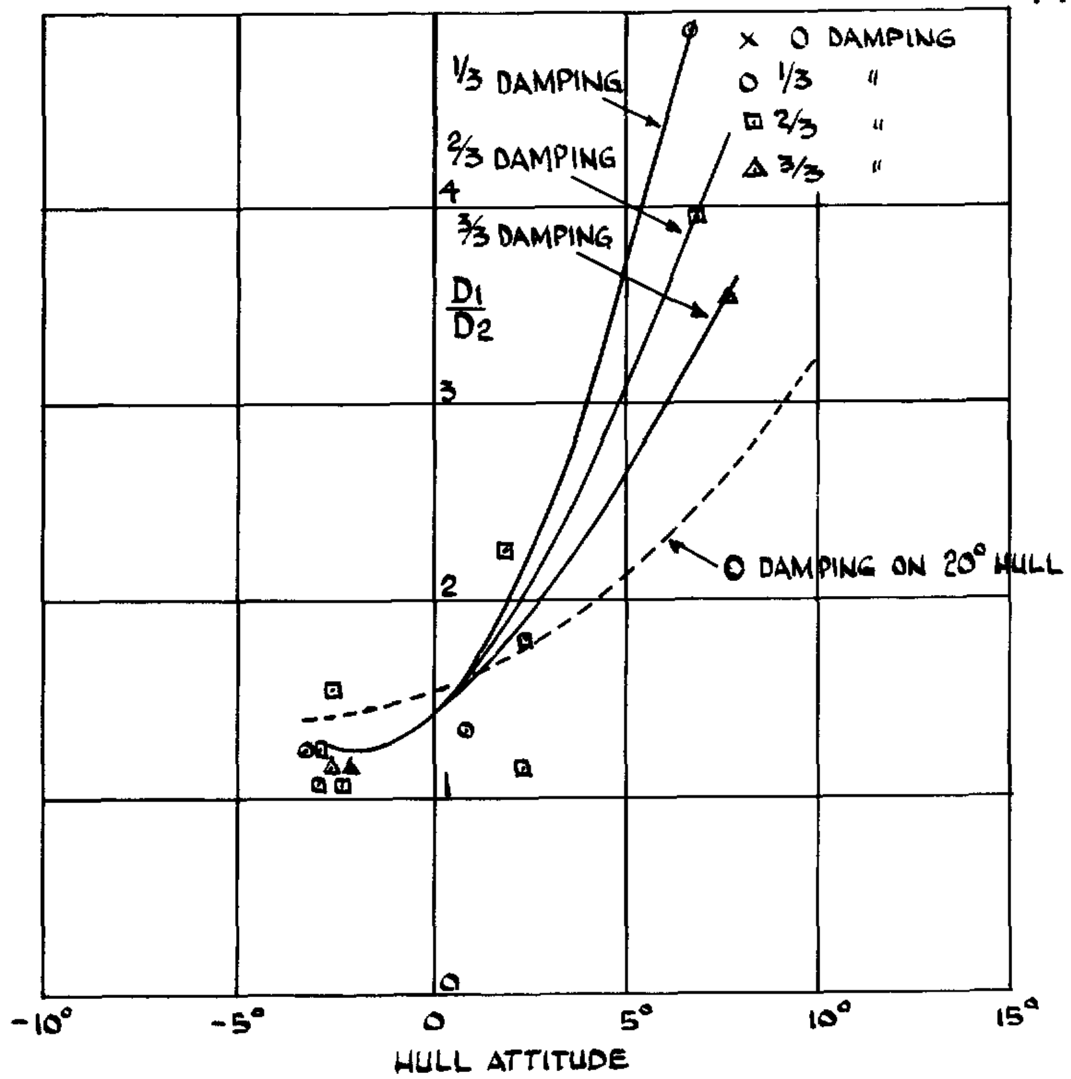

VARIATION OF $\frac{D_1}{D_3}$ WITH INITIAL ATTITUDE AND DAMPING (DIAPHRAGM 5 ON 10° HULL)

FIG 74

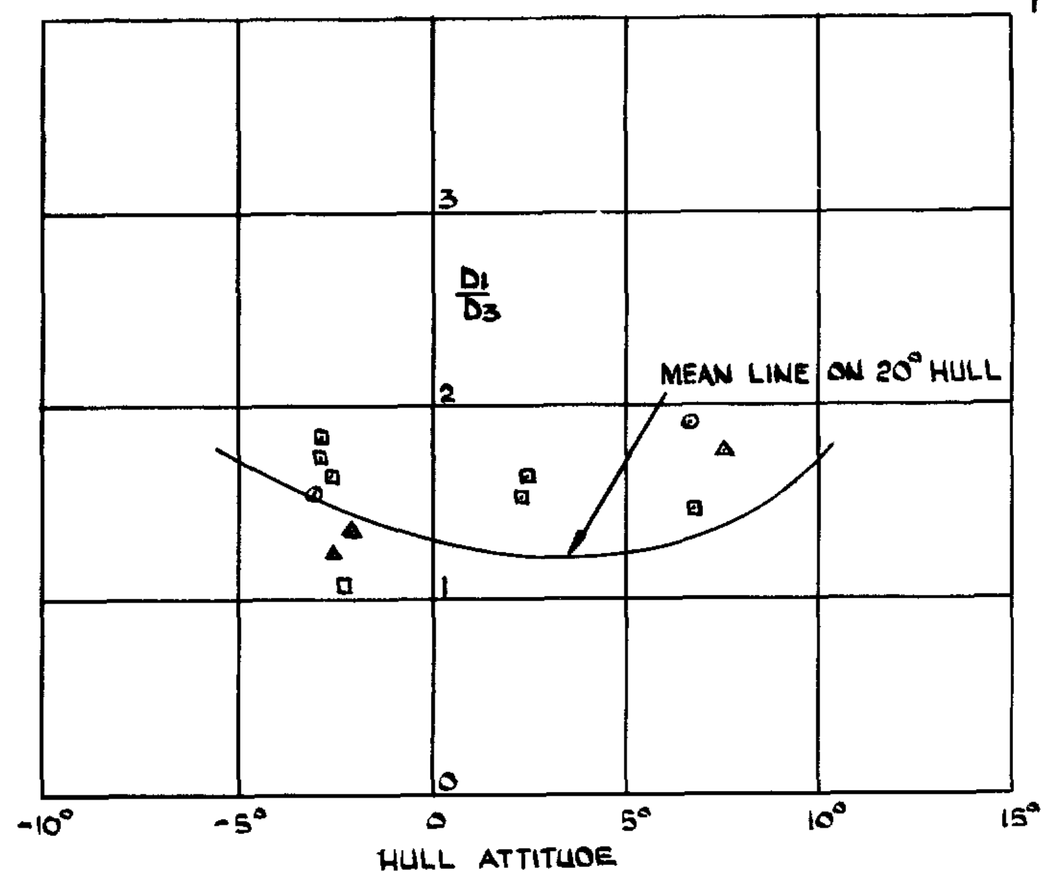

VARIATION OF $\frac{D_1}{D_3}$ WITH INITIAL ATTITUDE AND DAMPING (DIAPHRAGM 10 ON 10° HULL)

FIG. 75

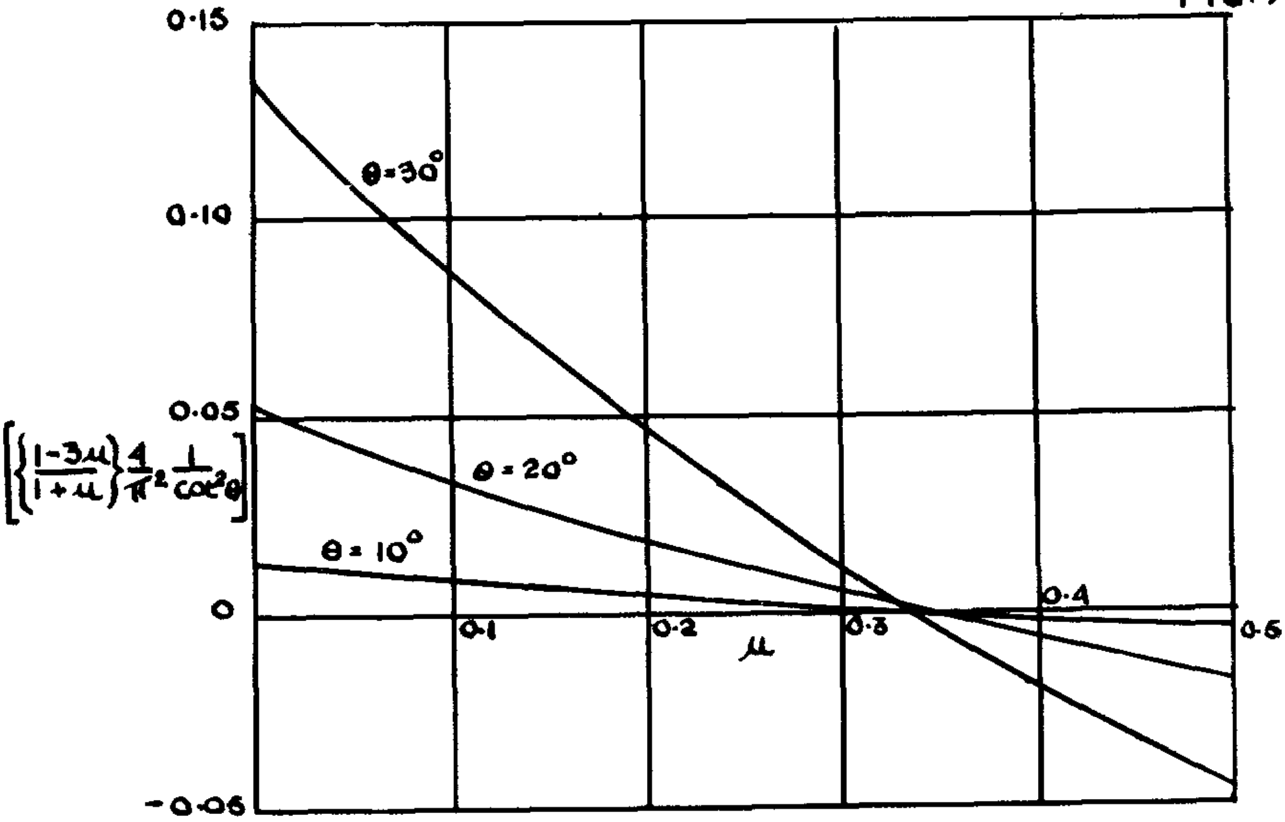

VARIATION OF TERM $\left[\left\{\frac{1-3\mu}{1+\mu}\right\}\frac{4}{\pi^2}\frac{1}{\cot^2\theta}\right]$ WITH μ

FIG 76

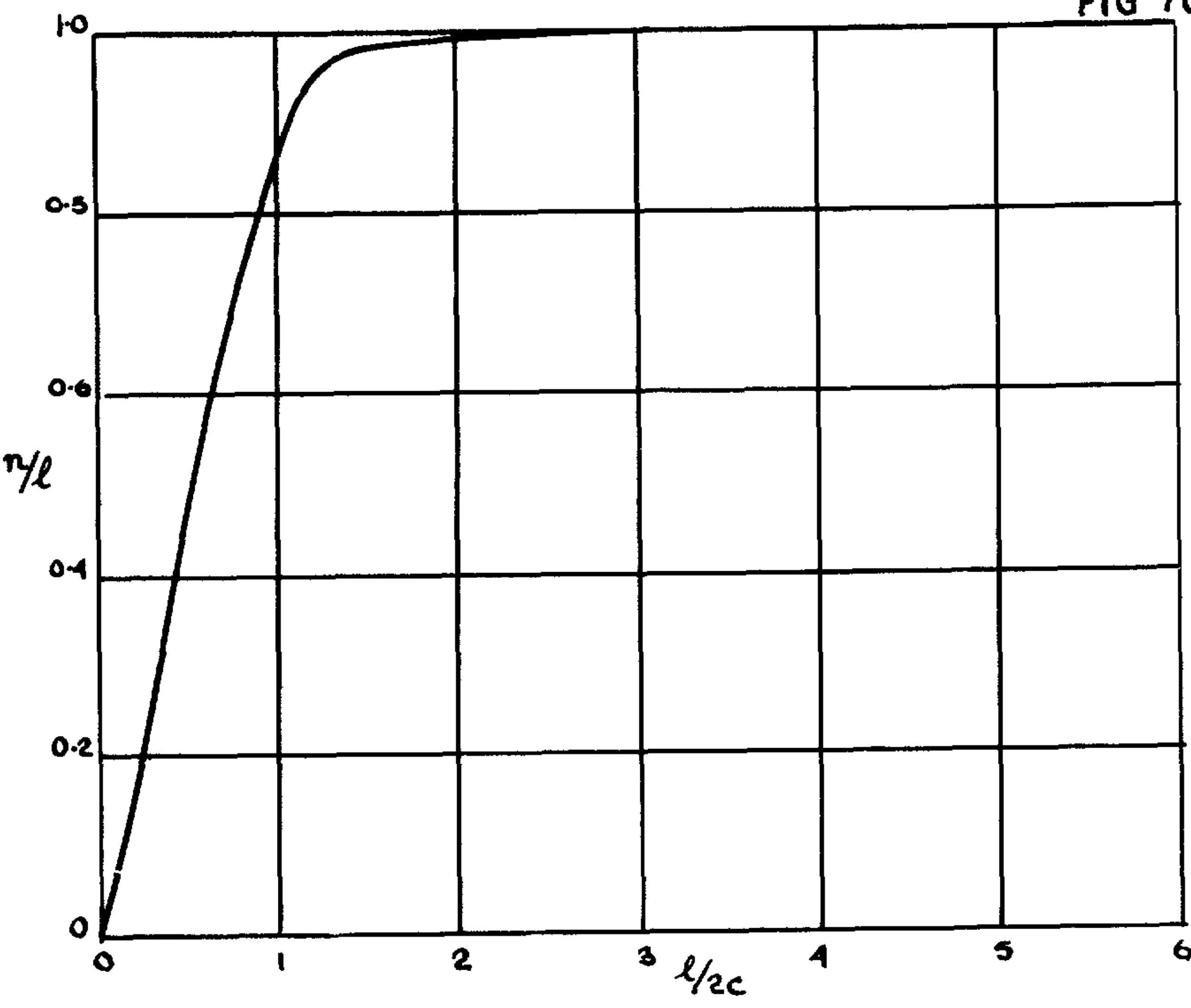

CORRECTION FACTOR n/l TO GIVE EFFECT OF $l/2c$

FIG 77

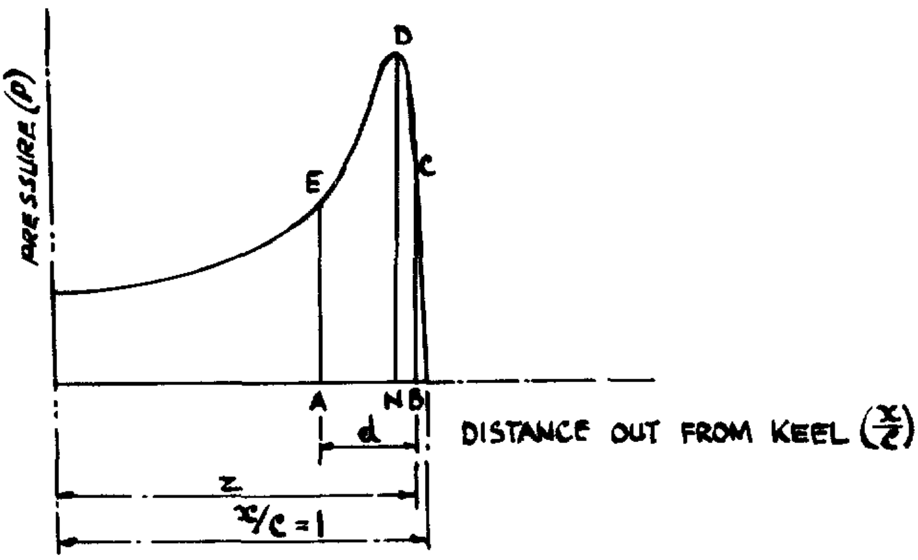

PRESSURE DISTRIBUTION DURING IMPACT

FIG 78

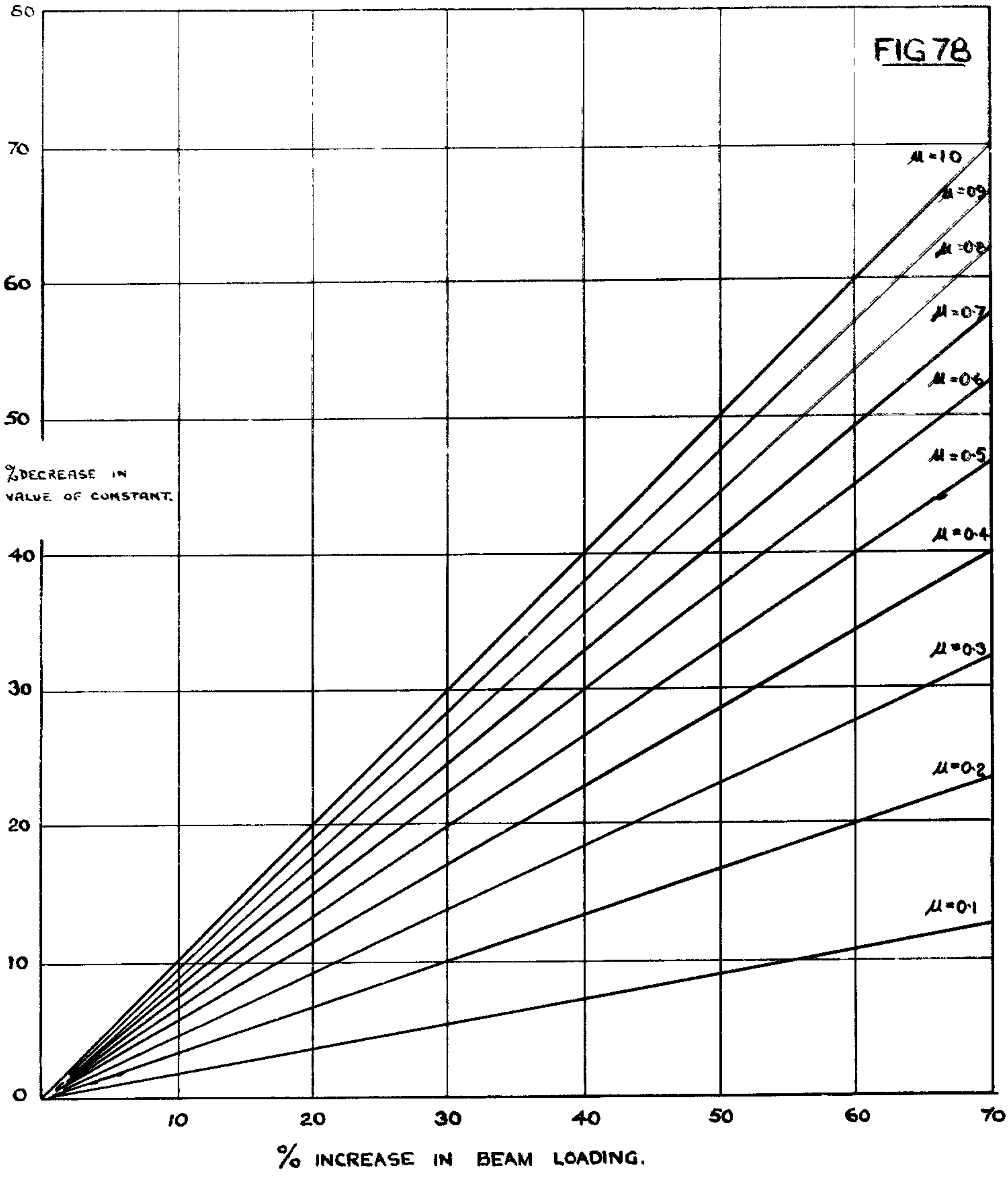

FIG 79.

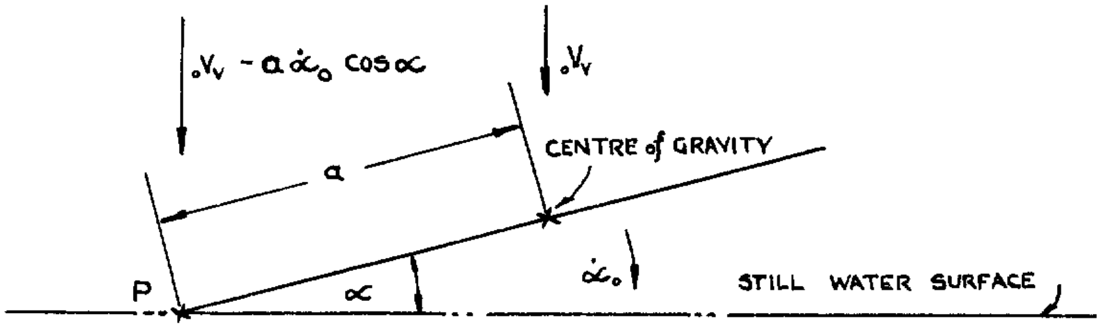

DIAGRAM SHOWING IMPACT OF WEDGE AT FINITE ATTITUDE.

FIG. 80.

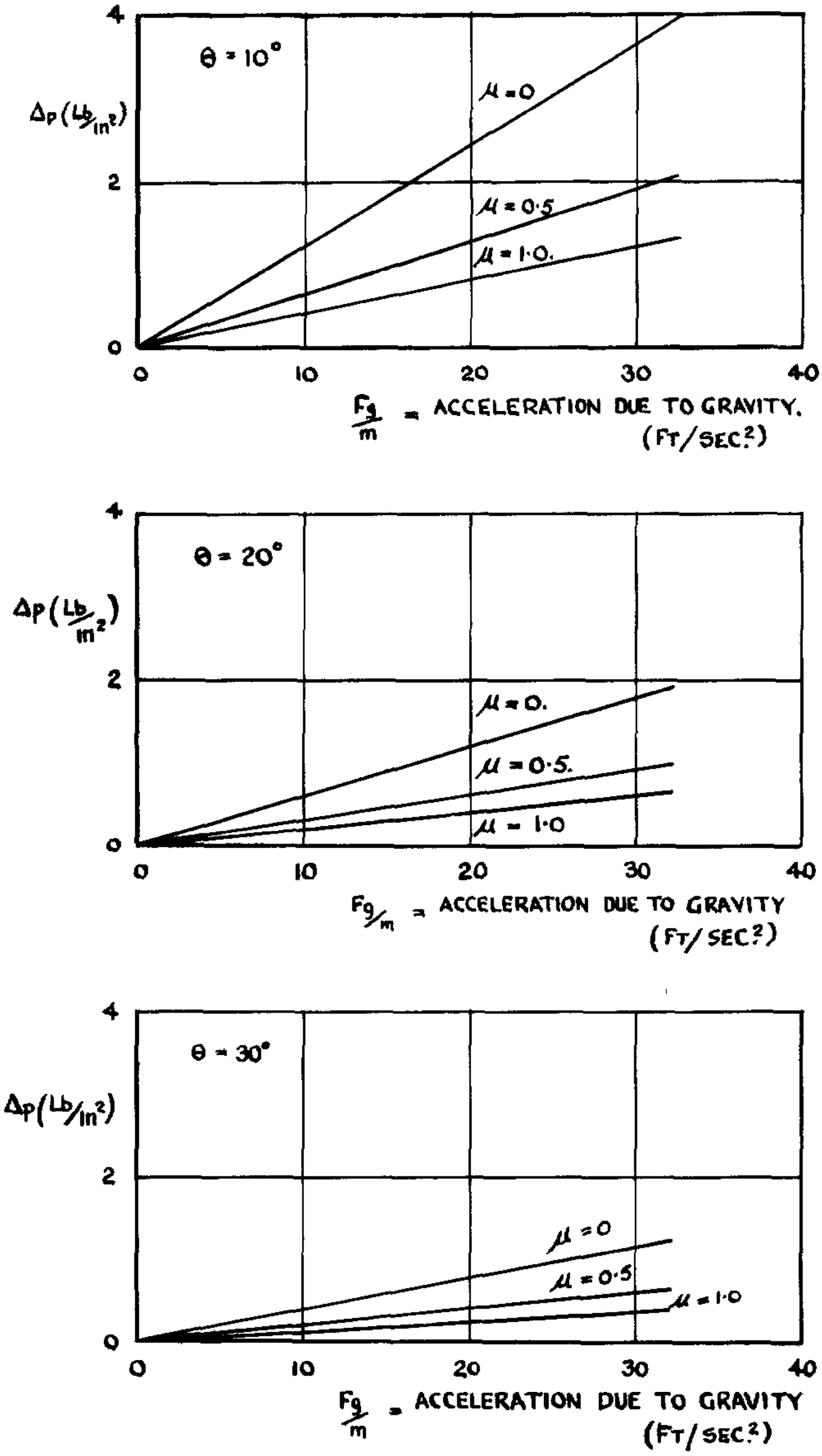

INCREASE IN P_{MAX} DUE TO GRAVITY AT C = 1·00 FT.

(NOTE :- IF C IS OTHER THAN UNITY MULTIPLY ABOVE VALUES OF Δp BY C)

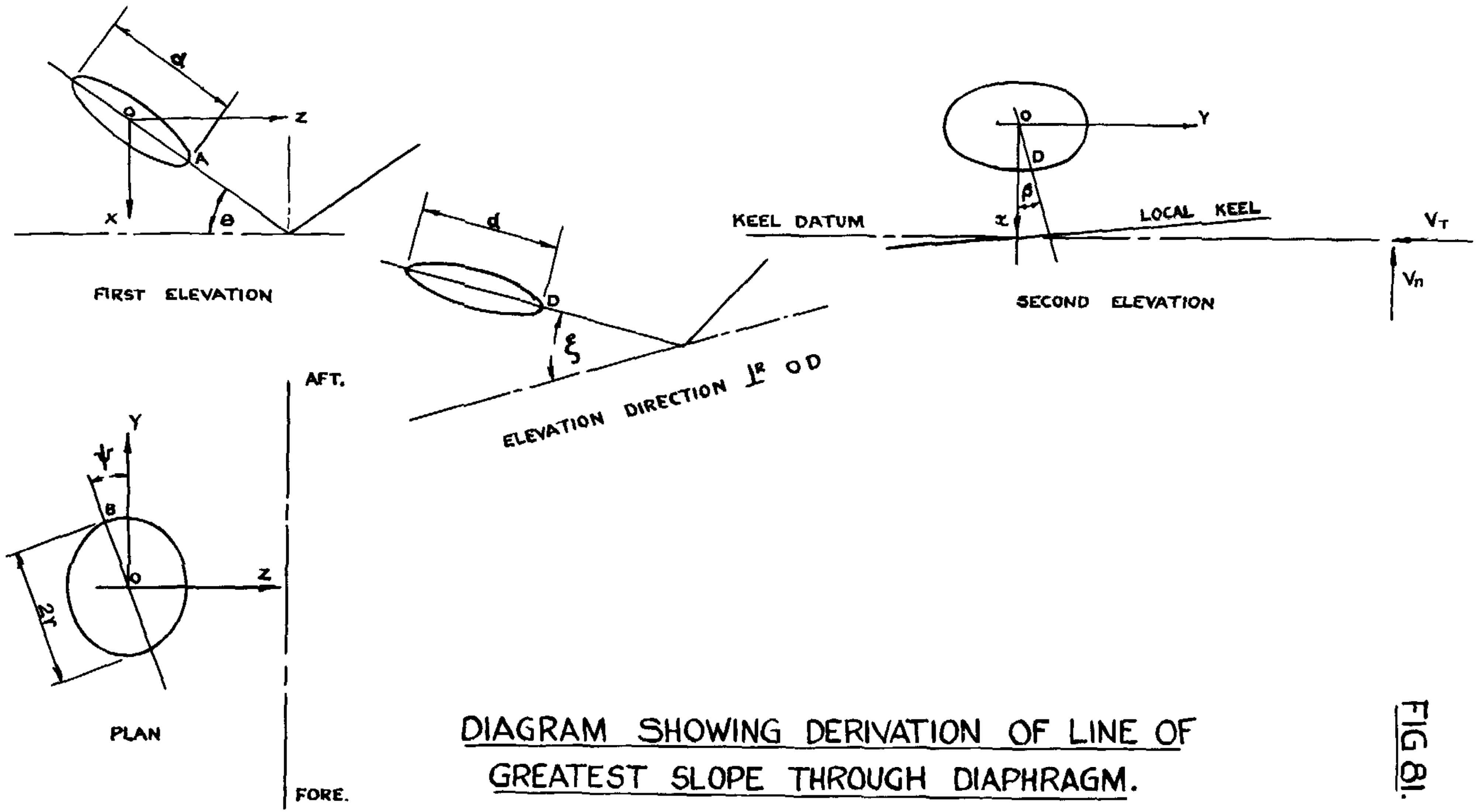

DIAGRAM SHOWING DERIVATION OF LINE OF GREATEST SLOPE THROUGH DIAPHRAGM.

FIG 81.

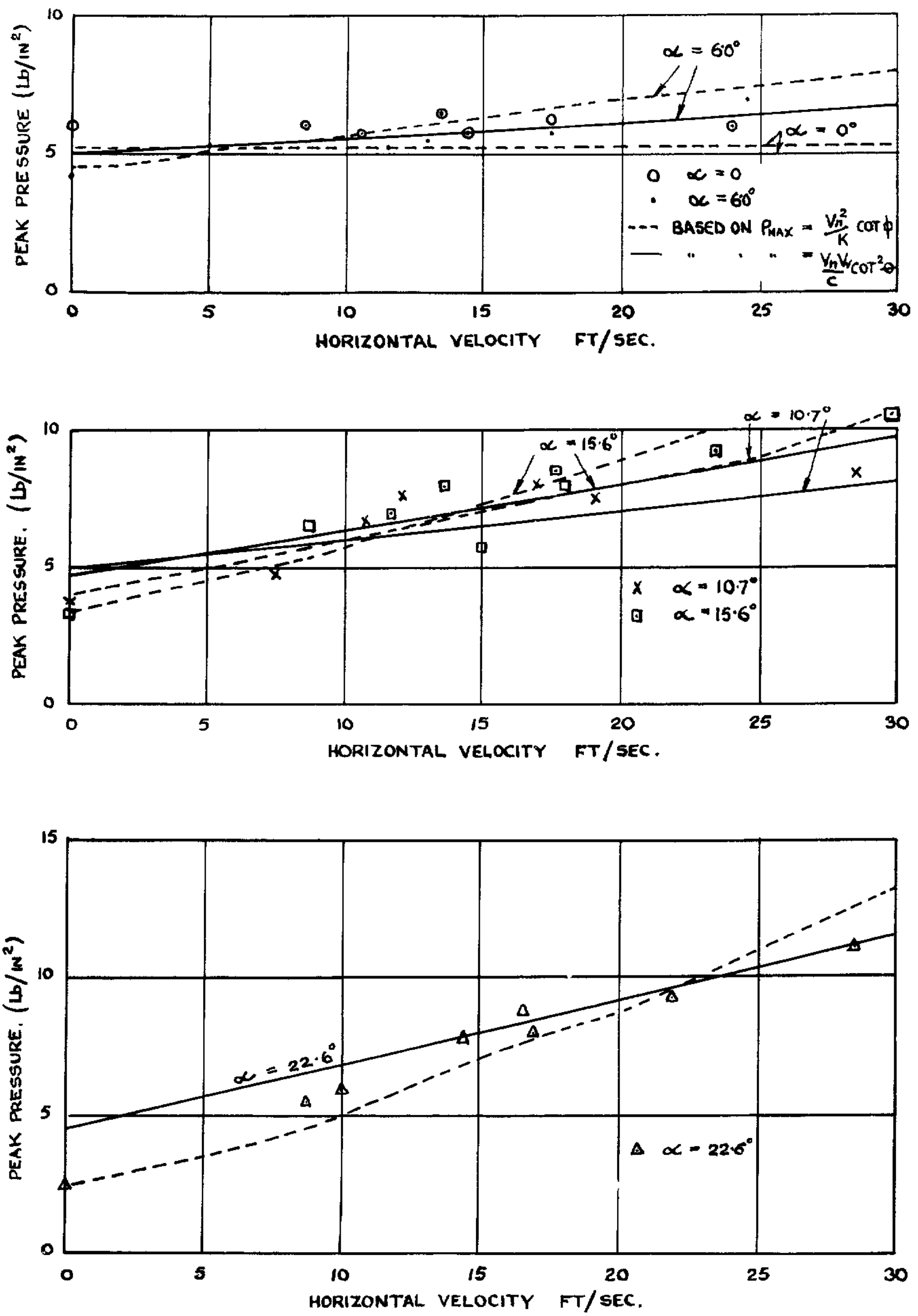

PEAK PRESSURE ON V-SHAPE AGAINST FORWARD SPEED FOR A CONSTANT VERTICAL VELOCITY OF 9.0 FT/SEC AND A CONSTANT DEAD RISE ANGLE OF 16°

FIG. 83

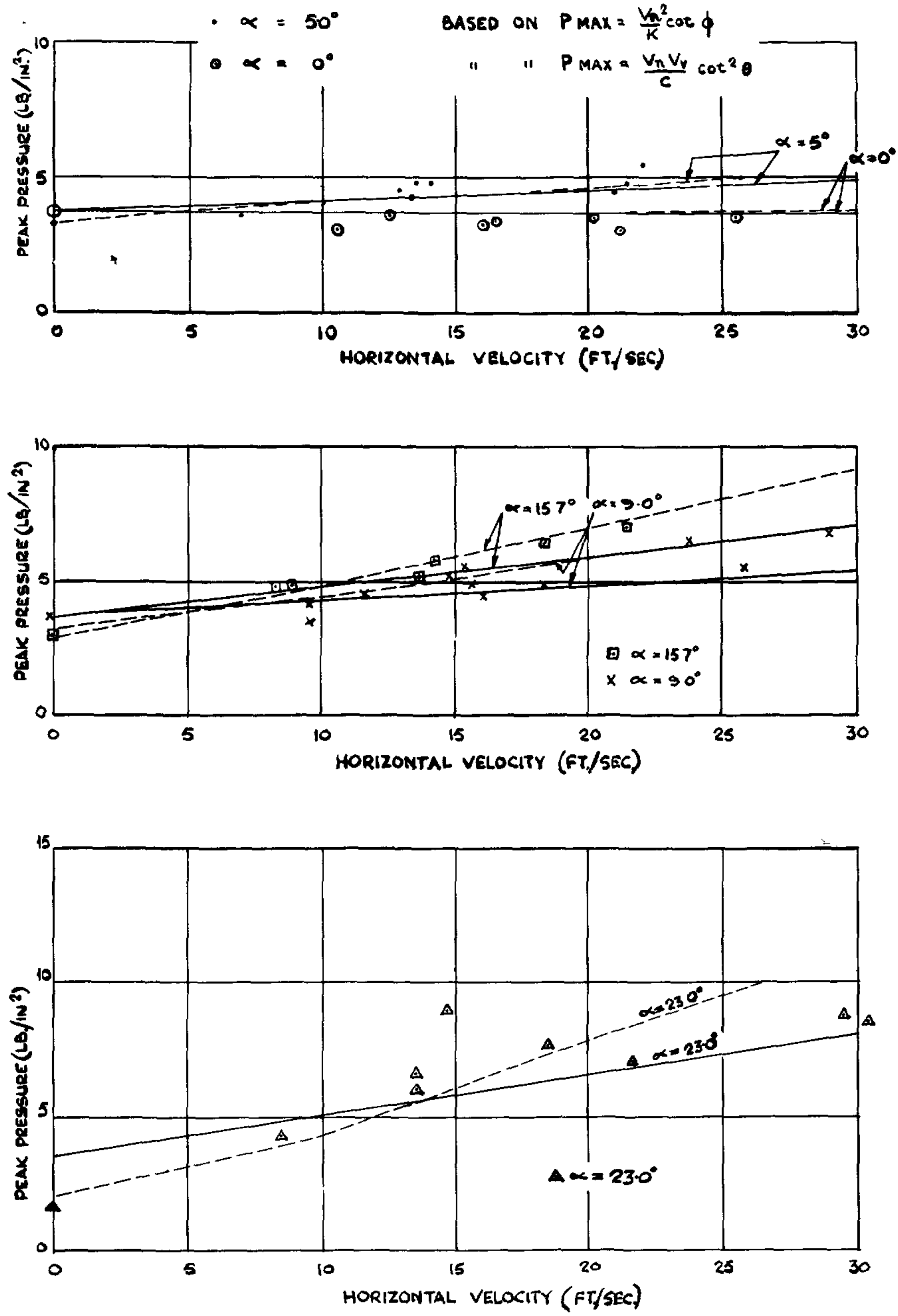

PEAK PRESSURE ON V- SHAPE AGAINST FORWARD SPEED FOR A CONSTANT VERTICAL VELOCITY OF 9.0 FT/SEC. AND A CONSTANT DEAD RISE ANGLE OF 22°

C.P. No. 4
(10057)
A.R.C. Technical Report

PRINTED AND PUBLISHED BY HIS MAJESTY'S STATIONERY OFFICE
To be purchased from
York House, Kingsway, LONDON, W.C.2 429 Oxford Street, LONDON, W.1
P.O. Box 569, LONDON, S.E.1
13a Castle Street, EDINBURGH, 2 1 St. Andrew's Crescent, CARDIFF
39 King Street, MANCHESTER, 2 1 Tower Lane, BRISTOL, 1
2 Edmund Street, BIRMINGHAM, 3 80 Chichester Street, BELFAST
or from any Bookseller

1950

Price 7s. 6d. net

PRINTED IN GREAT BRITAIN

S.O. Code No. 23-9006-4

D.S. 34602/K3